Title	THERMAL PROPERTIES OF SILICATE GLASSES(Dissertation_)
Author(s)	Hirao, Kazuyuki
Citation	Kyoto University ( )
Issue Date	1981-05-23
URL	http://dx.doi.org/10.14989/doctor.k2584
Right	
Type	Thesis or Dissertation
Textversion	author

THERMAL PROPERTIES OF SILICATE GLASSES

KAZUYUKI HIRAO

1 9 8 1

DEPARTMENT OF INDUSTRIAL CHEMISTRY

FACULTY OF ENGINEERING

KYOTO UNIVERSITY

THERMAL PROPERTIES OF
SILICATE GLASSES

KAZUYUKI HIRAO

1 9 8 1

DEPARTMENT OF INDUSTRIAL CHEMISTRY

FACULTY OF ENGINEERING

KYOTO UNIVERSITY

PREFACE

The studies presented in this thesis have been carried out under the direction of Professor Naohiro Soga at Kyoto University. The studies are concerned with a field of thermal properties of silicate glasses from very low temperatures to high temperatures.

The author wishes to express his sincere gratitude to Professor Naohiro Soga for his constant guidance and for his valuable advice throughout this work. The author wishes to thank Assistant Professor Rikuo Ota, Dr. Hanada and fellow graduate students for their useful discussions.

<div align="right">Kazuyuki Hirao</div>

Department of Industrial Chemistry

Kyoto university

1981

CONTENTS

CHAPTER 1

INTRODUCTION

Recently, the non-crystalline or amorphous state of solids is attracting much attentions of scientists and engineers because unusual but quite useful behaviors have been observed in many physical properties of glasses and are now being applied to develop new materials for device applications.[1)-5)] Such unusual behaviors are generally considered to be associated with the random or disordered structure of glassy state. Since the vibrations of atoms in solids are quite sensitive to the packing state of atoms, or to the atomic arrangement, the knowledge of thermal properties is useful to obtain information about the difference in structure between the glassy and crystalline states.[6)-8)] Among various thermal properties, heat capacity is the easiest to be dealt with from a theoretical point of view.

As for crystalline state, the behavior of heat capacity is well understood in a wide temperature range on the basis of Debye theory. At very low temperatures, the heat capacity obeys the T^3 law prescribed by the Debye theory and the characteristic temperature Θ_D obtained from this relationship agrees well with the value calculated from experimental sound velocities.[9)] In the low-to-moderate temperature range, it follows the Debye function based on Θ_D well. However, this situation does not hold for the glassy state.

It has been known that vitreous SiO_2, GeO_2 and Se show extra
heat capacities at very low temperatures compared with their crystal-
line states. This means that the T^3 law is inadequate to express
the heat capacity of a glass at very low temperatures. Zeller has
shown that a linear temperature dependent term is needed.
Although there are different types of glasses, they all show such
excess heat capacity. Thus, this phenomenon is considered to be
associated with a lack of periodicity or long range order.[10),11)]
Thus, in this temperature range, it seems possible to approach the
problem by considering a generalized simple disorder model.

A close look of the existing data of heat capacities of various
at low-to-moderate temperatures reveals that the Debye function based
on a single characteristic temperature is also inadequate to express
the heat capacity data in this temperature range.   Certainly, it
is easy to understand that the concept of Debye's elastic continuum
cannot be applied to multicomponent inorganic glasses, because
various types of atomic bonds exist due to the existence of framework
and interstitial cations connecting to bridging and non-bridging
oxygens. Thus, it is necessary to establish a more complicated
model in which all types of atomic bonds in the glassy state are
taken into consideration.

Other thermal properties such as thermal expansivity are
associated with atomic vibrations in a solid. Furthermore, the
Grüneisen parameter, which is important for the equation of state

of a solid, depends also on the nature of atomic vibrations. Thus, the above mentioned new models, either a generalized simple disorder model suitable for the very low temperature range or a more complicated model suitable for the low-to-moderate temperature range, should satisfy the behaviors of thermal expansion and Grüneisen parameter in the respective temperature range. Although a number of studies have been carried out in the past on thermal properties of glasses by various investigators, there exist little data useful to examine the above models.

In the present study, two glass models satisfying the above mentioned requirements were developed based on the theory of lattice dynamics. The heat capacity, thermal expansion coefficients and Grüneisen parameter were determined on alkali silicate glasses from very low temperatures to moderately high temperatures, and were used to examine the models developed. A particular emphasis was placed on the interpretation of the effect of the addition of network formers to silica network which is responsible to the pronounced anomalous thermal behaviors. Furthermore, the measurements were also made on alkali alumino silicate glasses to examine the applicability of the model to interpret the data of more complicated glasses.

REFERENCES

1.   N.F.Mott and E.A.Davies,

                "Electronic Processes in Non-Cryst.

                Materials", Clarendon Press, Oxford, 1971

2.   Proceedings of the eighth Int. Conf. on Amorphous and

      Liquid Semiconductors, ed. William Paul, Cambridge,

      Massachusetts, 1979

3.   Proceedings of the Int. Conf. on Frontier of Glass Science,

      ed. J.D.Mackenzie, Univ. California, Los Angeles, 1980

4.   Proceedings of 10th Int. Conf. on Physics of Semiconductors,

      Cambridge, Mass., 1970

5.   Proceedings of 14th Int. Conf. on Physics of Semiconductors,

      Bristol and London, 1978

6.   Proceedings of the Fifth University Conf. on Glass Science,

      ed. M.Tomozawa, Univ. Rensselaer, Troy, New York, 1980

7.   E.Prasad, M.Sayer and H.M.Vyas,

                J. Non-Cryst. Solids, 40, 119 (1980)

8.   Proceedings of Int. Conf., "The Structure of Non-Cryst.

      Materials", Cambridge, 1976

9.   C.Kittel,   "Introduction to Solid State Physics",

                John Wiley & Sons. Inc., New York, 1953

10.   D.Weaire and V.Srivastava,

                "Amorphous and Liquid Semiconductors",

ed. W.Spear, Univ. Edinburgh, 1977

11.   J.M.Ziman,   "Principles of the Theory of Solids",

Cambridge Univ. Press, 1972

CHAPTER 2

LATTICE DYNAMICS AND THERMAL PROPERTIES OF GLASSES

In this chapter, the theories of lattice dynamics are applied
to describe the thermal properties of glass. The main emphasis is
to obtain the equations which can be used to interpret the experi-
mental data of thermodynamic properties of silicate glasses in a
wide range of temperature as well as to clarify the difference in
vibrational properties between glassy and crystalline states.

It is generally considered that the glassy state has no long
range order and hence no periodic symmetry. Therefore, at high
frequencies, or when the wavelength becomes comparable with the
interatomic spacings, the vibrational modes become extremely complex.
However, most of inorganic glasses are considered to have the short
range order similar to crystals, so that the basic concept, such as
quasi-harmonic approximation, may still be applicable.

In the crystalline state, the quasi-harmonic approximation, in
which the normal modes are taken to be harmonic but the frequencies
vary with volume, has been used successfully to describe thermal
properties of a solid. Since heat capacity is determined mainly by
the normal mode frequencies of lattice vibrations and thermal expan-
sion is related to the volume dependence of the frequencies, it is
possible to discuss the thermal behaviors of a glass, once the vibra-
tional frequency spectrum and its volume dependence of the glass

become known.

From this point of view, in this chapter, a simple glass model system is assumed first, and the vibrational frequency spectrum for this model at low temperature range is obtained by modifying the existing theory of lattice dynamics applicable to crystals. As will be described in Chapter 4, the result thus obtained explains important features of thermal behaviors of fused silica and alkali silicate glasses qualitatively for the first time. It is not precise enough to describe the thermal behaviors of more complicated glasses quantitatively. In order to take care of the compositional variations and structural features of glasses in multicomponent systems, more than two vibrational frequency spectra are required. A theoretical approach to obtain the combined mode frequencies and their volume dependence for such a system is extremely complicated even at very low temperatures, and can not be made at the present time. However, at high temperatures where all of the vibrational frequency spectra follow closely to Debye or Einstein model,[1] it seems possible to describe the thermal behaviors of complicated glasses by means of the combination of more than two characteristic temperatures. On this basis, a model is developed in this section for silicate glasses in binary or ternary systems.

2.1 An analytically tractable simple model system

In order to interpret the experimental data of heat capacity and thermal expansion based on lattice dynamics, it is required to establish an analytically tractable model from which vibrational frequencies of the system can be calculated. Such a model has to be suitable to obtain an analytically closed expression for $\omega(k)$, with attention paid to its dependence on the local order in structurally disordered systems. In order to simplify the model, a glass is considered to be composed of atoms of a single species. Let $U_\alpha(n)$ be the α component of the displacement vector $U(n)$ of an atom located at the equilibrium position n. Then the time independent equation of motion obeyed by the $U(n)$ can be written in the form.

$$M\omega^2 U_\alpha(n) - \sum_m \sum_\beta K_{\alpha\beta}(nm)\{U_\beta(n) - U_\beta(m)\} = 0 \qquad (1)$$

where ω is the frequency, M is the atomic mass and K is the effective force constant. When a symbolic notation D is introduced as the dynamical matrix determining the eigenfrequencies of phonons for a fixed configuration of atoms in the system, Eq.(1) may be expressed as $(M\omega^2 - K)U = 0$ or $(\omega^2 - D)U = 0$ where $D = K/M$. When the distribution of atoms in the system is assumed to be homogeneous, the quantity D becomes diagonal with respect to k. Its explicit form is given by

$$\Psi_{\alpha\beta}(k) = \langle (1/N) \sum_n \sum_m D_{\alpha\beta}(nm)[1 - \exp\{-ik(n-m)\}] \rangle \qquad (2)$$

where N is the total number of the atoms in the system. Eq.(2) is easily transformed to be [2],[3]

$$\Psi_{\alpha\beta}(k) = (\delta/M) \int dn g_2(on) K_{\alpha\beta}(on) \{1-\exp(ikn)\} \qquad (3)$$

Here, $g_2(on)$ is the pair correlation function normalized to unity. Also, $\delta = N/V$ is the number density of the atoms in which V is the total volume of the system. It should be noted Eq.(3) reduces to a conventional expression for the dynamical matrix for a crystal lattice if all the atoms in the system are taken to be located at lattice points as given by the following equation,

$$\delta g_2(on) = \sum_m \delta(m-n) \qquad (4)$$

The main objective here is to obtain the qualitative properties of the eigenfrequencies of excitation modes given by Eq.(3). So, the interrelationship between such phonon-like excitations and crystal phonon is examined first. Eq.(3), when combined with Eq.(4), can be reduced to

$$\Psi(k) = (1/M) \sum_m K(on) [1-\exp(ikn)] = D_L(k) \qquad (5)$$

This is the conventional expression for the dynamical matrix for a crystal lattice. In terms of this quantity, we re-express $\Psi(k)$ as

$$\Psi(k) = D_L(k) + \Delta\Psi(k) \qquad (6)$$

As is well known, the eigenvalue of the dynamical matrix $D_L(k)$ is a periodic function of k. Therefore, it vanishes at reciprocal lattice points. The eigenvalues of the matrix $\Delta\Psi(k)$, however, generally remain finite at a lattice point $k=k_0$ in the reciprocal lattice space. Due to this fact, there arises a frequency gap which decreases with increasing local ordering and eventually vanishes in

the limit of complete order corresponding to the crystal lattice.
This result is to be expected from the lack of a kind of selection
rule, since the periodicity of the field is destroyed in our system.
Thus, a dispersion curve for frequencies may have a form as illustrated
in Fig. 1. It may be concluded that a dispersion curve as shown in
Fig. 1 is rather common to phonon like elementary excitations in almost
all types of disordered systems composed of atoms of a single species.
In fact, such a behavior has been observed experimentally for liquid
lead. Several numerical calculations and also the results of
computer simulation of molecular dynamics in classical liquids have
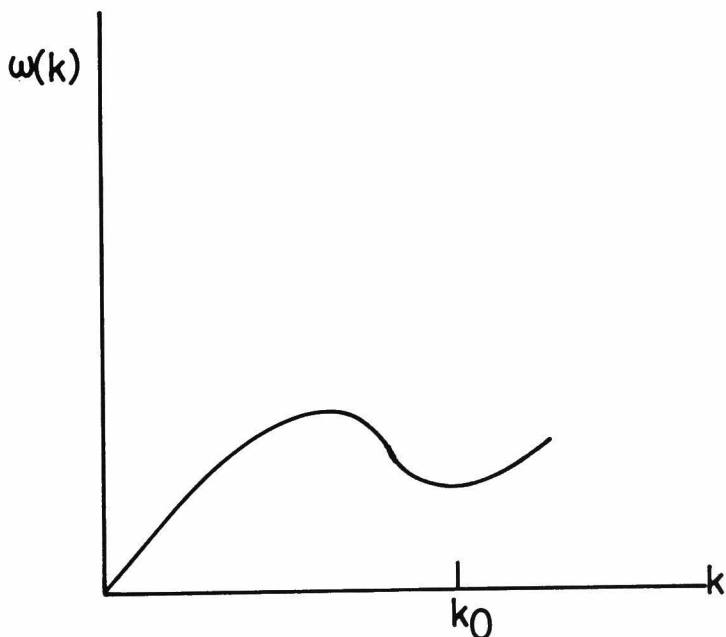given similar results.

Fig.1 Schematic feature of phonon eigenfrequencies
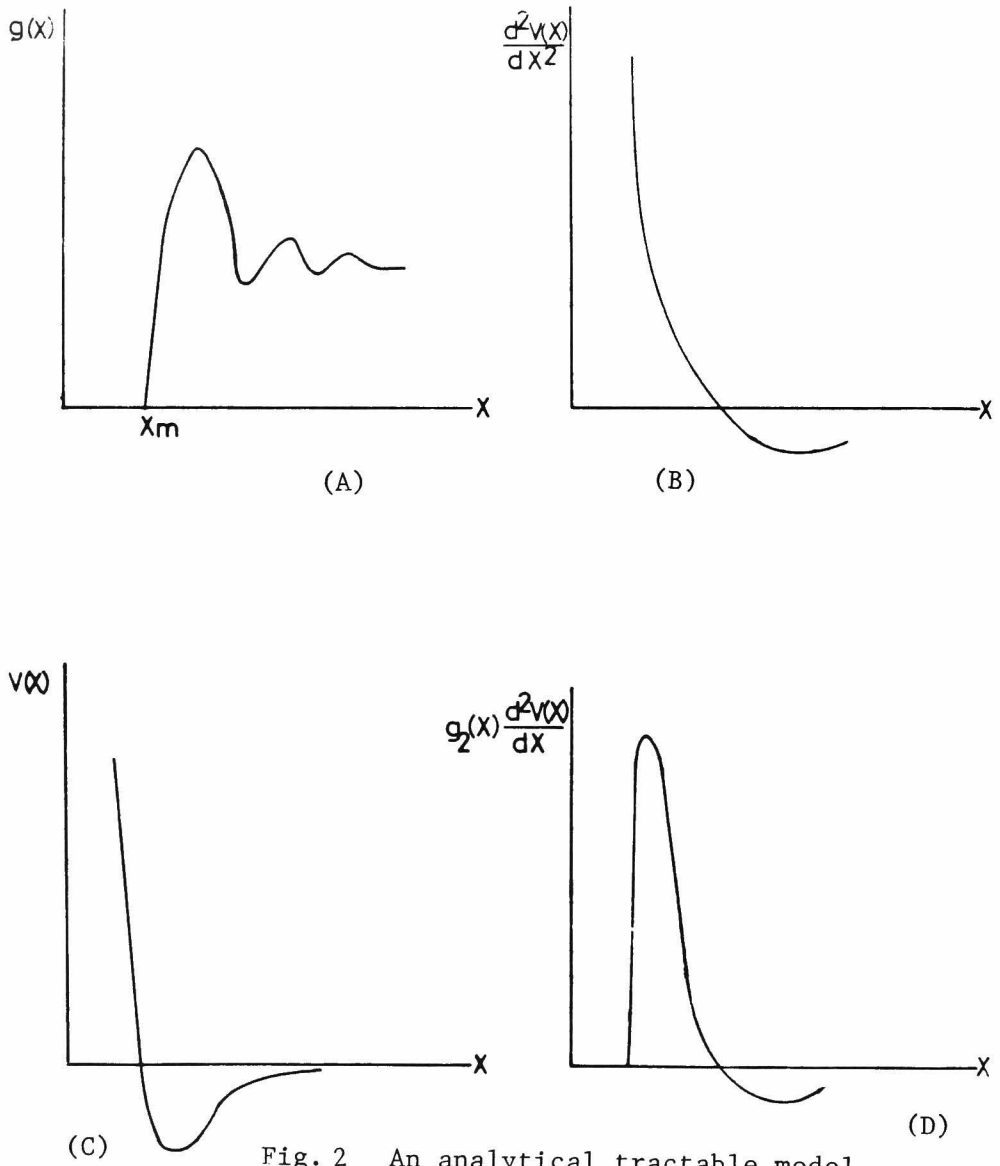$\omega(k)$ in a structure disorder system

Fig. 2　An analytical tractable model

In order to solve Eq.(1) and compare the theory with the experiments, the quantity $g_2(x) \cdot d^2V(x)/dx^2$ has to be expressed by an approximate simple form, which makes the above integral analytically tractable, but contains an essential feature of the disordered system. From a mathematical point of view, the product $g_2(x)V(x)$ or $g_2(x) \cdot d^2V(x)/dx^2$ is very sensitive to the value of $g_2(x)$ at small values of x. In the limit $x \to 0$, $g_2(x)$ vanishes sufficiently fast, so that the product should vanish. Thus, the peak value of the product is obtained for x just above x_m, when x_m is taken to be the smallest value of x for which $g_2(x)=0$. This behavior is illustrated in Fig.2. It is seen that the range of $V(x)$, and the long range behavior of $g_2(x)$ does not affect it. A dominant contribution to the product $g_2(x) \cdot d^2V(x)/dx^2$, therefore, comes from the region around x=a, where a is the average distance of nearest neighbour atoms in this model system. (Fig.3)

With these situations, we may use the following equation,

$$\delta g(x)(d^2v(x)/dx^2)=F(x)=\begin{cases} h^2-b^2(x-a)^2; & \text{for } a-h/b<x<a+h/b \\ 0 & ; \text{ otherwise} \end{cases} \quad (7)$$

The area S occupied by $F(x)$ is $\qquad S=4h^3/3b$

which is taken to be constant. Insertion of Eq.(7) into Eq.(3) we can obtain

$$\omega^2(k)=2K_L/M[1+\frac{3}{2}\{\frac{\sin(kd)}{kd}+\frac{\cos(kd)}{kd^2}-\frac{\sin(kd)}{kd^3}\}\cos(ka)] \quad (8)$$

where d=h/b is the half-width of the curve of $F(x)$. As shown above, Eq.8 can be rewritten as,

$$\omega(k) = [\omega_L(k)^2 + \Delta\omega(k)^2]^{1/2} \qquad (9)$$

Here, $\omega_L(k)^2 = (2K_L/M)(1-\cos(ka))$ is the squared frequency of phonons when the system constitutes a crystal lattice with lattice constant a.

$$\Delta\omega(k)^2 = 2K_L/M[1+3/2\{\frac{\sin(kd)}{kd}+\frac{\cos(kd)}{(kd)^2}-\frac{\sin(kd)}{(kd)^3}\}]\cos(ka)$$
$$(10)$$

This quantity is called here a frequency gap. It is expanded in powers of kd as follows;

$$\Delta\omega(k)^2 = \frac{2K_L}{M} \cdot \frac{3}{2}\sum_p^\infty (-1)^{p-1}(\frac{1}{(2P+1)!}\frac{2P+2}{2P+3}(kd)^{2P}\cos(kd)) \quad (11)$$

Thus, the quantity $\Delta\omega^2$ is shown to be directly connected with the width d. Here, an increase of the local order corresponds to a decrease of d and therefore of $\Delta\omega(k)^2$. Now it is possible to investigate the general behavior of phonon dispersion curves given by this function of k.
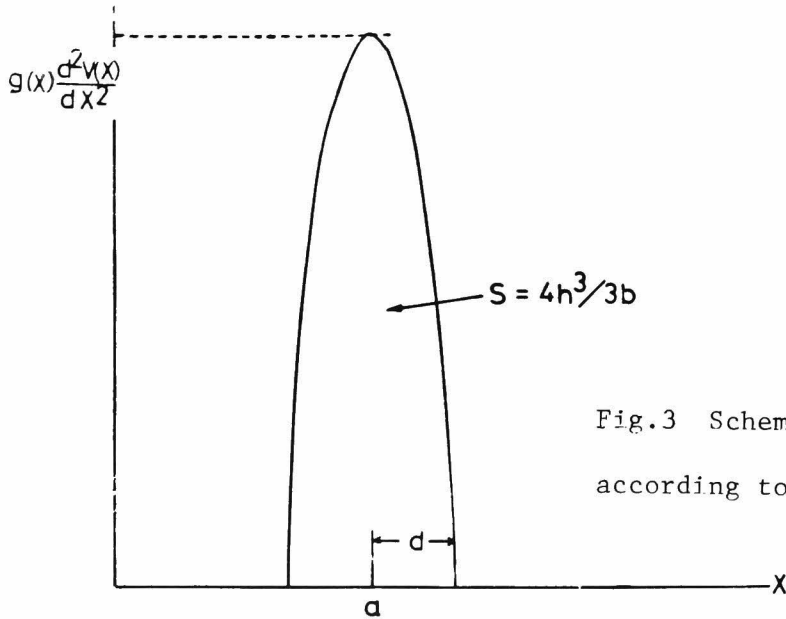

Fig.3 Schematic illustration according to Eq. 10

In the long wavelength region, the contribution of $\Delta\omega(k)^2$ to $\omega(k)^2$ can be neglected as compared with $\omega_L(k)$, and therefore $\omega(k)$ is little different from $\omega_L(k)$. This result is of course to be expected from the Debve theory. In this region, where the continum model holds, phonon dispersion curves are generally insensitive to the microscopic structure of the system. It is particularly interesting in the behavior of $\omega(k)$ near $k=2\pi/a$. It is seen that the phonon eigenfrequencies remain finite in the vicinity of $k=2\pi/a$, due to the presence of the factor $\Delta\omega(k)^2$. It is then shown that the function $\omega(k)$ has a minimum in this region with a gap which decreases as the local order increases. As in the case in Landau equation, let k_0 be the value of k at which such a minimum takes place. We then obtain Taylor's series for $\omega(k)$:

$$\omega(k)=\omega(k_0)+ (1/4\omega(k_0))[d^2\omega(k)^2/dk^2]_{k=k_0}(k-k_0)^2+\cdots \quad (12)$$

$$=\Delta + \{(k-k_0)^2/2\mu\} \quad (13)$$

where $\quad \Delta = \omega(k_0)$

is the frequency gap and $\quad \mu=2\omega(k_0)/[d^2\omega(k)^2/dk^2]_{k=k_0}$

is an effective mass of the elementary excitations.

This equation is the same as the Landau formula for elementary excitations in liquid helium.

Now the explicit expressions for k_0, Δ and μ defined above are obtainable. For this purpose, Eq.11 is approximated by

$$\Delta\omega(k)^2=(2K_L/M)\{(1/5)(kd)^2-(3/280)(kd)^4+\cdots\}\cos(ka) \quad (14)$$

$$=(2K_L/M)(1/5)(kd)^2\cos(ka)$$

By inserting this into Eq.8, an approximate value of k_0 is

$$k_0 a = 2\pi - (4\pi/5)(d/a)^2/[1-\{4\pi^2/5)+(2/5)\}(d/a)^2] \qquad (15)$$

$$= 2\pi - (4\pi/5)(d/a)^2/[1-(4\pi^2/5)(d/a)^2]$$

$$\Delta = (2/5)^{1/2}\omega_L(d/a) \qquad (16)$$

$$\omega_L^2 = 4K_L/M$$

is the maximum eigenfrequency of phonons in the case of the crystal lattice. A similar procedure yields an approximate result

$$(d^2\omega(k)^2/dk^2)_{k=k_0} = 1-(4\pi^2/5)(d/a)^2 \qquad (17)$$

From Eq.13, it becomes

$$\mu = 16\pi(d/a)/[5^{1/2}\omega_L a^2] - (4\pi^2/5)(d/a)^2 \qquad (18)$$

By eliminating the factor ω_L from Eq.16 and 18, the relationship between Δ and μ becomes,

$$\mu = (8\pi(d/a)^2/5)[\Delta a^2\{1-(4\pi^2/5)(d/a)^2\}] \qquad (19)$$

It is seen that the value of μ decreases as d/a decreases or the local order increases. The results of numerical calculations of phonon dispersion curves as given by Eq.8 are plotted in Fig.4, for d/a = 0.1, 0.2, 0.3, 0.4, 0.5 and 0.6.

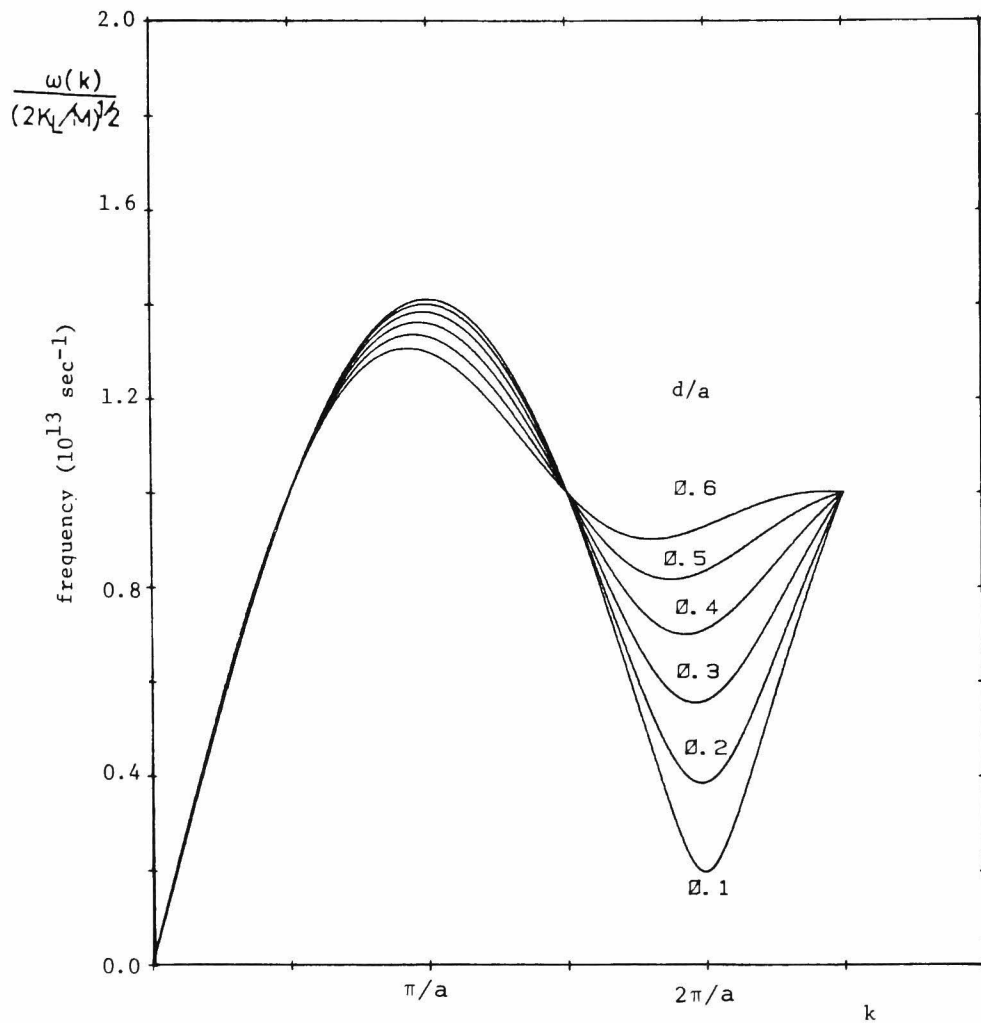This figure shows how phonon dispersion curves are modified as the local order changes.

Fig. 4   Phonon eigenfrequencies in a model structure
          disordered system for various values of d/a.

2.2   Frequency Spectrum and Low Temperature Specific Heat

It has become increasing clear that the low temperature specific
heat of solids in the glassy phase is   larger   than in crystal.
This difference is often referred to as an excess specific heat and
expressed by a term linear in temperature after Zeller.[4],[5] To get a
clear picture of it, the existing data were analyzed by the formula
$Cv = C_1 T + C_3 T^3$, and are shown as C/T vs T^2 in Fig.5. The existence
of $C_1 T$ term seems a characteristic of glassy state and insensitive
to structural detail of glass. Fulde and Wagner[6] have proposed a
model in noncrystalline solids which can account for the low temper-
ature anomalies in the specific heat of amorphous solids. Anderson[7]
has proposed an possible model where atoms occupy equally in
different equilibrium positions.

In the previous section, phonon dispersion curve was obtained
for a homogeneous but structurally disordered system like liquid
helium. In this section, it is tried to show that the phonon modes
based on such a simple system can yield an extra phonon density of
states in the low frequency region, which can account for the above
mentioned anomalies in the low temperature heat capacity of non-
crystalline solids.

As obtained in section 2-1, the dynamical matrix $\Psi(k)$ giving
the phonon eigenfrequencies as a function of wave vector k in a
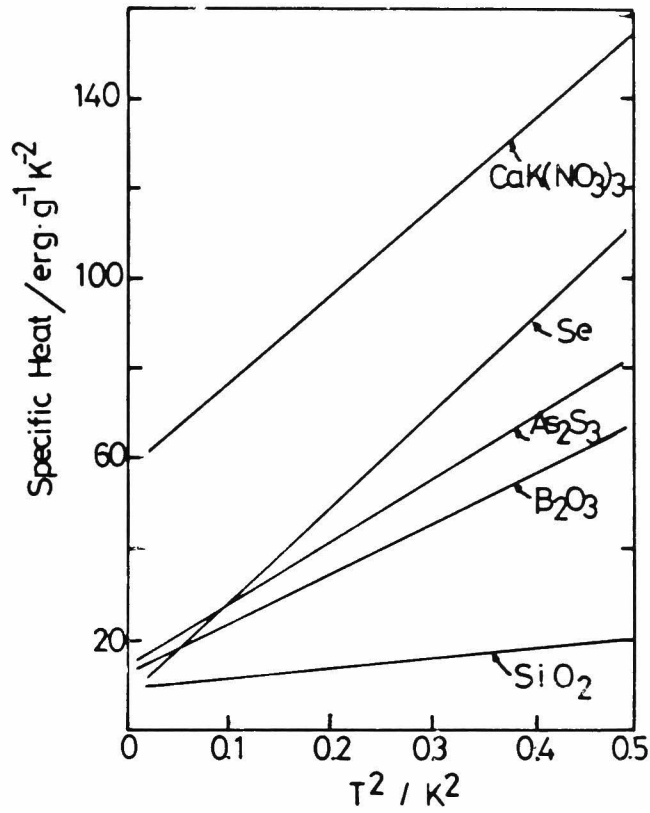non-crystalline solid composed of atoms of a single species is given by

Fig. 5 The low temperature specific heat
for various glasses

$$\Psi(k) = \omega(k)^2 = (2\delta/M) \int_0^\infty dx\, g_2(x)\, (d^2 v(x)/dx^2)\{1 - \cos(kx)\} \quad (20)$$

Let $\omega(k)$ be the eigenfrequency of such phonon modes with imaginary part $\Gamma(\omega^2)$.

Within the framework of the harmonic approximation, the factor arises if we take into account higher order correlations other than pairs. Then its contribution to the frequency spectrum $\delta(\omega)$ can be expressed in the form

$$\delta(\omega) = (2\omega/\pi) \, \mathrm{Im}\left[\int \frac{f(k)\, dk}{\Omega^2 - \omega(k)^2} \right] \quad (21) \qquad \Omega^2 = \omega^2 - i\Gamma(\omega^2)$$

where $f(k)dk$ is the number of modes between k and $k+dk$ and $\mathrm{Im}[A]$ denotes the imaginary part of A. In the case of crystal lattice, the quantity $f(k)$ is nonzero and becomes $V/(2\pi)^3$ only in the first Brillouine zone, where V is the volume of unit cell. In our case, however, such a relation can no-longer be used since the conventional reduced-zone scheme does not hold. In the followings, it is assumed that both of $\omega(k)$ and $f(k)$ are spherically symmetric. This approximation is equivalent to assuming the pair correlation function to be spherically symmetric. Thus only those correlations which exist in the case of simple liquids are taken into account. Although this is a zero order approximation for glassy state, there exist some experimental indications that the structure factor of several simple substances in non-crystalline phase is not very different from that in liquid phase. Eq.21 reduces to

$$\delta(\omega) = 8\omega \text{ Im}[\int_0^\infty \frac{f(k)k^2 dk}{\Omega^2 - \omega(k)^2}] \qquad (22)$$

Insertion of Eq.13 in the previous section into Eq.22 gives

$$\delta^{(r)}(\omega) = 8\mu\omega\text{Im}[\int_0^\infty dx \frac{f(k+k'(x))(k+k'(x))^2 + f(k-k'(x))(k-k'(x))^2}{(\Omega^2 - x^2)k'(x)}$$

$$(23)$$

$$k'(x) = [2\mu(x-\Delta)]^{1/2} \qquad (24)$$

where r denotes the roton-like part of the frequency spectrum.
In view of the fact that in the case of a crystal lattice f(k) is
step function with a cut-off wave vector corresponding to the first
reciprocal lattice vector k, we take f(k) as shown in Fig. 6
It should be noted that the uncertainty Δk in wave number k in
disordered systems increases as k increases and that the integrated
value of f(k) over the whole wave number space must be equal to the
total number of atoms in the system.

The expansion of the function $f(k \pm k')$ in Taylor's series gives

$$f(k+k') = f(k) + f'(k) k' + \cdots\cdots \qquad (25)$$

By combining Eq.25 with Eq.24, it becomes

$$\delta^{(r)}(\omega) = 16\mu\omega k^2 f(k) \text{ Im}[\int dx \frac{1}{(\Omega^2 - x^2)k'(x)}]$$

$$+ 16\mu\omega\{f(k) + 2k(\partial f/\partial k)\}\text{Im}[\int \frac{k'(x)}{\Omega^2 - x^2} dx]$$

$$= \delta_1^{(r)}(\omega) + \delta_2^{(r)}(\omega) \qquad (26)$$

Without detail calculations, the qualitative property of $\delta^{(r)}(\omega)$
can be obtained. By setting $\Gamma(\omega^2)$ equal to zero, Eq.24 reduces to

$$\delta^{(r)}(\omega) = \frac{16\mu\omega k f(\omega)}{[2\mu(\omega-\Delta)]^{1/2}}$$
$$+16\mu\omega\{f(k)+2k(\frac{\partial f(k)}{\partial k})\}[2\mu(\omega-\Delta)]^{1/2}$$
$$= \delta_{10}^{(r)}(\omega) + \delta_{20}^{(r)}(\omega) \qquad (27)$$

Introduction of the imaginary part would generally modifies the spectrum as shown in Fig.7. It also modifies the second term, but this modification is not so pronounced as compared with that due to the first term. The same result could be obtained by analogy of the energy spectra of electrons or phonons in disordered system. As seen from Fig.7, thus the behavior of $\delta^{(r)}(\omega)$ is almost constant in the vicinity of $\omega=\Delta$. The above result, when combined with the formula for the specific heat,

$$\Delta Cv^{(r)} = k_B\int d\omega \delta^{(r)}(\omega)(\frac{h\omega}{k_BT})^2 \frac{\exp(\hbar\omega/k_BT)}{[\exp(\hbar\omega/k_BT)-1]^2}$$
$$= (k_B/\hbar)T\int dx \delta^{(r)}(\frac{k_BT}{\hbar}x) \frac{x^2 e^x}{(e^x-1)^2} \qquad (28)$$

gives an excess specific heat $\Delta Cv^{(r)}$. Here, k_B is the Boltzmann constant and $\hbar$ is the Planck constant divided by 2π. The result obtained here depends on the frequency gap Δ in the phonon dispersion curve, and characterizes the local ordering in disordered systems.

As described above, the result by Zeller and Pohl shows that the specific heat of non-crystalline solids at very low temperatures is proportional to T. This proportionality can be obtained from the present model. It is seen from Fig.7 that the excess frequency
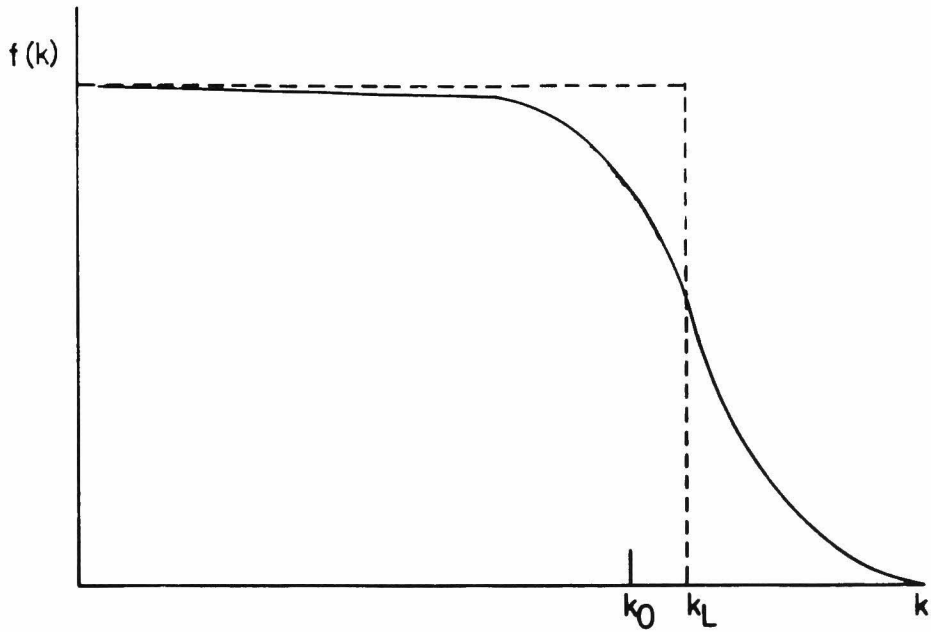
Fig. 6   Schematic behavior of the wave-number distribution
         function f(k).   The dotted line corresponds to
         the case of a crystal lattice

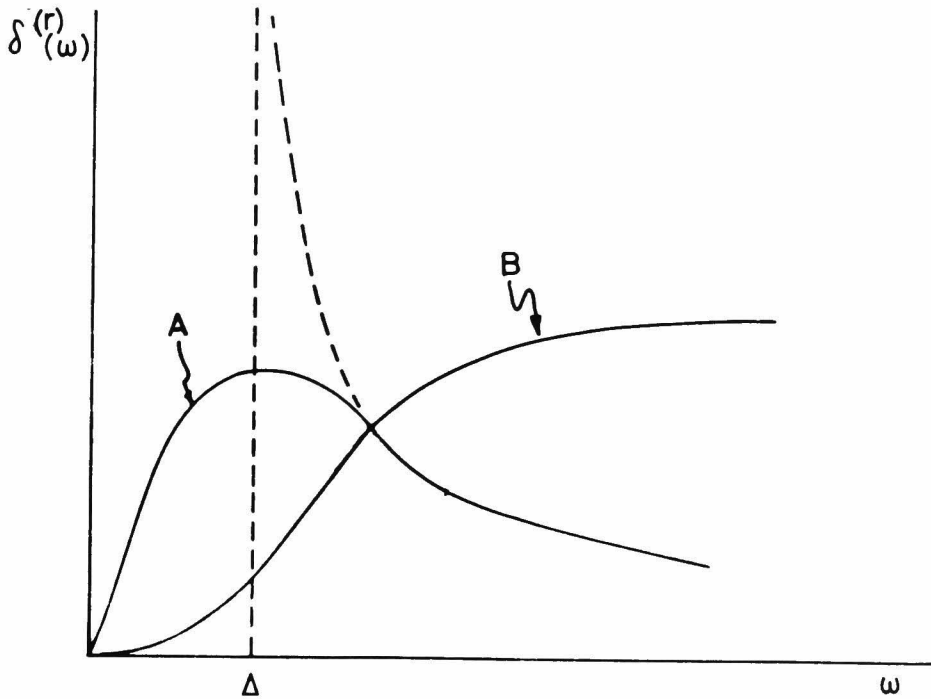Fig. 7   Schematic behavior of $\delta^{(r)}(\omega)$.
         Curves (A) and (B) represent $\delta_{10}^{(r)}(\omega)$
         $\delta_{20}^{(r)}(\omega)$

spectrum $\delta^{(r)}(\omega)$ is almost independent of ω above and in the vicinity

of Δ.   So, $\delta^{(r)}(\omega)$ can be approximated by

$$\delta^{(r)}(\omega) = \left\{ \begin{array}{ll} A\omega^n, & \omega < \omega_1, \\ A\omega_1^n, & \omega > \omega_1, \end{array} \right. \quad (n>1) \qquad (29)$$

where A is a constant. The quantities n and ω_1 are a positive

number greater than unity and a constant close to but smaller than Δ

, respectively. These values characterize the behavior

in the close vicinity of $\omega=0$ and $\omega=\Delta$,respectively. By putting Eq.29

into Eq.28, it becomes

$$\Delta C_v^{(r)} = (k_B^2/h) A\omega_1^n \, T \int_0^{\Theta/T} \frac{x^2 e^x}{(e^x-1)^2} \, dx \; + \; (k_B^2/h) AT \qquad (30)$$

$$x \int_0^{\Theta_4/T} [(\frac{k_B T}{h})^n \, x^n \; - \; \omega_1^n] \frac{x^2 e^x}{(e^x-1)^2} \, dx \; , \qquad \Theta_4 = h\omega/k_B$$

and Θ is a temperature corresponding to a cutoff frequency of $\delta^{(r)}(\omega)$

in the region $\omega > \omega_1$. At very low temperatures the quantity Θ/T can be

taken to be infinity. Thus, the first term of Eq.30 gives an excess

specific heat proportional to T. The second term depends on Θ_4 and n.

For liquid helium, the roton minimum in unit of degree Kelvin is

about 8K. In view of possible ordering in noncrystalline solids

higher than in the case of liquid helium, the quantity Θ_4 may be

smaller than 5K. For a sufficiently small value of Θ_4, the second

term in Eq.30 can be neglected in comparison with the first term.

Thus, the low temperature specific heat is expected to be linearly

dependent to absolute temperature. The validity of this result will

be checked in Chapter 4.

2.3   Low temperature thermal expansion and Grüneisen parameter

        deriving from the present simple model

Generally, a material expands on heating because the atomic

configuration corresponding to the minimum free energy changes with

temperature. The contribution to the free energy arises not only

from the potential energy of the atoms in the lattice but also from

their kinetic energy of vibration. In Grüneisen's theory of thermal

expansion, the vibrational frequencies of a solid are assumed to be

dependent upon the interatomic separation and hence upon the volume.

When the behavior of the jth mode of vibration is conveniently

described by a dimensionless parameter, the Grüneisen parameter is

expressed by the equation, $\gamma_j = -d\ln\omega_j/d\ln V$ (31)

where ω_j is the vibration frequency of the jth mode and V is the

volume. Since vibration frequencies normally decrease as the

volume increases, the constant γ_i is positive.

When no external stress exist,   the condition for minimum free

energy, $\frac{dF}{dV} = 0$, leads to the relation, $dU/dV = 1/V \sum_j \gamma_j E_j$ (32)

where U is the potential energy and E_i the vibrational energy of the

jth mode. At very low temperatures, E_j is small so that $\frac{dU}{dV} = 0$;

i.e., the volume corresponds to the minimum of the potential

energy-volume curve. At higher temperatures, the larger values of

E_j require that $\frac{dU}{dV}$ become finite and positive, which is consistent

with a volume greater than that appropriate to the minimum of the

potential energy curve.

$- 25 -$

Grüneisen made the simplifying assumption that all the vibrational

modes of a solid react in the same way to a change in volume and

this equation is $\alpha = \gamma C_v \beta / V$, where α is the coefficient of volume

expansion of the solid, β the compressibility and Cv the specific

heat. Since all frequencies are not equally affected by a change in

volume, the Grüneisen equation becomes $\alpha = \beta/V \cdot \sum_j \gamma j \; dE_j/dT$ (33)

For an ideal Debye solid, $^{(8)}$ the frequency spectrum is a function of

$f(\nu) = a \nu^2$, and is cut off at a maximum $\nu_m = k\Theta/h$.

At this condition, γi is equal to γ or $-\dfrac{d\ln \nu_m}{d\ln V}$, which is constant.

In a real solid, γ becomes constant at higher temperatures

($\gamma = \gamma_\infty$ where $T > \Theta$) or at very low temperatures

($\gamma = \gamma_0 = -\dfrac{d\ln\Theta_0}{d\ln V}$ where $T < \Theta$).

This constancy has been proved for a number of crystalline solids.

Furthermore, the difference between γ_0 and γ_∞ is generally small.

For example, the experimental curve for copper after Barron shows

that $\gamma_\infty - \gamma_0 < 0.3$.

As described above, a number of glasses, particularly silicate

glasses with low alkali contents have negative values of thermal

expansivity at low temperatures. Two examples are shown in Fig.8.

From the above definition of $\gamma = \alpha V/\beta Cv$, the Grüneisen parameter must

become negative for these glasses, because other quantities V, β

and Cv are always positive. On the other hand, almost all glasses

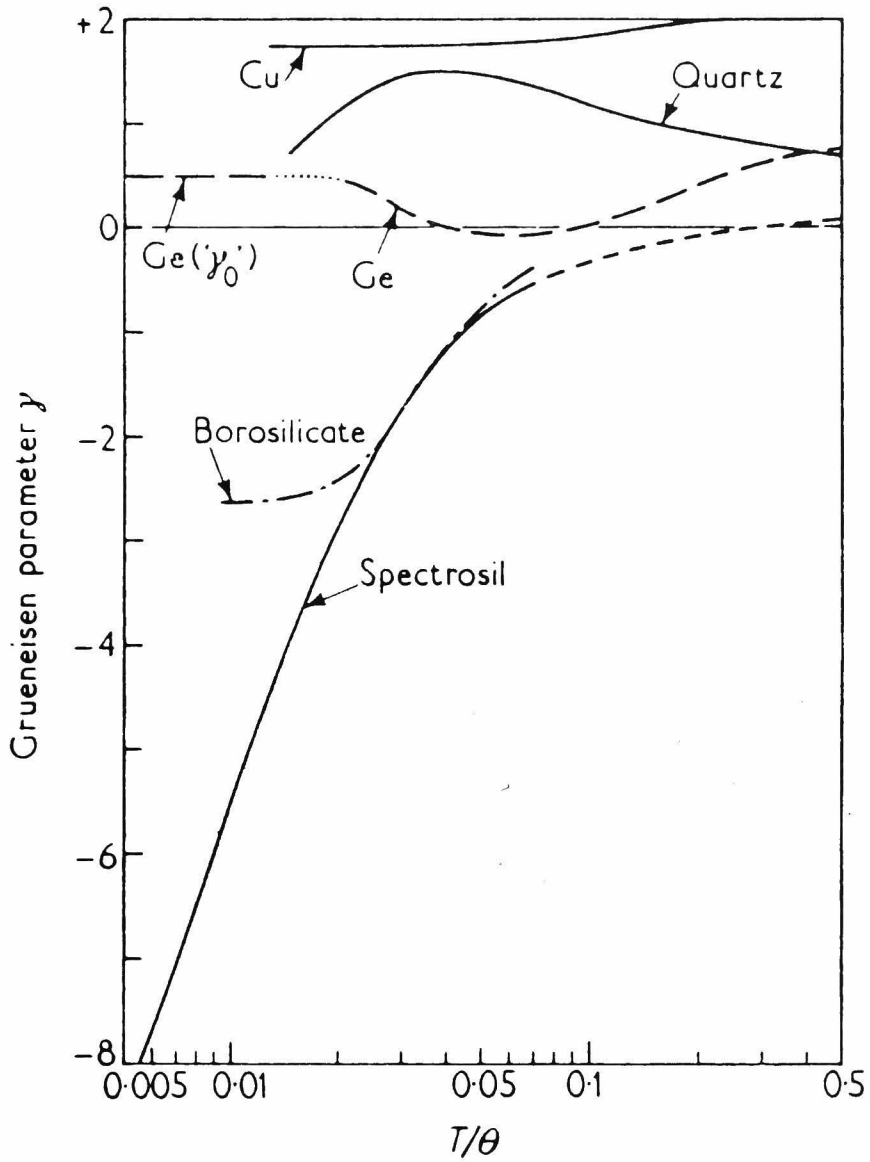have positive thermal expansion, and thus a positive Grüneisen

Fig.8 Variation of $\gamma = \beta V / C\chi$ with reduced temperature
T/Θ. Values of Θ are 340K (Cu), 600K (quartz),
380K (Ge) and 310K (borosilicate).
These data are from the following sources. (9)

parameter. Although various investigators have attempted to explain such variation in expansivity or Grüneisen parameter with temperature or composition from a structural point of view, no clear explanation has not been presented yet.

At any rate, whenever a model of glassy state is proposed, the model should show such a wide variation in thermal expansion or Grüneisen parameter from a negative to a positive value depending upon glass composition and temperature. So, it is attempted here to see whether the present simple model systems developed in the previous section satisfy this condition or not.

Since V is proportional to L^3, the Grüneisen parameter can be expressed in terms of ω and L by

$$\gamma = -\frac{d\ln\omega}{d\ln V} = -\frac{d\omega}{\omega} \Big/ \frac{dV}{V} = -\frac{V}{\omega} \cdot \frac{d\omega}{dL} \cdot \frac{dL}{dV} = -\frac{L}{3\omega}\frac{d\omega}{dL} \quad (34)$$

This indicates that the Grüneisen parameter can be calculated when the variation of ω with L is known. According to the results obtained for the present analytically tractable model system in section 2.1, ω can be expressed by

$$\omega = const. \left(\frac{d}{a}\right) + \frac{(k-k_0)^2}{2\mu} \quad (35)$$

where a is the average distance of nearest neighbour atoms and d is the half-width of the curve of $F(x)$, which specify the local order of the system. The above two equations give,

$$\gamma = -\frac{L}{3}\frac{1}{\omega}\frac{d}{dL}\left(\frac{d}{a}\right) = -\frac{L}{3a^2\omega}\left\{ a\frac{dd}{dL} - d\frac{da}{dL} \right\} \quad (36)$$

This equation shows that the behavior of depends on the variation

in d and a with respect to L, and that γ becomes negative when the
first term in parenthesis, involving the change in d with respect to
L, is larger than the second term involving the change in a with L.
However, the effects of composition and temperature on a and d can
not be given at this moment, further discussion based on Eq. 36 is
not possible.

In order to overcome this difficulty, an assumption is made that
the quantity $\beta=d/a$, which represents the "randomness" of the
disordered system, can be expressed as AL^N. This choice is based on
the fact that the equations can be analytically solved without any
other assumption, yet retain the characteristic feature of the model
described in the previous section. Qualitatively speaking, the
disorder existing in the supercooled glassy state becomes less as
temperature is raised. Thus, it may be considered that N is related
to $1/T$. By using this equation $\beta=AL^N$ and differentiating the disper-
sion equations in Chapter 2.1 with respect to L, the following
equation can be obtained for γ.

$$\text{(37)}$$

$$\gamma = \gamma_L + \frac{N}{2} \frac{[\ 1/(2\pi\beta)^2 + \sin(4\pi\beta)\{1/(2\pi\beta)+1.5/(2\pi\beta)^3\}]}{[1+3\{\cos(2\pi\beta)/(2\pi\beta)^2-\sin(2\pi\beta)/(2\pi\beta)^3\}\cos(2\pi\beta)]}$$

The results of the numerical calculations for different values of β
and N are shown in Fig. 9. In this figure, the Lennard-Jones
potential is assumed as the interatomic forces. The crystalline
state, in which no variation in force constant exists, shows a

constant value of $\gamma=0.5$ for any k. The glassy state, on the other
hand, shows a large variation in γ with k, as given in Fig.9.
As observed in this figure, the energy density is highest at near
$2\pi/a$. Thus, in order to see the variation in γ with β and N, the
values of γ at $2\pi/a$ are plotted in Fig.10 as a function of β (=d/a)
with at constant N. Since β is defined as the randomness of the
disordered system and thus is considered to be dependent on glass
composition, this figure gives the effect of glass composition on
γ at constant N. The same data are plotted in Fig.11 as a function
of N at constant β. Since N is related to 1/T, this figure gives
the effect of temperature on γ. From this figure, it is clear that
γ becomes negative at low temperature easily for a glass having a
large degree of randomness, while γ stays positive for a glass
having only a minute degree of randomness even at extremely low
temperatures. This result will be applied to interpret the experi-
mental data in Chapter 4.
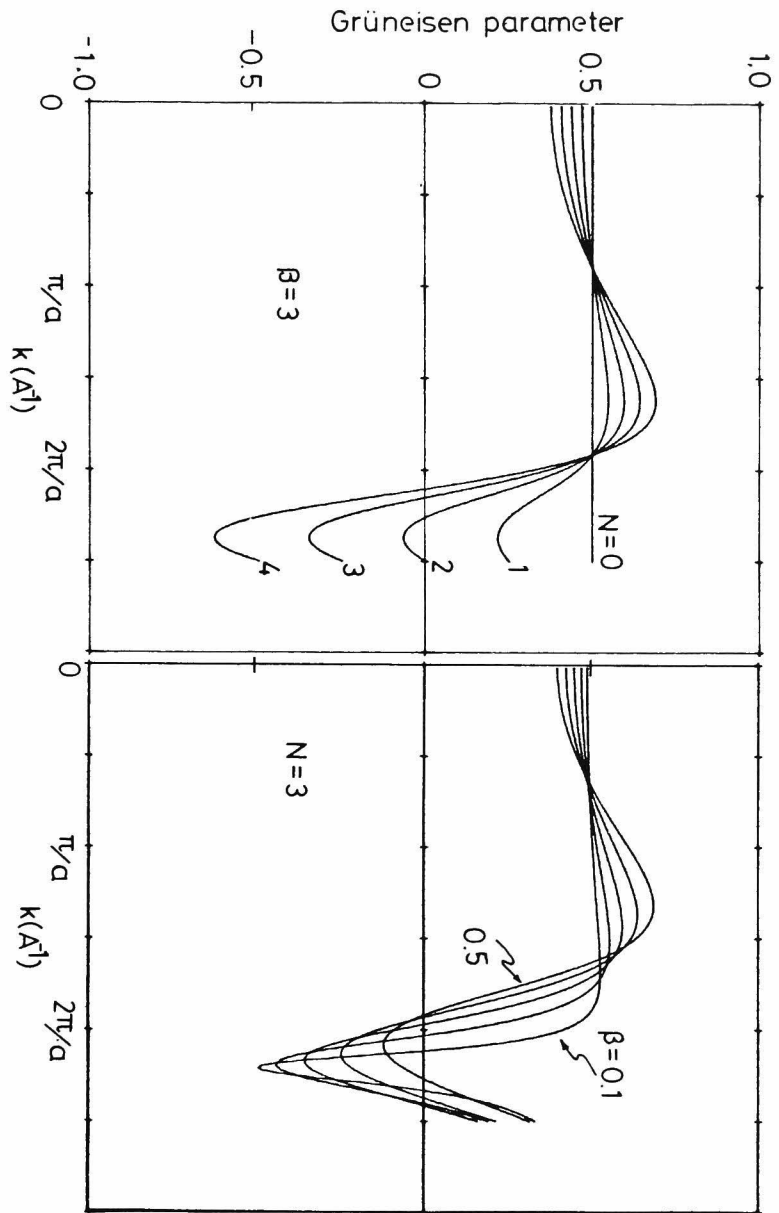
Fig.9 Grüneisen parameter as a function of N and β
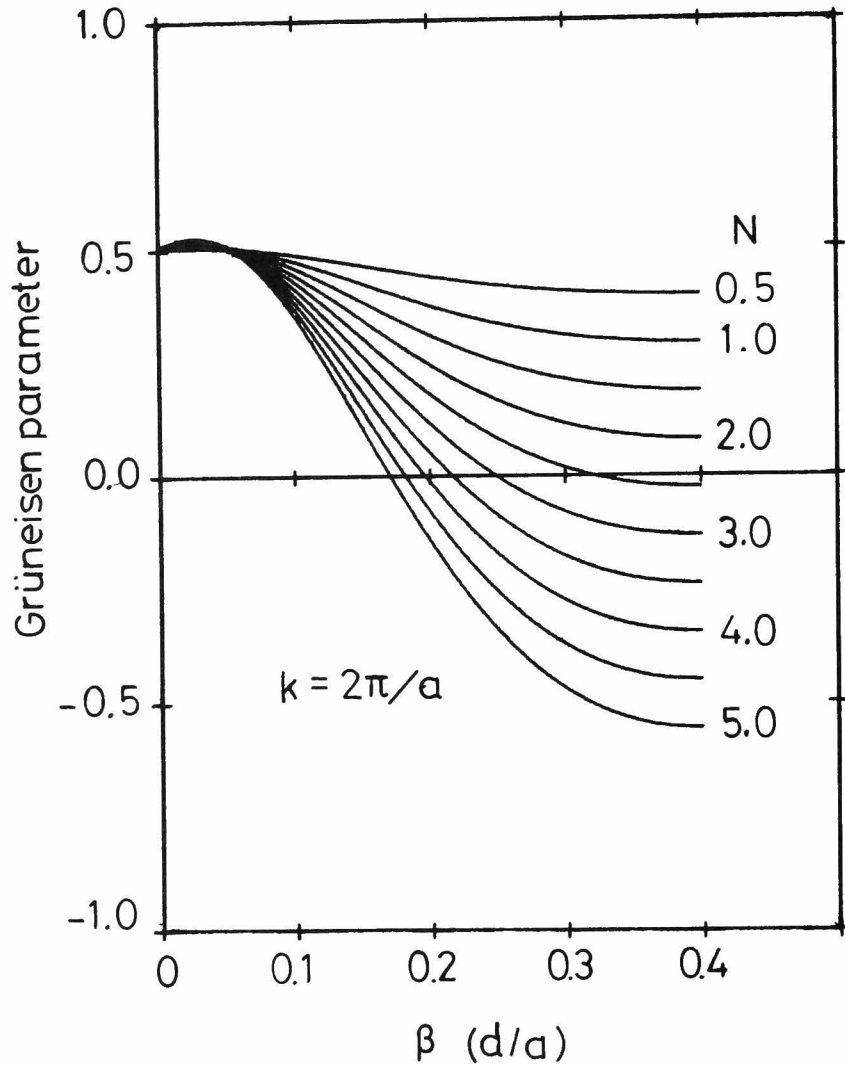
Fig.10 The variation of Grüneisen parameter at k=2π/a
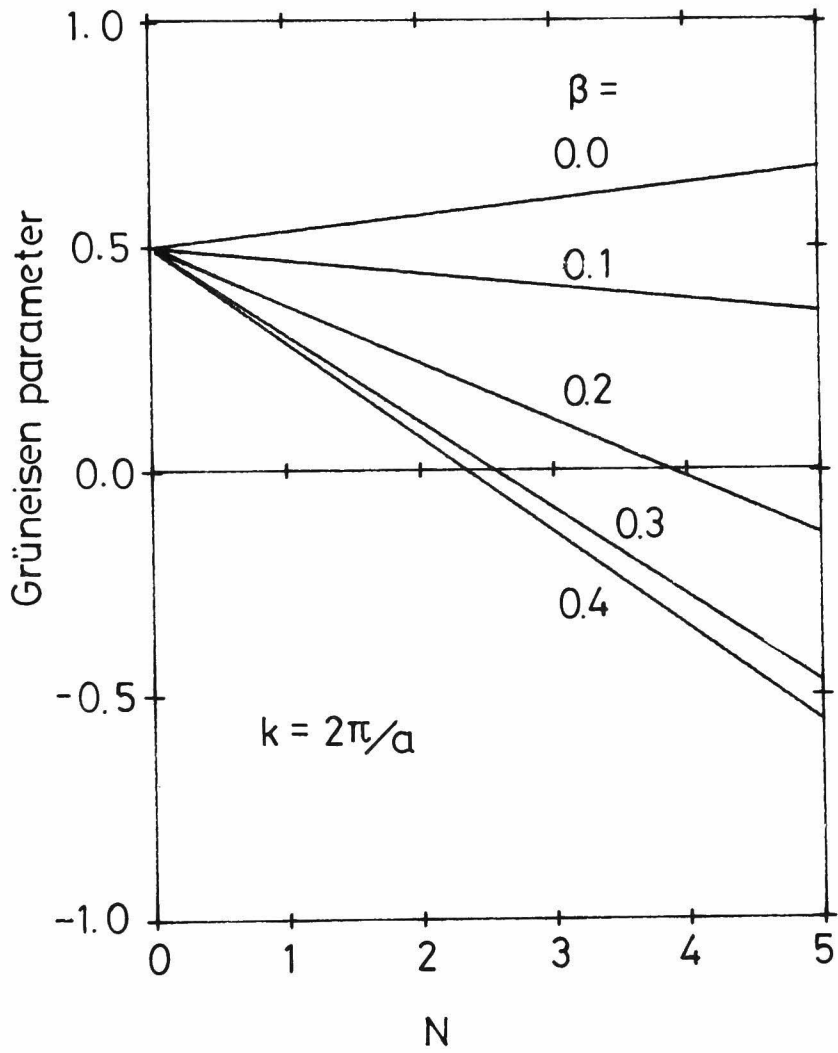
Fig.11 The variation of Grüneisen parameter at k=2π/a

2.4   Problems associated with application of the present

        simple model to complicated glass systems

As described in the previous section, the phonon dispersion

curve for a disordered system is different from that of an ordered

system at low temperatures. However, at high temperatures, the

contribution due to such disorder to the total heat capacity becomes

very small and the continuum model of specific heat applicable to

crystals is suitable also for simple glasses as expected from the

analytically tractable model treated in the previous section.

In this case, the frequency distribution function of the vibrations

can be assumed to follow the Debye model where 3N frequencies from

zero to some ν_m are picked out of the infinite frequency spectrum

of the continuum vibrations. By introducing this limiting maximum

frequency ν_m, Debye's theory takes into account the atomic nature

of the structure of solids, but it assumes that the continuum is

isotropic and the propagation velocity of elastic waves does not

depend on direction. In this sence, the glassy state is an ideal

case. Then the thermal energy of a solid is taken to be the sum of

the energies of 3N waves corresponding to the excitation of the

energy levels of the lattice with frequencies from 0 to ν_m.

Although the continuum model of specific heat is only a first

approximation, it turned out to be very fruitful, mainly due to the

fact that in this theory separate energy levels are ascribed to the

normal modes of the lattice as a whole and not to vibrations of the
individual atoms. By using the simple frequency distribution func-
tion, Debye obtained the following equations for the vibrational
energy of a solid and the specific heat

$$U = \int_0^{\nu_m} \varepsilon \, ds = 9N/\nu_m^3 \int_0^{\nu_m} \frac{h \nu^3 \, d\nu}{e^{h\nu/kT} - 1} \qquad (38)$$

$$U = 3RT \cdot 3 \left(\frac{\Theta}{T}\right)^3 \int_0^{\Theta/T} \frac{x^3}{e^x - 1} \, dx \qquad (39)$$

$$Cv = 3R \left[12 \left(\frac{\Theta}{T}\right)^3 \int_0^{\Theta/T} \frac{x^3 \, dx}{e^x - 1} - \frac{\Theta/T}{e^{\Theta/T} - 1} \right] \qquad (40)$$

where, $\quad h\nu_m/kT = \Theta/T \; ; \quad h\nu/kT = x$

Debye's theory has been applied successfully to describe the
temperature dependence of specific heat in a number of solids.
The fact that the characteristic temperatures of a simple solid
determined from Debye's theory coincide with those obtained from
elastic constants and other methods have proven the validity of
Debye's model. However, recent experimental and theoretical work
have disclosed that Debye's theory is not precise enough to a number
of solids. They include organic and inorganic high polymers having [10]-[17]
chained or layered structures with metallic, ionic, covalent or
hydrogen bonds in both crystalline and amorphous state. This means
that the simple model described in the previous section is not

precise enough to describe the thermal behaviors of more complicated glasses quantitatively even at high temperatures, because the simple modes involve only one characteristic temperature. Thus the simple model has to be modified to take care the change in vibrational frequency spectrum for complicated glasses in which chained or layered structures may exist.

It has been known that specific heat is very sensitive to the structural features of solids, or to the way in which atoms and molecules are bound each other. For example, the specific heats of diamond and graphite, which are different modifications of the same substance, differ approximately by a factor of 7 at about 100K and by a factor of 23 at 50K. A similar difference exists also between red and black phosphorus, or between rhombic and monoclinic sulfur. Moreover, the specific heat of graphite does not obey Debye's T^3 law exactly. It is clear that the frequency distribution of the eigenvibrations is different from that of Debye's theory and that the frequency distribution function of the model must contain the spectra arising from such structural features of a solid.[18),19)]

The contribution of such structural features may be obtained by considering the existence of macromolecules with chain-like or layer structures, as treated by Tarasov. Let us assume first that a solid is composed of a large number N of atoms which do not interact with each other. On the basis of the Debye assumption,

the vibrational state of a linear chain of atoms can be represented as eigen vibrations of a one dimensional continuum. By introducing a cut off frequency in the vibrational spectrum to account for the discrete atomic structure of the chain molecule, the number of frequencies dS_1 in the interval $(\nu, \nu+d\nu)$, becomes,

$$ds_1 = g_1(\nu) d\nu = 3N \nu_m^{-1} d\nu \qquad (41)$$

where N and ν_m are taken to satisfy the following condition.

$$\int_0^{\nu_m} g(\nu_1) d\nu + 2\int_0^{\nu_m} g(\nu_t) d\nu = 3N \qquad (42)$$

This separate writing of the frequency distribution functions for different directions of polarization, and therefore of the specific heat relations, is due to the fact that the longitudinal and transverse vibrations can have entirely different frequencies for the same wavelength. For a two dimensional network of atoms, the number of frequencies dS_2 in the interval $(\nu, \nu+d\nu)$, becomes,

$$g_2(\nu) d\nu = 6N \nu_2^{-2} \nu d\nu \qquad (43)$$

When generalized, the waves of one direction of polarization in p-dimensional continuum can be expressed.

Polarization in an p-dimensional continuum can be expressed by

$$g_p(\nu) d\nu = pN \nu_m^{-p} \nu^{p-1} d\nu \qquad (44)$$

The distribution of eigenvibrations of a p-dimensional continuum (p=1,2 or 3), and the Plank-Einstein expression for the mean energy per degree of freedom yield

$$U_p = \int_0^{V_m} h\nu(\exp\tfrac{h\nu}{kT} - 1)^{-1} pN\nu_m^{-p} \nu^{p-1} d\nu \quad (45)$$

for waves of one direction of polarization, and a total energy of

$3U_p$, assuming elastic isotropy and taking the mean value of ν_m.

Setting, as before,

$$x = \frac{h\nu}{kT} \quad \text{and} \quad \Theta_m = \frac{h\nu_m}{kT}$$

we obtain

$$U_p = pR\frac{T^{p+1}}{\Theta^p} \int_0^{\Theta/T} \frac{x^p dx}{e^x - 1} \quad (46)$$

Differentiating, we find from dU_m/dT, the specific heat

$$C_p = p(p+1)R\left(\frac{T}{\Theta}\right)^p \int_0^{\Theta/T} \frac{x^p dx}{e^x-1} - pR\frac{\Theta}{T}\left[\exp\frac{\Theta}{T} - 1\right]^{-1} \quad (47)$$

Taking, as in Debye's theory, some average value of the characteristic

temperature for the longitudinal and transverse vibrations, the total

specific heat for all the 3N modes is effectively threefold the above

value.

$$C_p = 3p(p+1)R\left(\frac{T}{\Theta}\right)^p \int_0^{\Theta/T} \frac{x^p dx}{(e^x-1)} - 3pR\frac{\Theta}{T}\left[\exp\frac{\Theta}{T} - 1\right]^{-1} \quad (48)$$

Integrating-by-parts as we did in deriving (40), this boils down to

$$C_p = 3pR\left(\frac{T}{\Theta}\right)^p \int_0^{\Theta/T} \frac{x^{p+1} e^x}{(e^x-1)^2} dx \quad (49)$$

This yields in the three possible cases.

a) Debye's three-dimensional continua

$$p=3; \quad D_3\left(\frac{\Theta_3}{T}\right) = 9R\left(\frac{T}{\Theta_3}\right)^3 \int_0^{\Theta/T} \frac{x^4 e^x dx}{(e^x-1)^2} \quad (50)$$

b) layers or two-dimensional continua

$$p=2; \quad D_2\left(\frac{\Theta_2}{T}\right) = 6R\left(\frac{T}{\Theta_2}\right)^2 \int_0^{\Theta/T} \frac{x^3 e^x dx}{(e^x-1)^2} \quad (51)$$

c) chains or one-dimensional continua

$$p=1; \quad D_1\left(\frac{\Theta1}{T}\right)=3R\left(\frac{T}{\Theta_1}\right)\int_0^{\Theta/T}\frac{x^2 e^x dx}{(e^x-1)^2} \quad (52)$$

When the equation $e^{x/2}-e^{-x/2}=2\sinh(x/2)$ is used,

a) $$p=3; \quad 36R\left(\frac{T}{\Theta_3}\right)^3\int_0^{\Theta/T}\left(\frac{x}{2}\right)^4 sh^{-2}\left(\frac{x}{2}\right)dx \quad (53)$$

b) $$p=2; \quad 12R\left(\frac{T}{\Theta_2}\right)^2\int_0^{\Theta/T}\left(\frac{x}{2}\right)^3 sh^{-2}\left(\frac{x}{2}\right)dx \quad (54)$$

c) $$p=1; \quad 3R\left(\frac{T}{\Theta_1}\right)\int_0^{\Theta/T}\left(\frac{x}{2}\right)^2 sh^{-2}\left(\frac{x}{2}\right)dx \quad (55)$$

The above equations hold when no interaction between molecules exist.
In solids, however, chain-like or layer-like molecules can not exist
independently and thus some interactions should appear among them.

2.5   A model for complicated glass system

So far, the frequency distribution functions have been derived

for the models in which atoms of one kind are dispersed homogeneously

in space or they form polyatomic chains or layers. [20)-23)] The question

naturally arise as to what extent the theory of specific heat of

monoatomic materials is applicable to glasses, which are mainly

polyatomic and complex systems. It is considered that the frequency

distribution functions at extremely low temperatures for the glasses

containing more than three kinds of atoms become extremely compli-

cated as the distance of nearest neighbour atoms ((a) in Fig. 2)

varies depending upon the species chosen as well as the chemical

composition of glasses. Thus it is almost impossible to obtain the

frequency distribution function at extremely low temperatures

suitable for estimating low temperature heat capacities of these

complicated glasses. At moderate to high temperatures, however, it

seems possible to treat the problem based on the fact that the heat

capacity of crystals having a simple structure but containing more

than two kinds of atoms can be described quite well in this temper-

ature range by only one Debye characteristic temperature.

As described in the previous section, the glass structure may

consist of chained or layered molecules. Therefore, the strong

interaction forces between the atoms inside the chain or the layer

as well as the weak interaction forces between atoms in adjacent

chains or layers have to be taken into account.

Obviously, a structure of interacting chain molecules by no means has the frequency spectrum of a linear continuum cut-off at ν_{max}. In the low frequency part of the spectrum, where the wavelength is much larger than the maximum distance between neighboring chains, the solid behaves as a three-dimensional isotropic continuum, and therefore the low frequencies are governed by the Debye formula. For the high frequencies, on the other hand, it is important to know the frequency spectrum of interacting macromolecules. Thus, the spectrum of an interacting chain structure may be divided into two parts.

1) $3N_1$ high frequency modes from ν_{max} to ν_1 with a one dimensional continuum distribution (increment dS_1)

2) $3N_2$ low frequency modes from ν_1 to 0, with a three-dimensional continuum distribution (increment dS_3)

where $3N = 3N_1 + 3N_2$ and

and $\qquad 3N_1 = 3N - \int_0^{\nu_1} dS_3,$ while $\quad dS_1 = 3N_1(\nu_{max} - \nu_1)^{-1} d\nu \quad (56)$

$\qquad dS_3 = 9N_2\nu_1^{-3} \nu^2 d\nu \qquad (57)$

Thus, we can obtain the frequency density function $g(\nu) = \dfrac{dS_1}{d\nu}$ according to (56) and (57).

The number of frequencies in the interval (ν_{max}, ν_1) is approximately in direct proportion to ν_1 and in inverse proportion to the maximum frequency ν_m, $3N_2 = 3N \dfrac{\nu_1}{\nu_{max}}$, $\qquad 3N_1 = 3N(1 - \dfrac{\nu_1}{\nu_{max}}) \qquad (58)$

From (56) and (57), we obtain for the vibrational energy $U_{1,3}$ of the

interacting chains,

$$U_{1,3} = 3N_1(\nu_{max}-\nu_1)^{-1} \int_{\nu_1}^{\nu_m} h\nu (exp\frac{h\nu}{kT}-1)^{-1}d\nu$$

$$+ 9N_2\nu_1^{-3} \int_0^{\nu_1} h\nu^3 (exp\frac{h\nu}{kT}-1)^{-1}d\nu \qquad (59)$$

From (58), setting $\quad x=\frac{h\nu}{kT}$, $\quad \Theta_1=\frac{h\nu_m}{k}$, $\quad \Theta_3=\frac{h\nu_1}{k}$

we obtain for the specific heat $C_{1,3}$ of the interacting chains,

$$C_{1,3} = 3R \frac{T}{\Theta_1} \int_0^{\Theta_1/T} \frac{x^2 e^x dx}{(e^x-1)^2} - \frac{\Theta_3}{\Theta_1} [\frac{3RT}{\Theta_3} \int_0^{\Theta_3/T} \frac{x^2 e^x dx}{(e^x-1)^2}$$

$$- \frac{9RT^3}{\Theta_3^3} \int_0^{\Theta_3/T} \frac{x^4 e^x dx}{(e^x-1)^2}] \qquad (60)$$

The frequency spectrum of a solid consisting of interacting two-dimensional layers is similarly divided into two parts. Then, the temperature dependence of the specific heat of a structure with interacting layers become

$$C_{2,3} = 6R (\frac{T}{\Theta_2})^2 \int_0^{\Theta_2/T} \frac{x^3 e^x dx}{(e^x-1)^2} - (\frac{\Theta_3}{\Theta_2})^2 [\frac{6RT^2}{\Theta_3^2} \int_0^{\Theta_3/T} \frac{x^3 e^x dx}{(e^x-1)^2}$$

$$- \frac{9RT^3}{\Theta_3^3} \int_0^{\Theta_3/T} \frac{x^4 e^x dx}{(e^x-1)^2}] \qquad (61)$$

Thus, it becomes possible to describe the heat capacity of a solid with interacting macromolecules by two characteristic temperatures.

The characteristic temperatures Θ_1, Θ_2 and Θ_3 have a definite meaning. For chain-type structures Θ_1 is the characteristic temperature of the solid when considered as a one-dimensional continuum. Θ_1 is determined by the elastic constant of the main bonds and is a

measure of this elasticity. Θ_3 is the characteristic temperature of

the chain structure when considered as a three-dimensional isotropic

continuum, in which the chains are linked by lateral interactions.

Θ_3 is obtained, independent of the calorimetric measurements, from

the sound velocity propagating across the chains. Fig. 12 shows

curves of the specific heat versus T/Θ_1. The top curves correspond to

the pure chain structures. The bottom curves represent Debye's theory.

The intermediate curves corresond to different degrees of interaction.

To extend the preceding treatment to more complicated glasses

such as containing modifying cations, alkali silicate and alkali

alumino silicate glasses, the vibrational energy of modifier in the

SiO_2 networks must be considered. In the present study, it is

assumed that the contribution of modifier-oxygen bonds can be given

by an Einstein function, following the treatment of Kelley for

crystalline silicates. Then, the heat capacity of these glasses

can be represented by three characteristic temperatures, two Debye, Θ_1

and Θ_3, and one Einstein, Θ_E.

Since Θ_1 and Θ_3 are properties of the glass lattice, their contri-

bution to the heat capacity is best described by the Debye model.

However, modifying cations result in local modes, which are considered

to contribute independently to the vibrational specific heat, in the

form of one Einstein function with the characteristic temperature Θ_E.

Consequently, Θ_E depends on the kind of modifying cations but not on
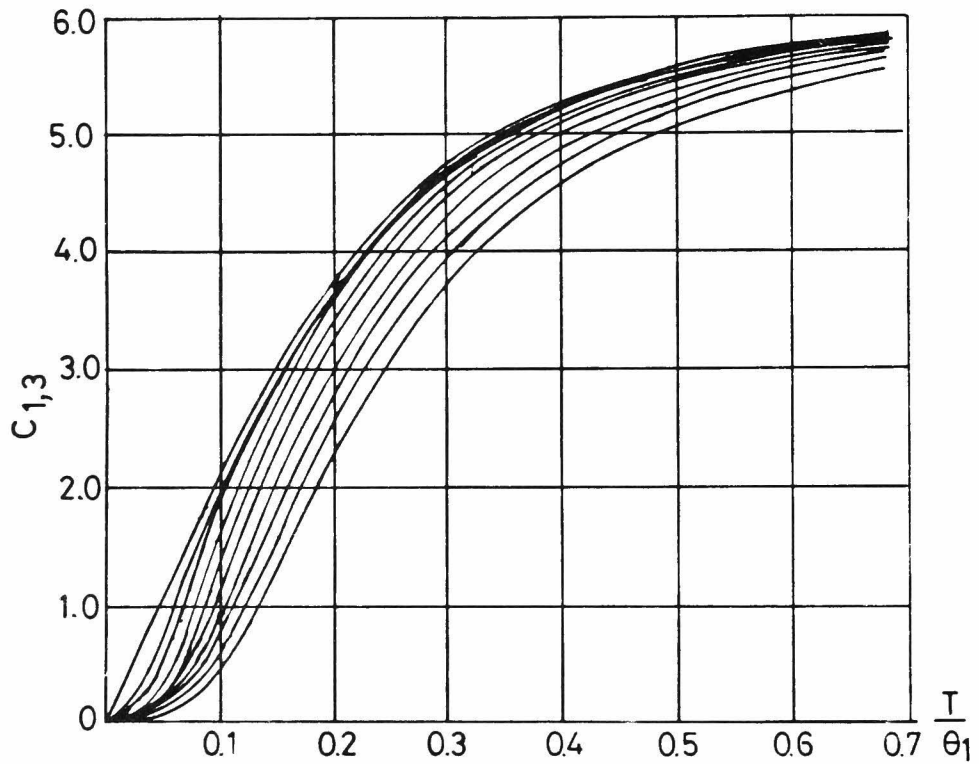
Fig. 12 Specific heat according to (60) at
different θ_3/θ_1
uppermost curve; $\theta_3/\theta_1 = 0$
lowest curve; $\theta_3/\theta_1 = 1$

their concentration.

The representative expression of the present three band model for the specific heat capacity, including these characteristic temperatures, is

$$C_v = C_{1,3} + 3R[x^2 e^x / (e^x - 1)^2] \quad (x = \Theta E / T) \quad (62)$$

Once the heat capacities of glasses are measured at various temperatures, Θ_1, Θ_3 and Θ_E can be determined numerically by a computer to verify the experimental data. However, in the case of low modifier content, the heat capacity due to modifying ions is small compared to the total heat capacity as expected from Eq.62. Thus, the uncertainty in Θ_E increases with decreasing modifier content. Although the real structure of silicate glass is unknown, it may be regarded as consisting of chains of SiO_4 tetrahedra connected by metal polyhedra, similar to those of silicate crystals. These chains may differ in the bond length, bond angle, number of tetrahedra in the repeat units, and type of interconnection, depending on the kind and amount of modifier in the glass. Such differences should cause a change in the lattice vibrational frequency spectrum and thus the value of Θ_1 and Θ_3. Therefore, it is possible to discuss the effect of modifier on the structure of the glass network by comparing Θ_1 and Θ_3 for various silicate glasses by the present three band model.

SUMMARY TO CHAPTER 2

Two glass model systems were considered theoretically to establish the vibrational frequency spectra and equations suitable to interpret the thermal properties of silicate glasses. The main results are as follows:

1. A homogeneous but structurally disordered system was found to possess the thermal property characteristic of the glassy state at very low temperatures. The phonon dispersion curve of the excitation modes for this system yielded an extra phonon density of states in the low frequency region, which gives an excess heat capacity at very low temperature. The phonon dispersion curve changed its shape depending upon the degree of local disorder of the system. Thus the magnitude of the excess heat capacity may be used to discuss the local disorder of glass. The same simple glass model system also gave the linear dependence of heat capacity on absolute temperature at very low temperatures, in accordance with the experimental results.

2. The Grüneisen parameter becomes negative at low temperatures easily for a glass having a large degree of randomness, while it stays positive for a glass having a minute degree of randomness even at very low temperatures. In addition to the randomness of the disordered system, which depends on the glass composition, the effect of temperature on Grüneisen parameter was introduced by considering two independent parameters, and a diagram showing the variation in

Grüneisen parameter with composition and temperature was constructed.

3. A more complicated glass system involving three different characteristic temperatures was formulated to represent the heat capacity data in the low-to-moderate temperature range. These three characteristic temperatures were taken to be related to the elastic interchain bonds of glass network, the lateral interaction of chains and the independent modifier-oxygen bonds. Thus, the nature of atomic bonds in various glasses or their structures can be discussed based on these three characteristic temperatures.

REFERENCES

1. C.Kittel,   "Introduction to Solid State Physics",
                      3rd ed. (Wiley), 193 (1966)

2. T.Rubin, H.W.Altman and H.L.Johnston,
                      J. Am. Ceram. Soc., 5, 5289 (1954)

3. R.D.McCammon and G.K.White,
                      Phys. Rev. Lett., 10, 234 (1963)

4. R.C.Zeller and R.O.Pohl,
                      Phys. Rev., B4, 2029 (1971)

5. R.B.Stephens, G.S.Cieloszyk and G.L.Salinger,
                      Phys. Lett., 38A, 215 (1972)

6. P.Fulde and H.Wagner,
                      Phys. Rev. Letters, 19, 1280 (1971)

7. P.W.Anderson, B.I.Halperin and C.M.Varma,
                      Phil. Mag., 25, 1 (1972)

8. P.P.Debye,   Ann. Phys., Lpz., 39, 789 (1912)

9. T.H.K.Barron,   Phil. Mag., 46, 720 (1955)

10. M.Blackman,   Proc. Roy. Soc., London, 148A, 384 (1935)

11. M.Blackman,   Proc. Roy. Soc., London, 159A, 416 (1937)

12. R.B.Leighton,   Rev. Mod. Phys., 20, 165 (1948)

13. W.H.Houston,   Rev. Mod. Phys., 20, 161 (1948)

14. L.Van Houe,   Phys. Rev., 89, 1189 (1953)

15. H.B.Rosenstock, Bull. Am. Phys. Soc., 111, 141 (1956)

16. M.Blackman,   Reports on Prog. in Physics, 8, 11 (1941)

17.   M.Blackman,   Handbuch der Physik, VII (1), (1956)

18.   V.V.Tarasov,   Dan, 46, 117 (1945)

19.   V.V.Tarasov,   Dan, 58, 577 (1947)

20.   W.De Sorvo,   J. Chem. Phys., 21, 168 (1953)

21.   A.S.Dworkin and D.J.Sasmor,

                          J. Chem. Phys., 21, 954 (1953)

22.   D.F.Smith and A.S.Brown,

                          J. Am. Chem. Soc., 78, 1553 (1956)

23.   T.Fukuroi and Y.Muto,

                          Sci. Rep. Res. Inst. Tohoku Univ.,

                          A8(3), 213 (1956)

CHAPTER 3

METHODS OF THERMAL PROPERTY MEASUREMENTS

Among various thermal properties, heat capacity and thermal
expansivity were investigated in detail in the present study by using
Low temperature calorimetry and Low temperature dilatometry.

Low temperature calorimetry was carried out by a newly constructed
calorimeter in order to determine the heat capacity of various glasses
and crystalline compounds as a function of temperature from 1.6K to
400 K. Low temperature dilatometry was undertaken on glass samples
by two types of dilatometers, one suitable for the measurements from
77 to 700 K , and the other for a very low temperature range from
4.2 to 400 K.

There are some problems associated with the measurements of heat
capacity and thermal expansivity at low temperature. Heat capacity
and thermal expansivity are important to the theories of thermo-
dynamics and the equations of state of solids, and they are defined
as the temperature derivatives of length and heat content, respec-
tively. Thus, it is better to determine the change in length or
heat content in a very small temperature interval, which requires
accurate measurements of temperature and length (or heat content)
as well as stability of the apparatus in the temperature range in
question. Most of the commercially available systems of measuring
thermal expansion and heat capacities are for a wide temperature

range from room temperature to high temperatures but not for low temperatures. Thus, it was necessary to construct the systems suitable for the present study.

In this chapter, the systems constructed and used for the present study are described in detail. The systems were tested by measuring some standard materials, the results of which are also given.

3.1 Low temperature calorimetry

The heat capacity at constant pressure is generally obtained by measuring the heat added on a calorimeter vessel insulated thermally from its surrounding and the resulting temperature change ΔT after maintaining the calorimeter at a certain temperature. The general requirements for the vessel are mechanical and chemical stabilities, good thermal diffusivity, and low electric conductivity among others. To satisfy these requirements, the system capable of measuring heat capacity of solids from 1.6 to 400 K was designed and constructed. It is basically similar to the one successfully used by Seki, for various solids, and consists of cryostat, calorimeter, and measuring system.[1),2)]

Cryostat

The cryostat used was of adiabatic type and made essentially of metallic materials. The primary function of this cryostat assembly is to maintain a calorimeter vessel at any desired temperature in a thermally insulated state, so that virtually no heat is exchanged between the calorimeter and its surroundings even when an electric heater of the calorimeter vessel is turned on during measurements. In order to eliminate heat exchange between the calorimeter and its environment due to gas convection and establish adiabatic conditions, it is necessary to maintain a high vacuum (less than 10^{-6} mmHg at room temperature). To achieve this condition, the vessel was connect-

ed through pipe to a separate evacuation system equipped with a liquid nitrogen trap, an oil-diffusion pump and a rotary pump.

Various precausions were taken to minimize the heat conduction through electric lead wires in the cryostat. The wires were drawn into the cryostat through the inlet of leads. After passing through the evacuation tube, these leads were thermally anchored to the thermal station. The leads were then anchored to the smaller cylindical part of the liquid nitrogen container. All the lead wires were vanished tightly with glyptal lacquer (G.E. adhesive No. 7031), particularly at the place where they were thermally anchored.

Calorimeter

The cross sectional view of the calorimeter constructed in the present study is shown in Fig.1-A. The main body of the calorimeter consisted of a sample container, an adiabatic jacket, an upper flange of the calorimetric envelope with pipes for evacuating the system to the order of 10^{-6} mmHg and for feeding in a heat conduction gas of helium. It was attached to the flange of vessel by means of a ring shaped well-annealed copper spacer. The sample container was suspended by four thin constantan wires from the top portion of the adiabatic jacket. The adiabatic jacket was in turn suspended from the upper block of stainless steel. The sample container (Fig.1-B) was made of copper (0.1 mm in thickness) with a central well for setting a heater. The eight radial fins silver-soldered to the well and to the inside

hermetic seal

vacuum pipe

Cu-O ring

terminal

radiation shield

outer jacket

inner jacket

sample vessel
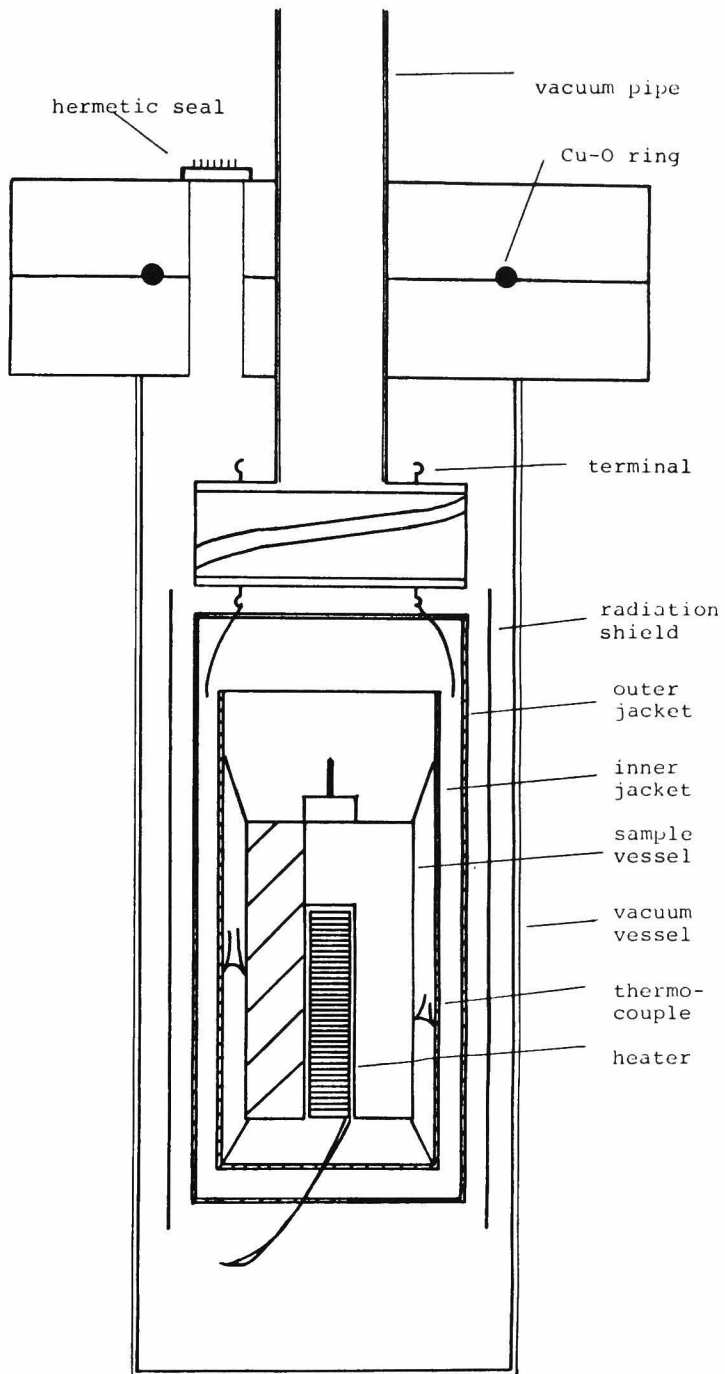
vacuum vessel

thermo- couple

heater

Fig. 1-(A) Sectional drawing of the calorimeter assembly

wall of the container provided a good thermal contact of the sample
with the container. The size of the main body of the container was
30.8 mm diameter and 52.3 mm long. The total weight of the container
was about 20 g.

Although the well was machine-drilled so as to be fitted with the
heater assembly, it was necessary to fill the gap with beryllia cement
at the entrance portion of the well and with silicon varnish on the
heater in order to reduce the temperature gradient in the container.
The adiabatic inner jacket was a thin walled copper cylinder with a
diameter of 4 cm, and a length of 9.0 cm. The metallic body of the

(a)

Cap

hook

vessel

thermo-
meter

copper
holder

bundle

heater

radiation

radiation
plate

Germanium
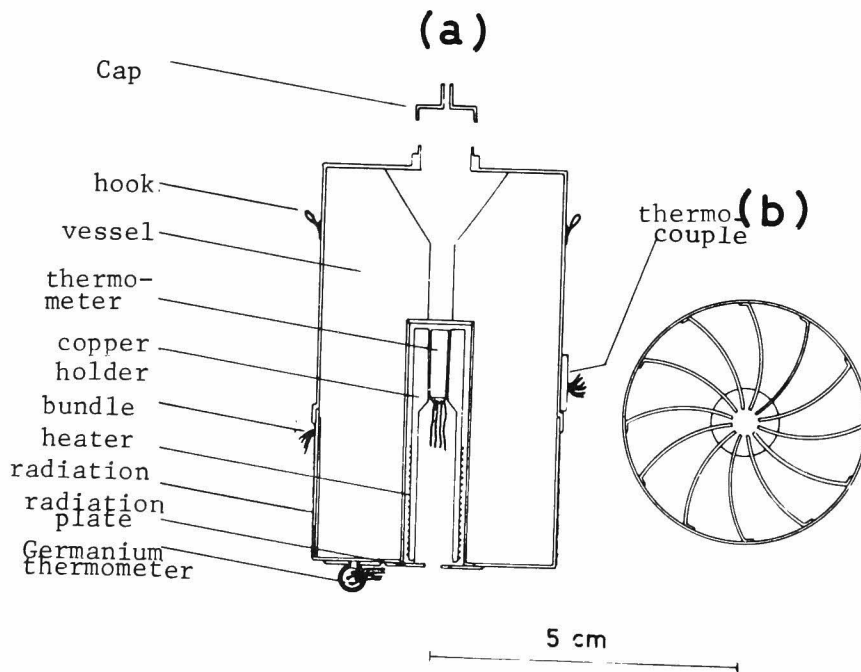thermometer

thermo **(b)**
couple

5 cm

Fig. 1-(B) Sectional drawing of the calorimeter vessel

jacket was coated with thin aluminium seal and the manganin heater of 200 ohms insulated with GE cement was fixed on the jacket non-inductively . The same heater was also attached on the outer jacket.

The temperature difference between the outer surface of the container and the inner surface of the jacket, was detected by a three junction chromel-alumel thermocouple. The junction of the thermocouple was insulated with a small thin piece of cellophane adhesive tape and inserted tightly into copper bands. The voltage difference between two thermocouples at the jacket and the sample container was amplified with an microvoltmeter (±10μV in full scale). This amplified voltage was fed into a servo-circuit, which controls the heater current of each portion of the jacket. The output current was adjusted automatically from 0 to 500 mA, responding to the measured temperature. The adiabaticity between the inner jacket and the outer jacket was checked by two thermocouples placed on them and maintained in the same way as described above.

After a powdered sample was packed into the sample container, a small amount of helium gas was introduced through a narrow copper tube in order to help the container to reach an thermal equilibrium state in a short time. The tube was pinched off to keep it gas-tight after dehydration in vacuum.

The electric power produced in the calorimeter heater was obtained by measuring the current and the voltage applied on the heater.

The potential drop across the calorimeter heater was measured in the conventional way with a DC volt meter, using a standard resistor (10 ohm) as a reference. The heating interval, usually 900 sec, was measured on a digital counter, which was also used as an automatic digital on-off switch. The energy supply was so adjusted that the temperature elevation in this heating period was 10 deg. in the loaded condition. For such heating rate, interval equilibrium in the sample container could be attained within 5 minutes after heating was stopped. . The EMF of a working thermocouple was measured by a potentiometer in conjunction with a galvanometer. The output voltage of the galvano-meter was recorded on a X-T recorder. When the automatic adiabatic control was working in order, the temperature difference could be kept within 10^{-2} deg. at any temperature below room temperature for the period of equilibration. The whole circuit is shown schematically in Fig.2(A). The servo circuits for automatic control system and relay are shown in Fig.2(B) and 2(C).
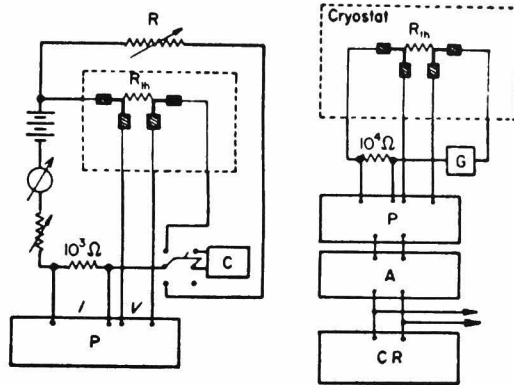
Heater Circuit (left)   Thermometer circuit (right)

R_{th} Heater R_{th} Resistance thermo-
                                                     meter

R   Heater equivalence   G   Constant current
       resistance   generator

C   Chronometer   P   Potentiometer

P   Potentiometer   A   Amplifier

                                          CR   Chart recorder

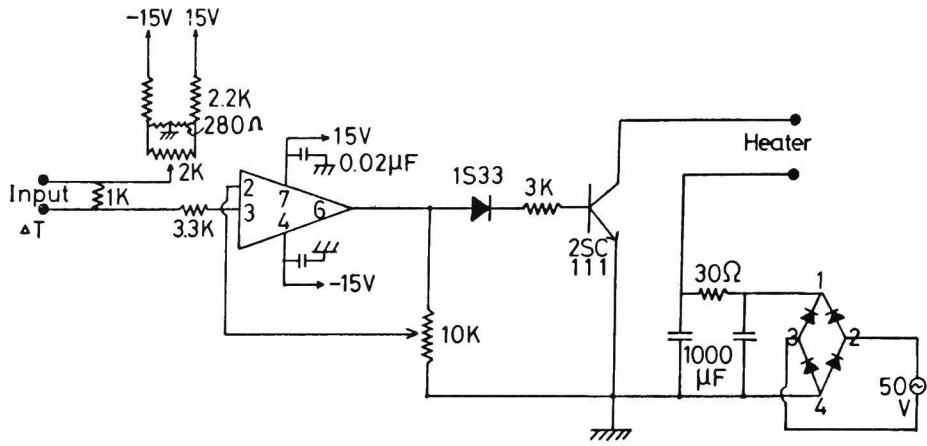Fig.2(A) Electric circuit for heat capacity measurement

Fig.2(B) Servo circuit for automatic control system
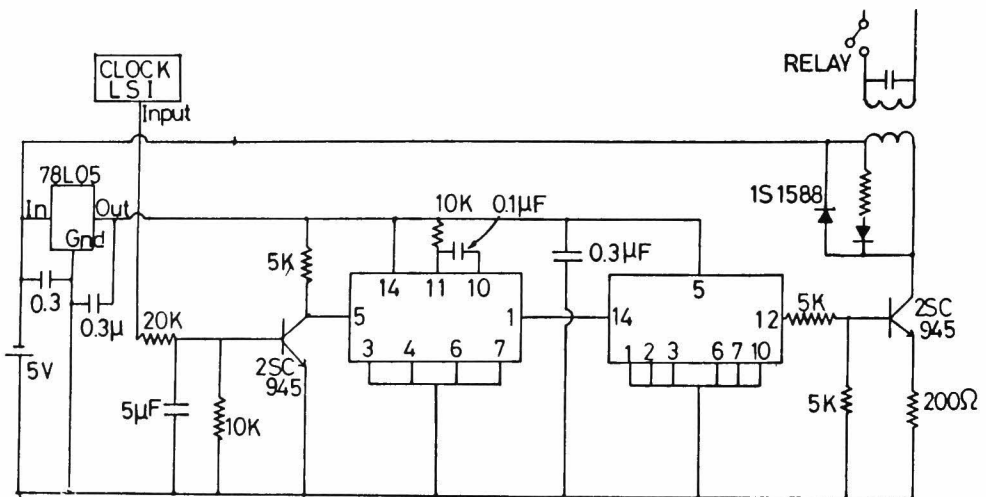

Fig.2(C) Servo circuit for relay.

3.2   Low temperature dilatometry

Among various methods of measuring the change in length with temperature, a vitreous silica differential dilatometer using a differential transformer was designed and constructed. The system was suitable for the temperature range from 4.2 to 300 K. It consisted a base plate, two inner chambers, the dilatometer system and the cryostat, as shown schematically in Fig. 3.

Dilatometer system

The dilatometer system consisted of the quartz parts, the aluminium sleeve and radiation shields shown in Fig. 3. A quartz support tube of 53 cm long was attached by epoxy resin to the base plate. The inside of the support tube was bored to provide precision sliding fits with the quartz platform and quartz push rod guide. The push rod was a 600 mm long quartz tube. The specimen was about 5 mm in diameter and 30 mm in length and its ends were ground flat and parallel. It was placed in a 7 mm OD, 20 mm long copper holder to reduce the temperature gradient along the specimen length. The Au,Co-Cu thermocouples and a germanium thermometer were attached to the specimen to measure the specimen temperature. The bottom of the holder was ground flat and perpendicular to the side wall. Both the specimen and the holder were removable through a window in the support tube. The specimen and the lower portion of the support tube and push rod were positioned inside an aluminium cylindical sleeve, which served as a heat shield to minimize the temperature gradient in the specimen

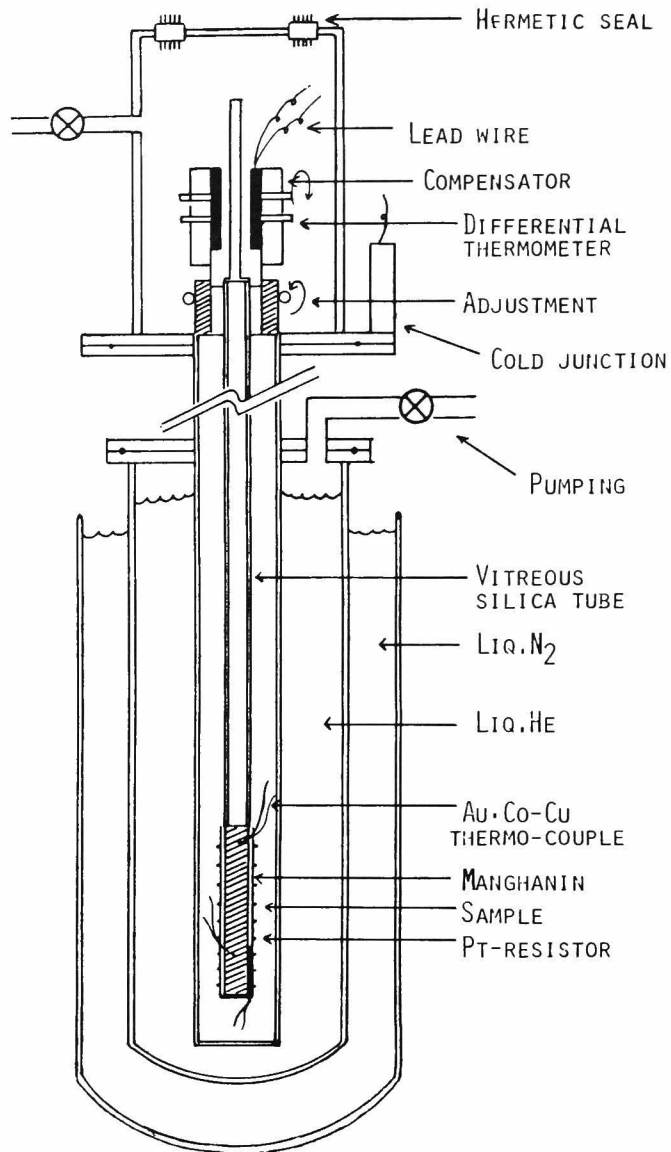HERMETIC SEAL

LEAD WIRE

COMPENSATOR

DIFFERENTIAL
THERMOMETER

ADJUSTMENT

COLD JUNCTION

PUMPING

VITREOUS
SILICA TUBE

LIQ. N_2

LIQ. HE

AU·CO-CU
THERMO-COUPLE

MANGHANIN

SAMPLE

PT-RESISTOR

Fig. 3 Sectional drawing of the dilatometer

environment.

Electrical circuit

To achieve an accurate constant heating rate of the dilatometer, a program controller with a SCR unit was used. The temperature was monitored by a Pt resistance thermometer. The electrical circuit is shown schematically in Fig. 4. The equilibrium temperature was also measured with the germanium resistance thermometer in conjunction with a six-dial double thermofree microvoltmeter.

The output voltage from the differential transformer, which corresponds to the expansion of dilatometer, and that from thermo-couples were alternatively measured on a digital voltmeter and printed every ten seconds, or in a time interval corresponding to a rise of one degree. These printed data were fed into a computer and the calculation was made by using the least square method to obtain the thermal expansion coefficient at various temperatures.
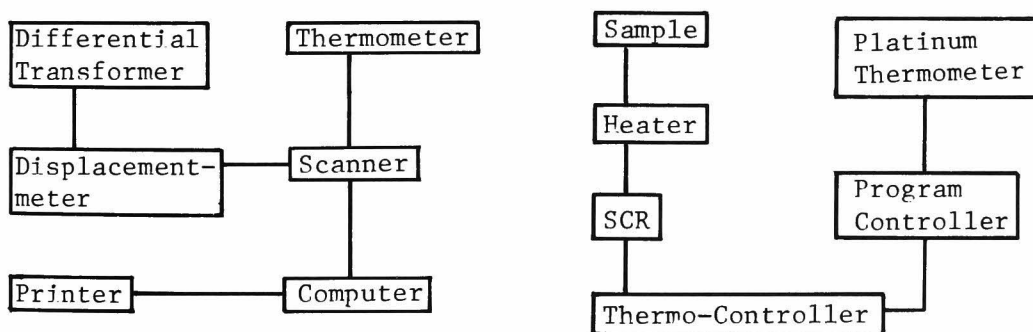
Fig.4 Electric circuit for thermal expansion measurement

3.3   Calibration of thermometers and thermocouples

The determinations of thermal quantities that appear in any second law equation requires the temperature measurements on the thermodynamic scale. In the present study a germanium thermometer and various types of thermocouples were used. For high temperatures, the Plank radiation formula may be used to determine the values of temperature on the thermodynamic scale. For low temperatures, the measurement of magnetic susceptibility of an ideal paramagnetic salt which obeys the Curie's law or the Curie-Weiss law is suitable, to determine the temperature.[2] In any case, accurate measurements of values of temperature on the thermodynamic scale are fraught with experimental difficulties. The usage of any method or system requires some calibration beforehand.

Calibration of germanium thermometers

The germanium resistance thermometer (Cryocal, Inc., CR1000) used in this study was calibrated against the standard germanium thermometer, which belongs to the Low Temperature Laboratory in the Faculty of Science in Kyoto University. The resistance value of these germanium thermometers was ca. 1000 ohm at 4.2 K and the calibration current of ca. 5 microampere was chosen to avoid excessive joule heating. The values of resistance measured are shown in Fig. 5 as a function of temperature.

In the case of germanium thermometers, no established functional relationship exists between temperature and resistance, but the cali-

bration data were generally fitted to the following formula.[3]

$$T = \sum_j cof_j (logR)^{j-1}$$

For the present thermometer, the data were arranged by dividing the temperatures into three range and using the following equations.

From 1.6 K to 10 K,

$$T = COF(1,5,1)(logR)^0 + COF(1,5,2)(logR)^1 + COF(1,5,3)(logR)^2$$
$$+COF(1,5,4)(logR)^3 + COF(1,5,5)(logR)^4$$

From 10 K to 60 K,

$$T = COF(2,5,1)(logR)^0 + COF(2,5,2)(logR)^1 + COF(2,5,3)(logR)^2$$
$$+COF(2,5,4)(logR)^3 + COF(2,5,5)(logR)^4$$

From 60 K to 100 K,

$$T = COF(3,8,1)(logR)^0 + COF(3,8,2)(logR)^1 + COF(3,8,3)(logR)^2$$
$$+COF(3,8,4)(logR)^3 + COF(3,8,5)(logR)^4 + COF(3,8,6)(logR)^5$$
$$+COF(3,8,7)(logR)^6 + COF(3,8,8)(logR)^7$$

The COF values are shown below as COEFFICIENT.

```
(        COEFFICIENT(1,  5,  1)= -0.187728886151D+03
(        COEFFICIENT(1,  5,  2)=  0.941535407835D+02
(        COEFFICIENT(1,  5,  3)= -0.169523648642D+02
(        COEFFICIENT(1,  5,  4)=  0.132765432465D+01
(        COEFFICIENT(1,  5,  5)= -0.385026266090D-01
(        COEFFICIENT(2,  5,  1)= -0.150999991070D+02
(        COEFFICIENT(2,  5,  2)=  0.216599473981D+02
(        COEFFICIENT(2,  5,  3)= -0.573203932972D+01
(        COEFFICIENT(2,  5,  4)=  0.573395216695D+00
(        COEFFICIENT(2,  5,  5)= -0.200917910759D-01
(        COEFFICIENT(3,  8,  1)=  0.419080539577D+03
(        COEFFICIENT(3,  8,  2)= -0.252267361458D+03
(        COEFFICIENT(3,  8,  3)=  0.287001333214D+02
(        COEFFICIENT(3,  8,  4)=  0.170253315658D+02
(        COEFFICIENT(3,  5,  5)= -0.685705612353D+01
(        COEFFICIENT(3,  8,  6)=  0.108126083146D+01
(        COEFFICIENT(3,  8,  7)= -0.819530079577D-01
(        COEFFICIEMT(3,  8,  8)=  0.247421322414D-02
```
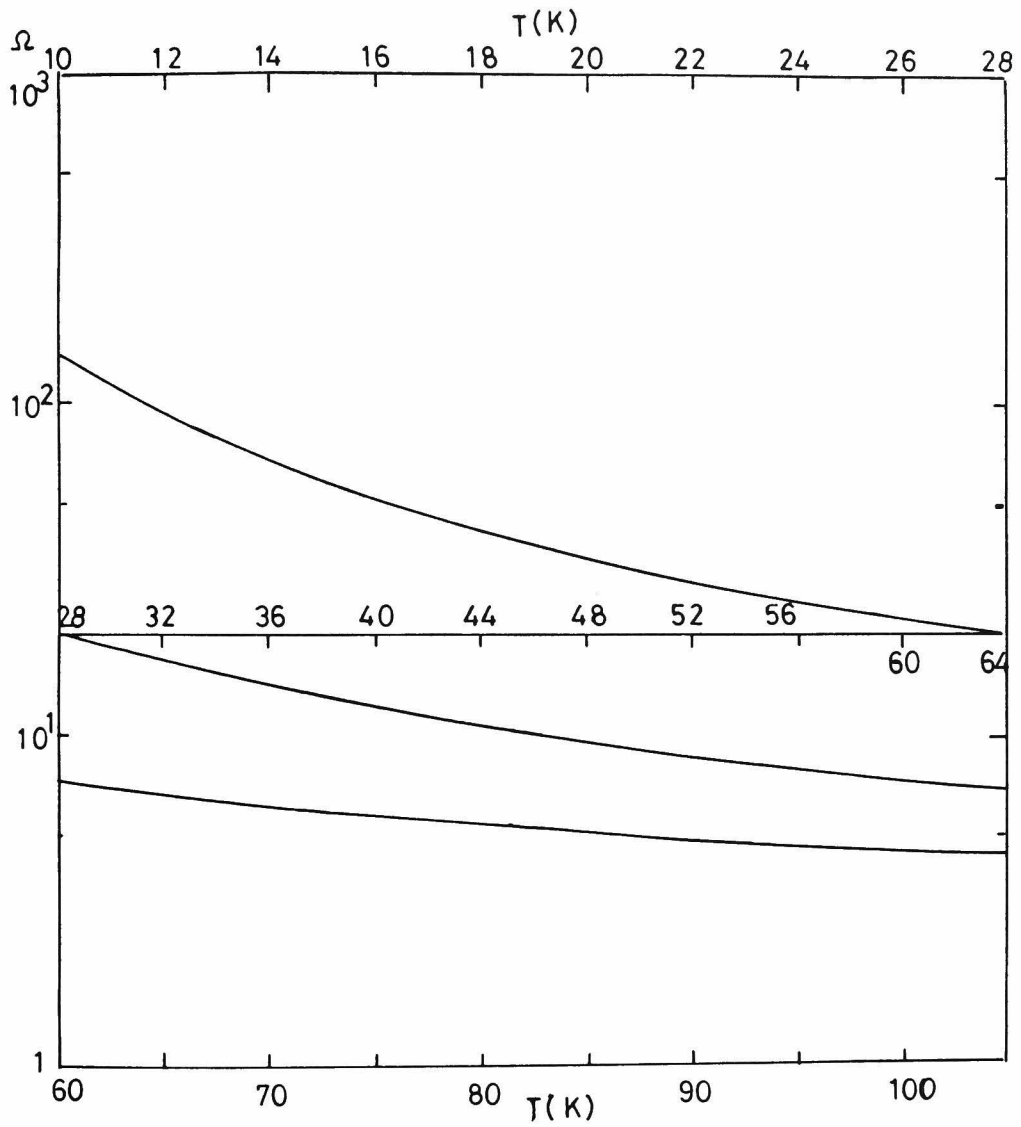
Germanium thermometer
CR 1000
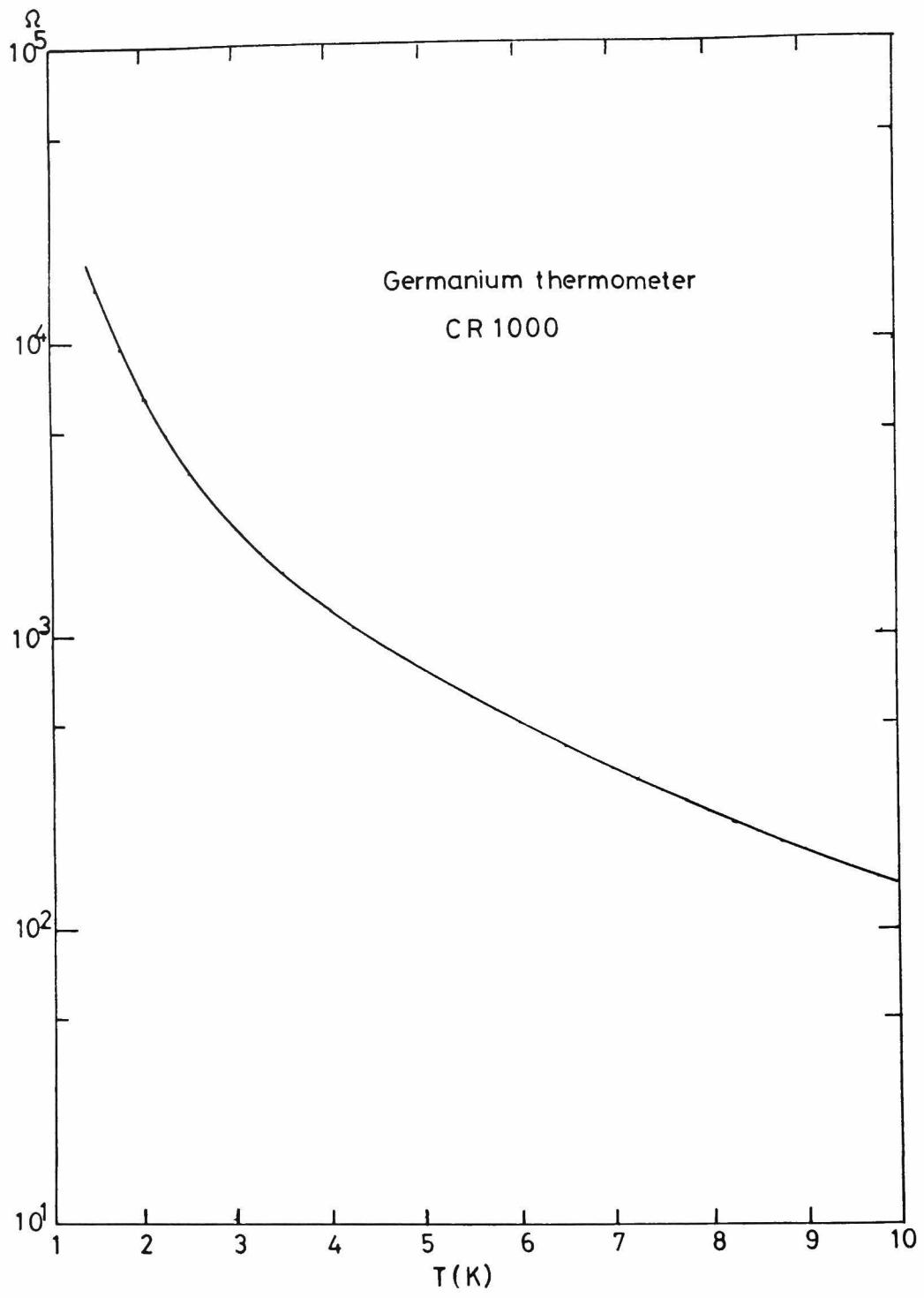
Fig. 5 Calibration of germanium resistance thermometer

The calibration of thermocouple

Among many ways of measuring cryogenic temperatures, the usage
of thermocouples is simplest and most useful. In the present study,
three thermocouple combinations, Chromel versus Alumel thermocouple,
Constantan versus Copper thermocouple and Gold-2.1 at % Cobalt versus
Copper thermocouple, were used depending upon the temperature range
studied. Constantan versus Copper and Chromel Alumel thermocouples
are suitable for use above liquid nitrogen temperature but not below,
because of their relatively low sensitivity at very low temperatures.
Gold-Cobalt one has sufficiently large thermoelectric power against
copper at near liquid helium temperature so that it can be used
together with Germanium resistor thermometer. A number of thermo-
couples were tested by determining their thermoelectric potential
at two different temperatures at liquid nitrogen and ice or liquid
helium temperatures. From this test, only thermocouples which showed
the same values listed in the literature, were selected.[4),5)] However,
some thermocouples, particularly the one with gold-cobalt alloy were
found to vary in thermoelectric power with time. Therefore, many
measurements were carried out to test the time variation.
Three thermocouples were tested over a period of a month, and the
thermocouple which showed only about 1% change was selected.

3.4   Preliminary experiments for testing measuring systems

In addition to the calibration of thermometers and thermocouples, all the systems constructed in the present study for determining heat capacity and thermal expansivity were tested by measuring these quantities of a standard material.

Calorimeter system

The reliability of the present calorimeter was examined by measuring the heat capacity of a standard sample of α-Al_2O_3 from 77 to 300 K. The deviation of the present values from these of Furukawa[3] is shown in Fig.6. Most of the observed points fall within $\pm$ 2% in relative deviation from the smoothed curve. This agreement was sufficient for the present study.
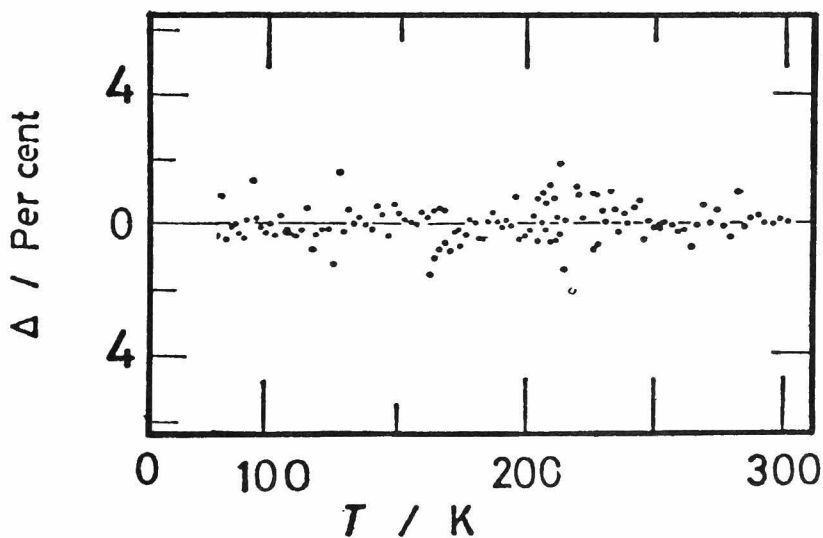

Fig. 6 Calibration of the calorimeter about α-Al_2O_3

Dilatometer system

By the present system, the difference in thermal expansivity between the specimen and vitreous silica is detected. Thus, the thermal expansion of vitreous silica used for the support tube has to be added to obtain the true thermal expansion coefficient of the sample.

The thermal expansion of a vitreous silica sample, which was cut from the same rod used for the dilatometer, was measured in the capacitance dilatometer. The experimental procedure has been described in detail by Nakamura.[7] The sample was in the form of cylinder (2mm in diameter and 5mm in length) in the capacitance cell, as shown schematically in Fig.7. The result is shown in Fig.8 , which also gives the data for Spectrosil by Gibbon.[8],[9] A small amount of difference between Gibbon's is observed at 20K. This may be attributed to experimental error or to a difference in fictive temperature or thermal history of glasses, which are known to exist in different glass samples.

However, the present values of vitreous silica are not so much different from those of Gibbon, and in the range of 80 to 293 K they may be expressed by the following equation.

$$\alpha \times 10^6 = -1.416 + 9.581 \times 10^{-3}T$$
$$-5.991 \times 10^{-6}T^2 - 1.564 \times 10^{-8}T^3$$

At lower temperatures, thermal expansion was so small that the poly-nomial function $\alpha = -(3.5 \pm 0.1) \times 10^{-10}T^3 degK^{-1}$. In order to obtain thermal
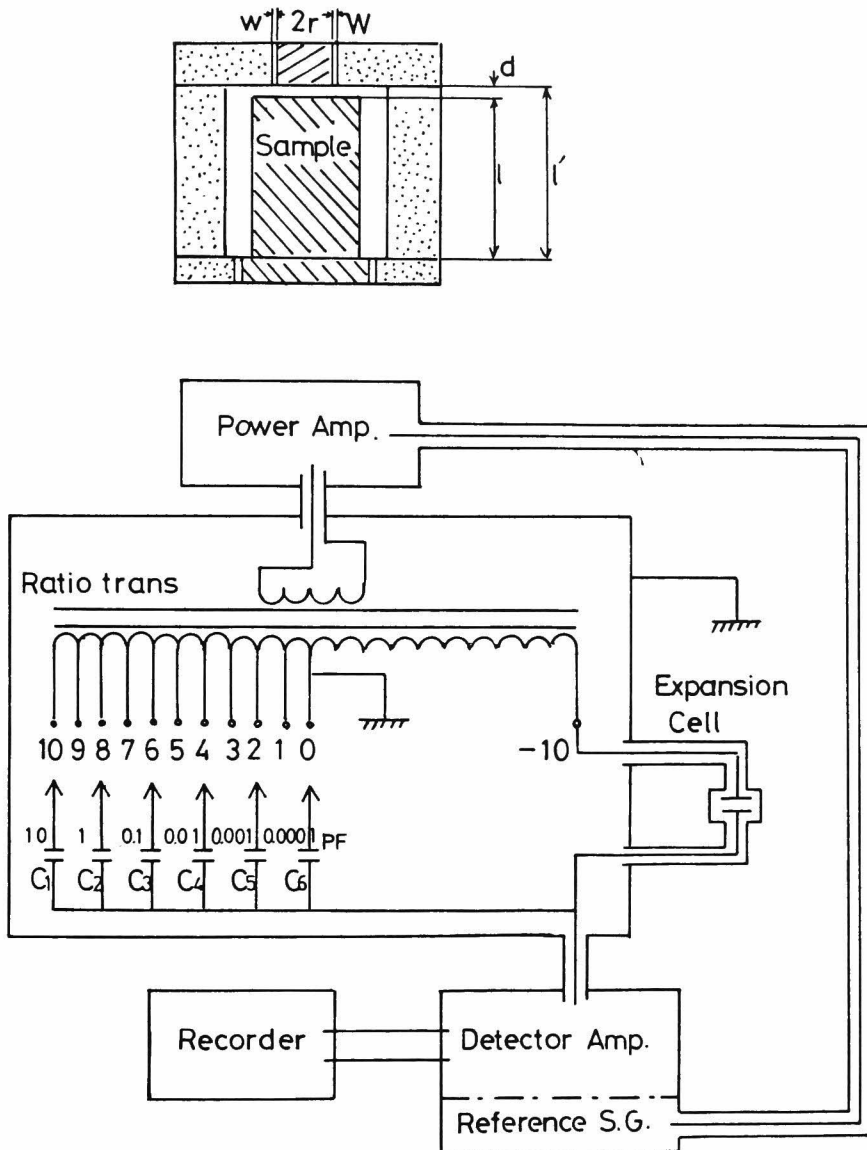
Fig. 7 Apparatus for capacitance dilatometer

expansion coefficient of a sample at low temperatures, thermal expan-
sion of vitreous silica, at 5 K, 10 K, 15 K etc, was taken from the
thermal expansion curve given by Gibbon and added to the thermal
expansion of sample determined at the same temperature. Indeed,
these values were tried to fit to a fourth order equation.
Thermal expansion coefficient was obtained by differentiating this
equation. Although the correction for finite ΔT has to be made, the
magnitude of the correction them at low temperatures is estimated to
be about 0.06×10^{-6}/K, which is negligible in our purpose.

The dilatometer was tested against copper as a standard
copper is the first of a series of materials that are to be certified
as the thermal expansion standards by the National Bureau Standards.[10]
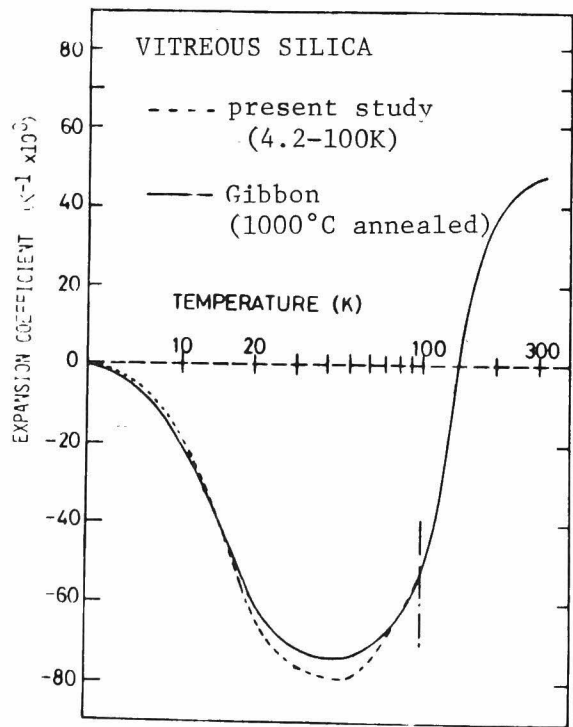
Fig. 8 Result of vitreous silica
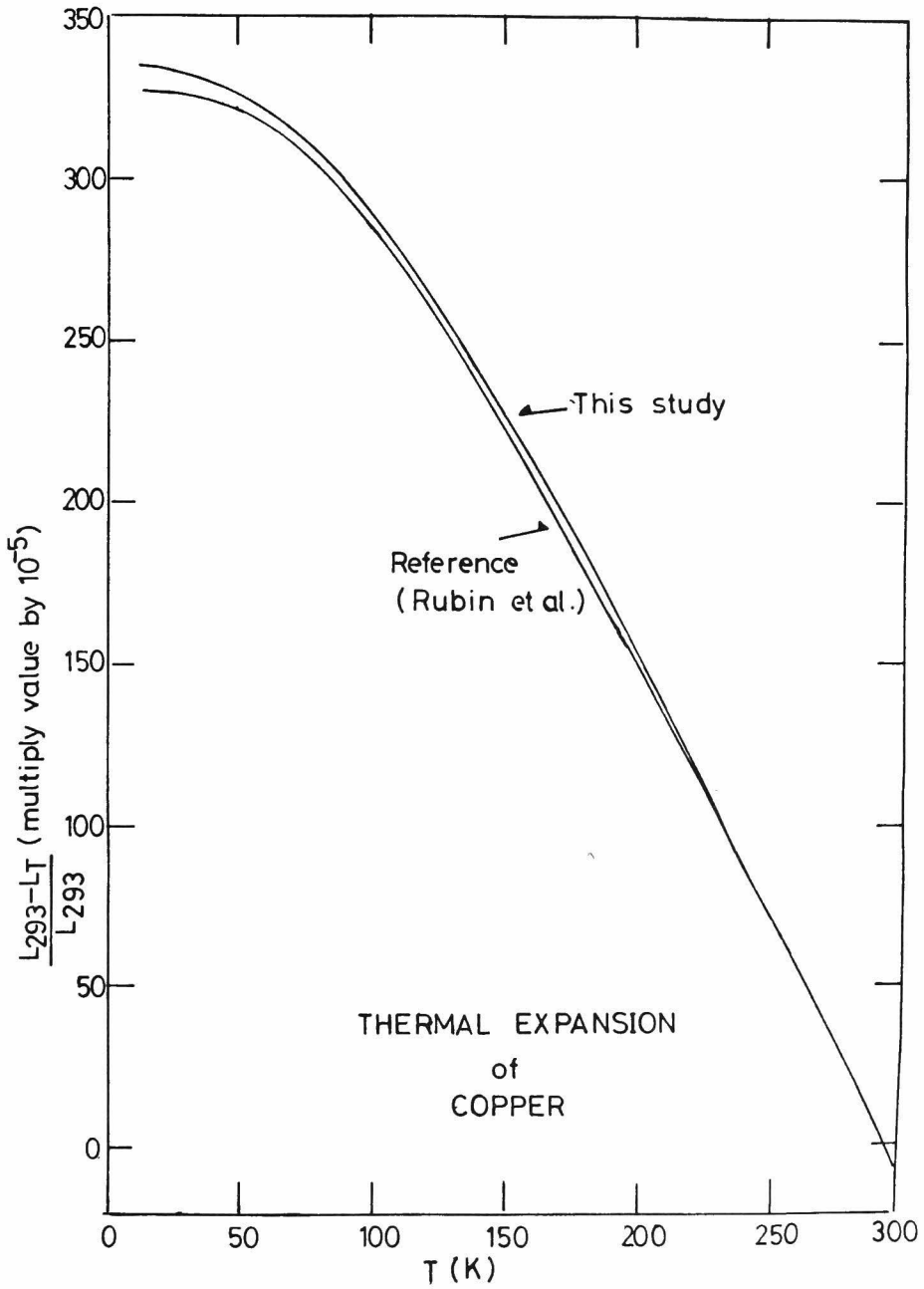
Fig. 9   Calibration of the dilatometer about copper

A heating rate of 3.0°C/min. was used for all measurements. The fourth order polynomial was fitted to the expansion data for each of the five specimens in the temperature ranges from 10 to 50 K and 50 to 300 K, in order to obtain the values of expansion coefficient. A comparison with the data in literature is shown in Fig. 9. The maximum probable inaccuracy in expansion is ±3.0% at 10K, ±1.8% at 20 K and ±1.5% at 30 K. Relative or random errors between samples are considered to be less than this.

SUMMARY TO CHAPTER 3

The methods used in this study to determine heat capacity and thermal expansion coefficient from very low temperature to moderately high temperatures were described in details.

1. The low temperature calorimeter system, newly designed and constructed, was found to be useful for the measurements from 1.6 to 400K, by using α-Al_2O_3 as a standard sample. The deviation of the measured values from those in literature was within $\pm$ 2% in the entire temperature range.

2. The vitreous silica differential dilatometer designed and constructed by using a differential transformer, was suitable for the temperature range from 4.2 to 300K. The standard sample used was copper and the agreement between the measured and the reported value was within 3% at 10K, 1.8% at 20K and 1:5% at 30K.

REFERENCES

1.   H.Chihara and M.Nakamura,

                    Bull. Chem. Soc. Japan, 5, 133 (1972)

2.   G.K.White,   "Experimental Techniques in Low Temperature

                    Physics", Clarendon, Oxford (1959)

3.   J.L.Riddle, G.T.Furukawa and H.H.Plumb,

                    NBS Monograph, 126 (1973)

4.   T.J.Quinn and J.P.Compton,

                    Rep. Prog. Phys., 38, 151 (1975)

5.   R.L.Powell, M.D.Bunch and R.J.Corrueeini,

                    Cryogenics, 1, 139 (1961)

6.   D.C.Ginnings and G.T.Furukawa,

                    J. Amer. Chem. Soc., 75, 522 (1953)

7.   Y.Nakamura and K.Sumiyama,

                    Inst. Phys. Conf. Ser., 39, 522 (1978)

8.   T.A.Hahn and R.K.Kirby,

                    "Thermal expansion", AIP Conference

                    Proceedings, 3, 13 (1971)

9.   D.F.Gibbons,   J. Phys. Chem. Solids, 11, 246 (1959)

10.   G.K.White,   "Thermal expansion", AIP Conference

                    Proceedings, 3, 59 (1971)

11.   T.Mamiya, K.Nomura and Y.Masuda,

                    J. Phys. Soc. Japan, 28, 380 (1970)

12. B.B.Triplett, Phys. Rev. Letters, 27, 1001 (1971)

13. S.S.Shinozaki and A.Arrott,

    Phys. Rev., 152, 611 (1966)

14. G.Seidel, P.H.Keesom,

    Rev. Sci. Instr., 29, 606 (1958)

15. N.E.Phillips, Phys. Rev., 114, 676 (1959)

16. O.V.Lounasmaa, Phys. Rev., 114, A1620 (1964)

17. B.W.Veal and J.A.Rayne,

    Phys. Rev., 135, A442 (1964)

18. L.J.Neuringer and Y.Shapira,

    Rev. Sci. Instr., 40, 1314 (1969)

19. K.Hirao and N.Soga,

    Rev. Sci. Instr., to be published (1981)

20. K.Hirao, N.Soga and M.Kunugi,

    J. Am. Ceram. Soc., 62, 570 (1970)

CHAPTER 4

THERMAL PROPERTIES OF ALKALI SILICATE GLASSES

AT VERY LOW TEMPERATURES

As described briefly in Chapter 1, many silicate glasses show
anomalous excess specific heat near 10K. This phenomenon is certainly
related with other anomalous behaviors of silica glass, such as
negative thermal expansion, and the positive temperature and negative
pressure derivatives of elastic moduli. White[1] et al. has suggested
that these anomalies are associated with low lying modes of atomic
vibrations. In silica glass, these modes are considered to be bond
bending motions of network formers, that is Si-O-Si. If so, the
addition of network modifiers such as alkali oxides to the network
formers should suppress these modes by hindering the bond bending
motions of Si-O-Si, since the inside space of network is filled by
network modifiers. Thus, it might be expected that the anomalies
mentioned above should become less with increasing alkali content.
This trend has been observed experimentally in thermal expansion and
elastic moduli of alkali silicate glasses. However, no data exist
on low temperature heat capacities of alkali silicate glasses.

In order to know quantitatively the effect of network modifiers
on the excess heat capacity and thus the number and frequencies of
the excess modes associated with network formers, an attempt was made
in this study to measure the specific heats of several sodium silicate
glasses at very low temperatures. Then, the thermal expansions of

the same glasses were measured in the same temperature range in order to obtain the correlation between thermal expansivity and heat capacity. In addition, the thermal expansions of lithium and potassium silicate glasses were measured to obtain the effect of the size of network modifiers. These results were used to discuss the conclusions derived theoretically on the basis of a simple glass model in Chapter 2.

4.1 Preparation of glass samples

Several glasses in the system Na_2O-SiO_2 were prepared from reagent grade Na_2CO_3 and SiO_2. The batches of the prescribed compositions were melted in Pt crucibles in a silicon carbide resistance furnace at 1200°C to 1500°C depending on composition, stirred with a Pt rod, allowed to stand until bubble-free, poured into a stainless steel mold, and annealed in a furnace. The glasses obtained were crushed into powder (150 mesh in size), and then lastly cooled through the glass transition region at a rate of about 25K/min. to give them a constant thermal history. In addition to sodium silicate glasses, lithium or potassium silicate glasses were also prepared in the same manner as sodium silicate glasses but with reagent grade Li_2CO_3 or K_2CO_3.

4.2 Heat capacity at very low temperature

The heat capacities of glass samples were determined by using a calorimeter described in Chapter 3. The values of Cp for sodium

silicate glasses of the compositions of $Na_2O \cdot 1.5SiO_2$, $Na_2O \cdot 2SiO_2$, $Na_2O \cdot 4SiO_2$ and SiO_2 from 1.6 to 60K are listed in Table 1-4. The lowest temperature of 1.6K was attained by using evacuation of liquid helium. Fig.1 is the plot of Cp/T^3 (J/mol·K) against T, together with the result for vitreous silica by Flubacher.[2],[3] This figure shows that the values of Cp/T^3 are not independent of T for all glasses, indicating that the specific heat of these glasses do not obey the Debye continuum theory at very low temperatures. It is clear that other temperature dependent terms than a T^3 term is required to describe their specific heats. A close look of this figure also shows that the excess specific heat is not so sensitive to the compositional variation. This means that the quantity of excess modes in silicate glasses does not vary so much with the addition of sodium oxide.

It is generally accepted that sodium oxide separates linked SiO_4 tetrahedra, fills the inside space of the network and thus leads to a general weakening of the network structure. If the low modes were to arise only from the bending of the Si-O-Si angle, they should be greatly affected by the change in angular ordering which take place by adding sodium oxide. However, the present experimental result does not support this consideration. As described in Chapter 2, it is expected from a simple glass model system that an excess heat capacity appears even though no bending motion exists. Thus, it may be concluded that the excess heat capacities of silica glass

and alkali silicate glasses do not reflect the easiness of bending

motions of the network structures but they are mainly due to the

randomness of glass structure.

Fig.1(B) is shown for an another plot, Cp/T versus T^2.
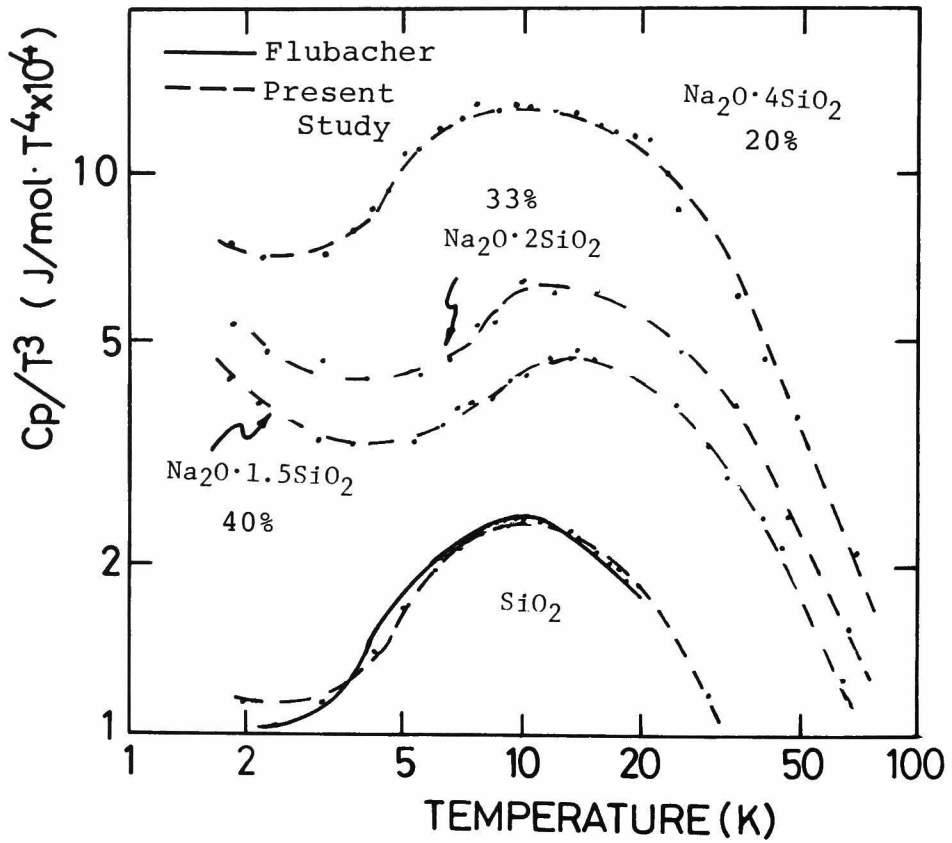
Fig.1(A) Specific heat for sodium silicate glasses
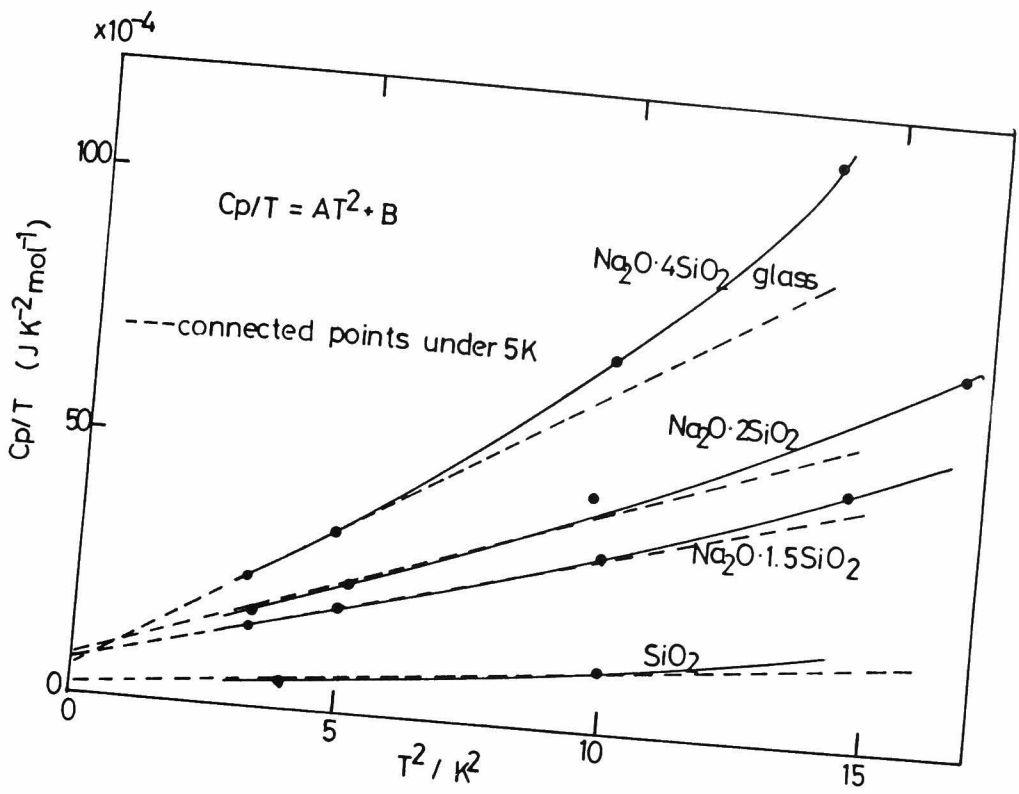
Fig.1(B)   Another plot for specific heat

The figure shows axes with C_p/T ($J K^{-2} mol^{-1}$) on the vertical axis (×10^{-4}) and T^2/K^2 on the horizontal axis. Equation shown: $C_p/T = AT^2 + B$. Curves labeled $Na_2O \cdot 4SiO_2$ glass, $Na_2O \cdot 2SiO_2$, $Na_2O \cdot 1.5SiO_2$, and SiO_2. Legend: --- connected points under 5K.

Table 1 Heat Capacity for SiO_2 glass

T	Cp/T^3	Cp/T^3
K	$J/mol \cdot K^4$ $\times 10^4$	$J/g \cdot K^4$ $\times 10^6$
1.99	1.16	1.93
3.15	1.15	1.91
4.28	1.42	2.37
5.12	1.71	2.84
6.09	1.98	3.29
7.05	2.18	3.64
7.95	2.30	3.83
9.32	2.38	3.96
10.08	2.43	4.05
11.25	2.42	4.04
12.06	2.37	3.95
13.23	2.33	3.88
14.15	2.26	3.77
15.23	2.11	3.50
16.05	2.10	3.50
17.29	2.00	3.33
18.15	1.95	3.25
19.03	1.86	3.10
20.16	1.83	3.05
30.31	1.17	1.95
41.32	0.75	1.25
50.98	0.53	0.89

Table 2. Heat Capacity for $Na_2O \cdot 1.5SiO_2$ glass

T	Cp/T^3	Cp/T^3
K	$J/mol \cdot K^4$ x10^4	$J/g \cdot K^4$ x10^6
1.84	4.33	2.85
2.23	3.94	2.59
3.13	3.36	2.21
3.80	3.31	2.18
5.01	2.69	1.77
5.50	3.34	2.20
6.51	3.59	2.36
7.10	3.86	2.54
7.70	3.95	2.60
8.51	3.98	2.62
9.49	4.29	2.82
10.56	4.38	2.88
11.90	4.70	3.09
13.60	4.71	3.10
14.12	4.87	3.20
15.51	4.70	3.09
24.90	3.89	2.56
30.21	3.28	2.16
33.72	2.89	1.90
41.52	2.43	1.60
46 53	2.16	1.42
66.24	1.26	0.83

Table 3. Heat Capacity for $Na_2O \cdot 2SiO_2$ glass

$\dfrac{T}{K}$	$\dfrac{Cp/T^3}{J/mol \cdot K^4 \; x10^4}$	$\dfrac{Cp/T^3}{J/g \cdot K^4 \; x10^6}$
1.83	5.44	2.99
2.26	4.81	2.64
3.10	4.68	2.56
4.07	4.34	2.38
5.51	4.42	2.43
6.51	4.70	2.58
7.65	5.44	2.99
8.50	5.49	3.01
10.03	6.44	3.53
11.99	6.19	3.40
15.51	6.21	3.41
24.92	4.88	2.68
34.01	3.86	2.12
46.01	2.44	1.34
65.63	1.55	0.85

Table 4. Heat Capacity For $Na_2O \cdot 4SiO_2$ glass

T	Cp/T^3	Cp/T^3
K	$J/mol \cdot K^4$ x10^4	$J/g \cdot K^4$ x10^6
1.80	7.47	2.47
2.19	7.07	2.34
3.13	7.13	2.36
3.72	7.92	2.62
4.12	8.64	2.86
4.57	9.34	3.09
5.01	10.82	3.58
5.45	11.00	3.64
6.14	11.99	3.97
7.02	12.51	4.14
7.57	13.30	4.40
8.67	12.85	4.25
9.59	13.21	4.37
10.62	13.09	4.33
12.05	12.85	4.25
13.77	12.75	4.22
15.79	12.12	4.01
17.36	11.79	3.90
19.32	11.58	3.83
20.84	11.39	3.77
23.07	9.91	3.28
24.66	8.55	2.83
34.84	6.01	1.99
40.55	4.62	1.53
48.43	3.63	1.20
69.02	2.12	0.70

4.3   Thermal expansion at very low temperatures

The thermal expansion of glass samples was determined by using a dilatometer described in Chapter 3.   The raw data were smoothed out to obtain thermal expansion coefficients as a function of temperature.   Fig.2 shows the results for sodium silicate glasses containing 0 to 40% of sodium oxide, together with potassium oxide.   The effect of the addition of sodium oxide on thermal expansion coefficient is shown in Fig.3, where α versus composition is plotted for different temperatures.   This figure indicates that α increases with increasing Na_2O content at low temperatures.   Fig.4 shows the results of lithium silicate glasses containing from 0 to 30 mol% lithium oxide.   The effect of the addition of lithium is shown also in Fig.5 where α versus composition was plotted for different temperatures.   In all cases, the thermal expansion coefficients appear to be essentially a linear function of alkali oxide content.   In comparison with the results of sodium silicate glasses, this figure shows that the thermal expansions of lithium silicate glasses are low.   The lithium silicate glass containing 10% Li_2O possesses negative thermal expansion coefficients below 35K.   Fig.6 shows T_N, below which thermal expansion coefficient has a negative value.   It is clear that the addition of sodium oxide gives a large effect on thermal expansion coefficient.
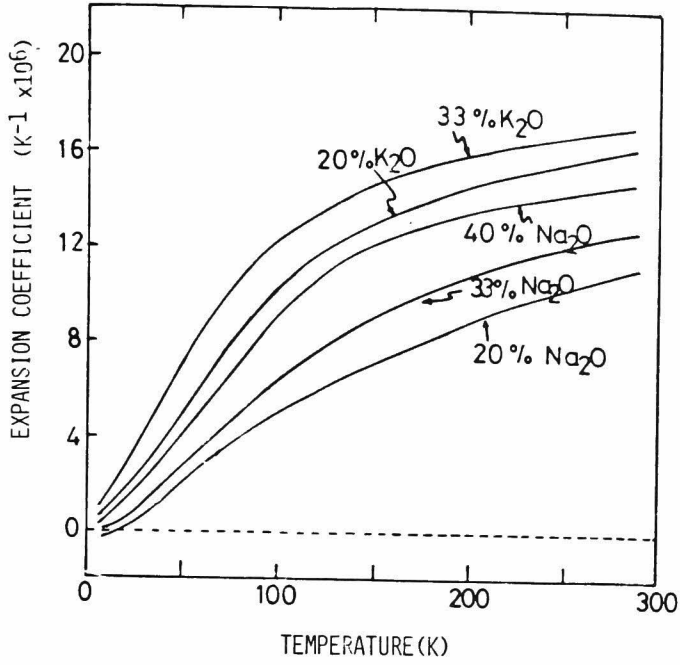
Fig. 2

Thermal expansion for
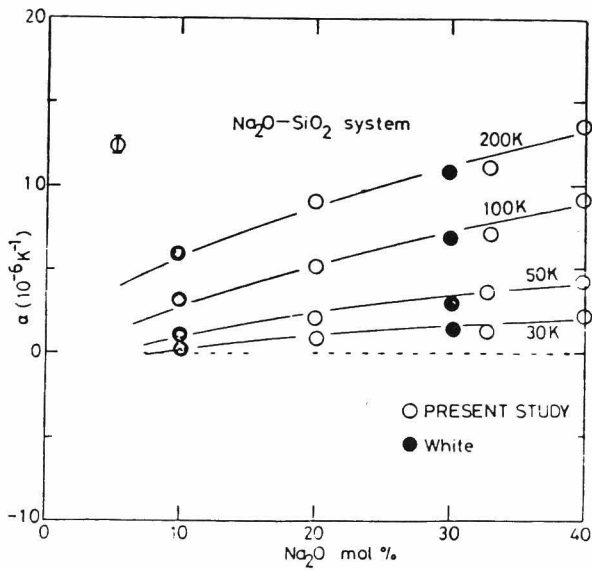
sodium silicate glasses

Fig. 3

Thermal expansion

coefficient versus

sodium content
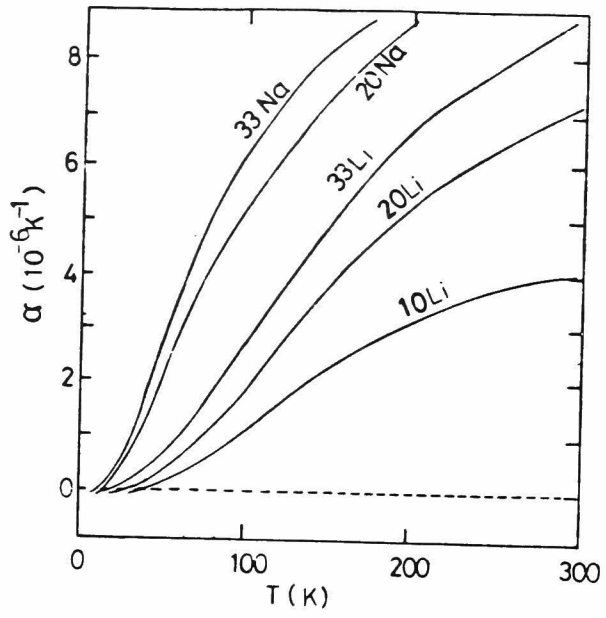
Fig. 4

Thermal expansion for

lithium silicate glasses
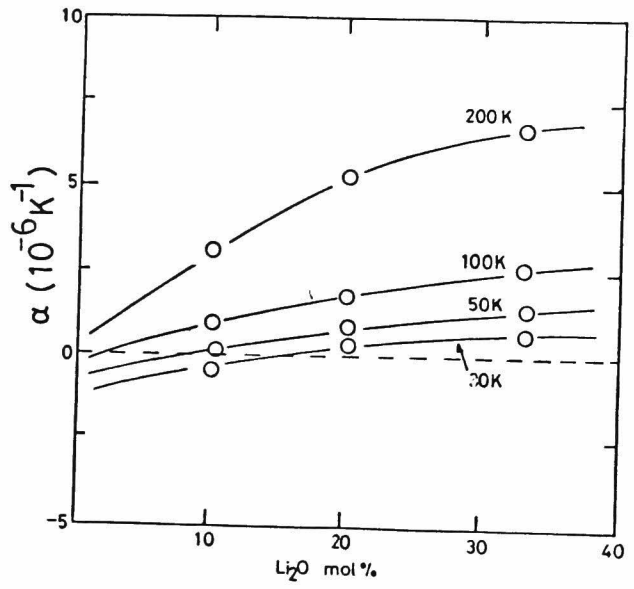
Fig. 5

Thermal expansion

coefficient

versus lithium content
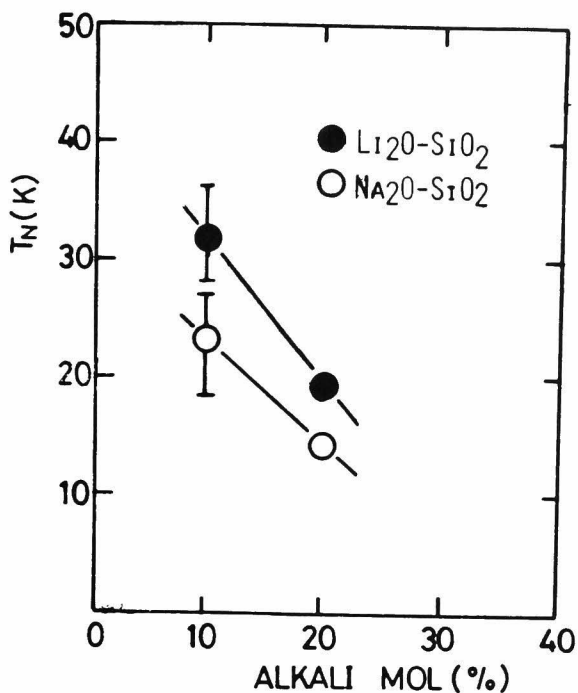
Fig.6

T_N versus alkali content

4.4 Grüneisen parameter and simple glass model system

In Chapter 2, it has been shown that the Grüneisen parameter of a simple glass model system is negative but it tends to become positive as the disorder or asymmetry of the glass system becomes less. This tendency can be examined based on the thermal data obtained in the previous sections. In order to obtain the thermal Grüneisen parameter, the knowledge of compressibility or bulk modulus for the glass is required. The values of bulk modulus for alkali silicate glasses were calculated from the sound wave velocities and density, and were shown in Table 5 along with the elastic Debye temperature. Since the temperature dependence of bulk modulus is very small, the values listed in Table 5 were used to calculate the

Grüneisen parameter at all temperatures. The error introduced by neglecting the temperature dependence of bulk modulus is estimated to be about 5%.

The values of thermal Grüneisen parameter are shown in Fig.7 as a function of normalized temperature, together with those obtained by White.[1] A small difference of about 5% between White's and the present values is considered to be due to the experimental error in thermal properties, particularly thermal expansion coefficients. It is clear from this figure that the negative Grüneisen parameter of vitreous silica is very much larger in magnitude and persists to much higher temperature than those of alkali silicate glasses. It reaches to a value of -5.5 at near $T/\Theta_D=0.01$, which is lower than the limiting value of $\gamma=-2.36$ calculated from the elastic data of Anderson.[4] The similar behavior of Borosilicate glass indicates that the substitution of small percent of boron atoms to silicon sites has little effect on the modes responsible for negative Grüneisen parameter. This result might be expected if these modes are associated with the transverse modes of the oxygen atoms.

On the other hand, the addition of network-filling atoms such as sodium ions in Fig.7 has considerable effect, and suppresses the negative Grüneisen function. At 40% Na_2O glass, γ becomes almost constant at all temperatures. In order to examine the effect of the difference in alkali ion, the temperature dependence of $\gamma(T)$ for alkali disilicate glasses was obtained and is illustrated in
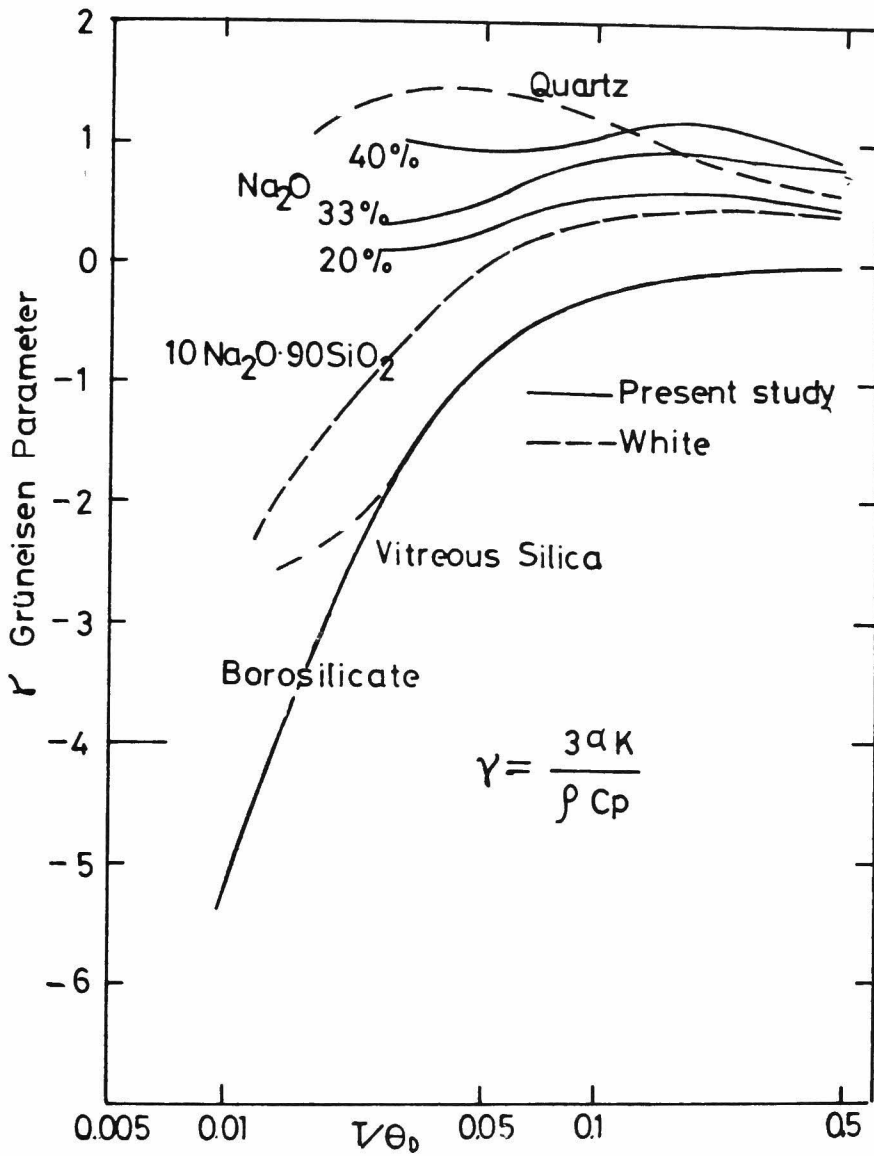
Fig. 7   Grüneisen function for alkali silicate
glasses

Fig.8. The value of γ decreases in the order, Cs>K>Na. Clearly, the Grüneisen parameter varies depending on the kind of alkali ions in the glass network. These structural aspects are connected with the packing density, which is represented by parameter $\frac{dd}{dL}$ discussed in Chapter 2. The increase in both amount and size of network filling atoms causes the increase in $\frac{dd}{dL}$ and thus the decrease in γ. In order to compare these experimental results with those obtained in Chapter 2 on the basis of the simple glass model system, the data are plotted as a function of $1/T$ so as to superimpose with the γ-N curves in Fig.11 in Chapter 2. A good agreement can be seen between these curves. Thus, it is concluded that the theory developed in Chapter 2 is suitable to explain the anharmonicity of alkali silicate glasses qualitatively.

Composition	ρ (g/cm^3)	V_p (km/s)	V_s (km/s)	Ks (Kb)	Θ_D (K)
Na$_2$O·2SiO$_2$	2.495	5.361	3.038	409.0	422.4
K$_2$O·2SiO$_2$	2.456	4.640	2.522	333.2	331.1
Cs$_2$O·2SiO$_2$	3.629	3.185	1.570	253.1	198.5
Na$_2$O·9SiO$_2$	2.288	5.565	3.478'	338.8	467.0
2Na$_2$O·8SiO$_2$	2.383	5.382	3.251	354.5	443.2
4Na$_2$O·6SiO$_2$	2.520	5.401	2.993	430.6	418.1

Table 5 Elastic constants and density for alkali silicate glasses
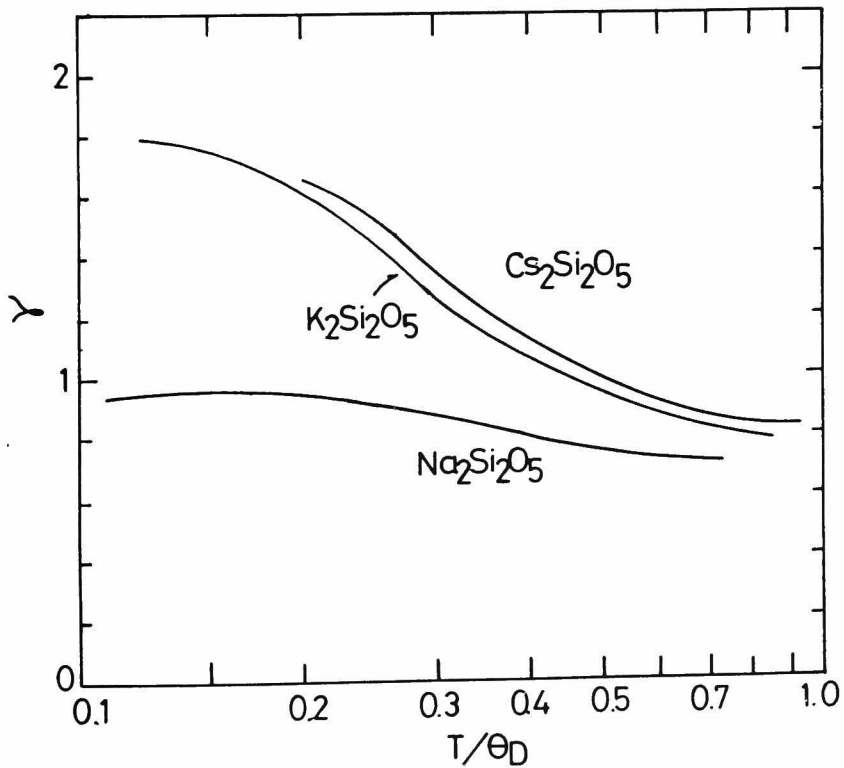
Fig.8 Grüneisen function for alkali disilicate glasses

SUMMARY TO CHAPTER 4

The heat capacity and thermal expansivity of vitreous silica and alkali silicate glasses were determined from 1.6K to 300K and the results were compared with the behaviors of thermodynamic properties of the simple glass model system obtained in Chapter 2. The main results obtained are summarized as follows.

1. The heat capacities of alkali silicate glasses at very low temperature did not obey the Debye continuum theory, and required other temperature dependent term than a T^3 term as prescribed by the simple glass model system. This excess heat capacity was not so sensitive to the compositional variation, indicating that this excess heat capacity does not reflect the easiness of bending motions of the network structures but arises mainly from the randomness of glass structure.

2. The thermal expansion coefficient increases with increasing Na_2O content at very low temperatures. This similar results were obtained for lithium containing glasses. The temperature T_N, defined as the temperature below which thermal expansion coefficient becomes negative, was found to be essentially a linear function of alkali content.

3. The Grüneisen parameter γ of vitreous silica was very much negative but this negative value was suppressed by the addition

of network-filling atoms such as sodium ions. At 40% Na_2O glasses, γ becomes almost constant like that of a stable crystalline solid. The tendency of alkali ions to suppress the negative behavior of γ was stronger with increasing alkali ion size. These results may be interpreted by the change in packing density due to the introduction of network modifiers into glass network.

The effects of temperature and compositional variation on Grüneisen parameter were in agreement with the general tendency of Grüneisen parameter of the simple glass model system obtained in Chapter 2.

REFERENCES

1.   G.K.White et al.,

                Phys. Rev., 112, 111 (1958)

2.   P.Fulbacher, A.J.Leadbetter et al.,

                J. Phys. Chem. Solids, 12, 53 (1959)

3.   J.G.Collins and G.K.White,

                Progress in Low Temperature Physics,

                4, 450 (1964)

4.   O.L.Anderson and G.Dienes,

                J. Non-Cryst. Solids, 449 (Ed. Frechette)

                (1960)

5.   E.F.Westrum,   Phys. Chem. Glasses, 9, 1 (1968)

6.   R.D.McCammon and G.K.White,

                Phys. Rev. Lett., 10, 234 (1963)

7.   W.B.Waniels,   Rev. Lett., 8, 3 (1962)

8.   O.L.Anderson,   J. Phys. Chem. Solids, 12, 41   1959

9.   A.J.Leadbetter,   Phys. Chem. Glasses, 9, 1 (1968)

10.   R.B.Stephens,   Phys. Rev., B8, 2896 (1973)

11.   A.J.Leadbetter and K.E.Wycherley,

                Phys. Chem. Glasses, 12, 41 (1971)

12.   R.G.Bohn,   J. Appl. Phys., 45, 2133 (1974)

13.   H.S.Chen and W.H.Haemmerle,

                    J. Non-Cryst. Solids, 11, 161 (1972)

14.   R.A.Fisher, G.E.Brodale, E.W.Hornung and W.F.Giauque,

                    Rev. Sci. Instr., 40, 365 (1969)

15.   G.K.White and J.A.Birch,

                    Phys. Chem. Glasses, 6, 85 (1965)

16.   E.W.Hornung, R.A.Fisher, G.E.Brodle and W.F.Giauque,

                    J. Chem. Phys., 50, 4878 (1969)

CHAPTER 5

THERMAL PROPERTIES OF ALKALI SILICATE GLASSES
AT LOW-TO-MODERATE TEMPERATURES

In the low-to-moderate temperature range, the phonon dispersion is no more significant, because the exciting frequency behaves as the Debye continuum. However, as described in Chapter 2, the simple Debye model is not suitable to describe the mode frequencies of multicomponent glasses, and the combination of more than two characteristic temperatures is required. The knowledge of these characteristic temperatures or the frequency distribution function obtainable from analysing heat capacity in the low-to-moderate temperature range is useful to discuss the nature of bond and structure of silicate glasses.

As for thermal expansion, many experimental studies have been carried out on various silicate glasses at room and high temperatures and it has been found that the expansion is sensitive to glass composition. However, in spite of its importance in discussing the anharmonic nature of chemical bonds in glass structure, the temperature dependence of thermal expansion coefficient has been studied little. So, the thermal expansion behaviors of alkali silicate glasses were determined in the low-to-moderate temperature range from 77 to 350K.

5.1   Heat capacities

The heat capacities of alkali silicate glasses including mixed alkali glasses were determined by using a calorimeter described in Sec.3.1.   The glass samples were prepared in the same manner as described in Chapter 4.1.   The values of Cp measured for various alkali silicate glasses from 80 to 300K are listed in Table 1-7 and shown in Fig.1-2.   It is clear that the heat capacity increases as alkali ions are changed from Na to K and from K to Cs, when compared at the same temperature.   The results for mixed alkali disilicate glasses are shown in Table 8, 9, 10 and in Fig.3.

In order to compare the heat capacity data of glasses having different alkali oxide/ silica ratios, the gram-atomic heat capacity was calculated by dividing the heat capacity per formula weight by the number of atoms in the formula.   The values of the gram-atomic heat capacity for mixed alkali glasses at 300K and 80K are shown in Fig.4 and 5, respectively.   While Cp decreases rapidly in all systems as alkali ions of large size are substituted by those of small size, Cp does not increase so much when small size ions are replaced by large size ions.   In other words, Cp deviates downwards from a linear line drawn between the values of two end members.

In order to show that the simple Debye model is not suitable to describe the heat capacities of alkali silicate glasses, an attempt was made to analyze the heat capacity data by means of the Debye theory.
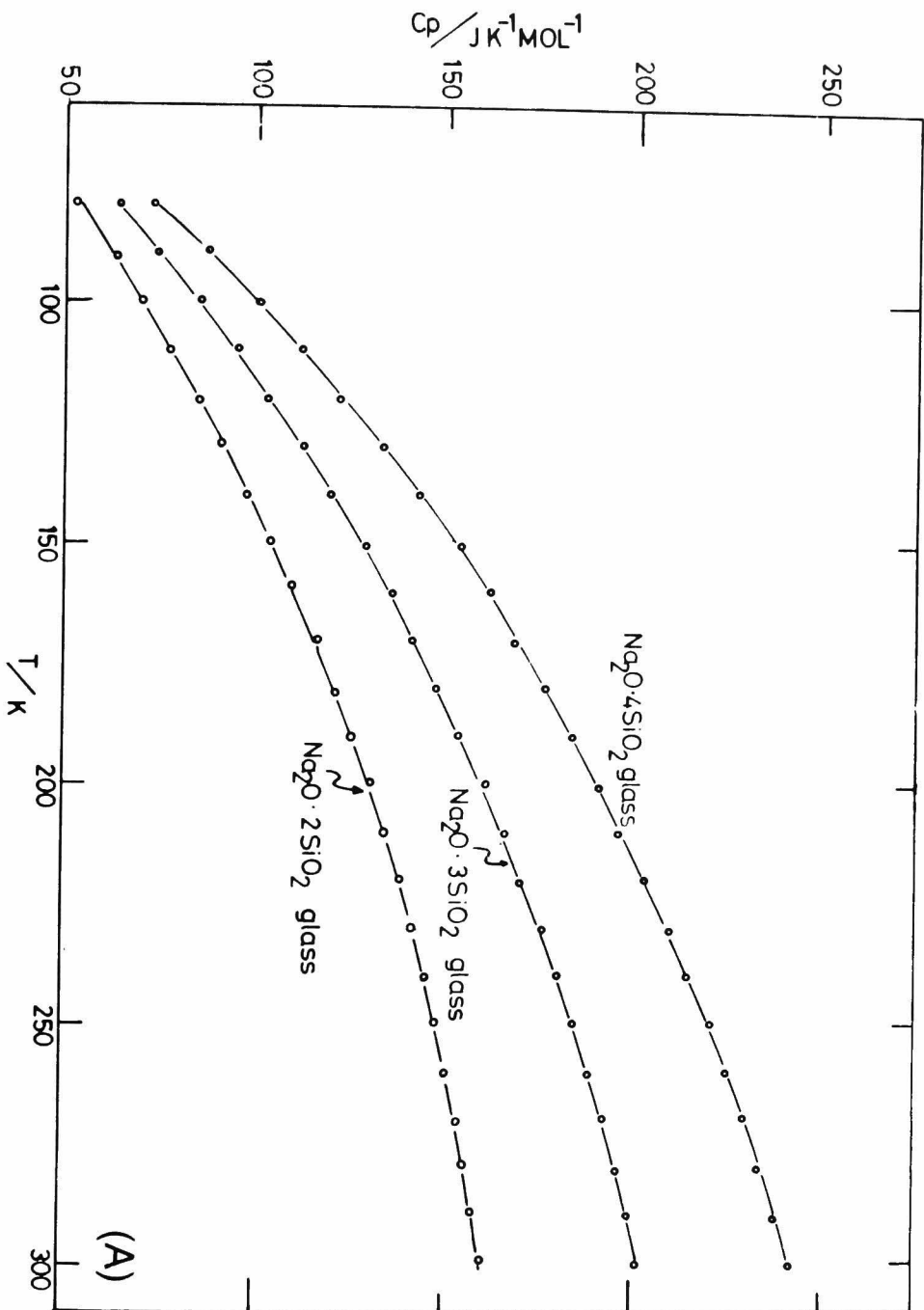
Fig.1　The temperature dependence of the low temperature
specific heat of $Na_2O \cdot mSiO_2$
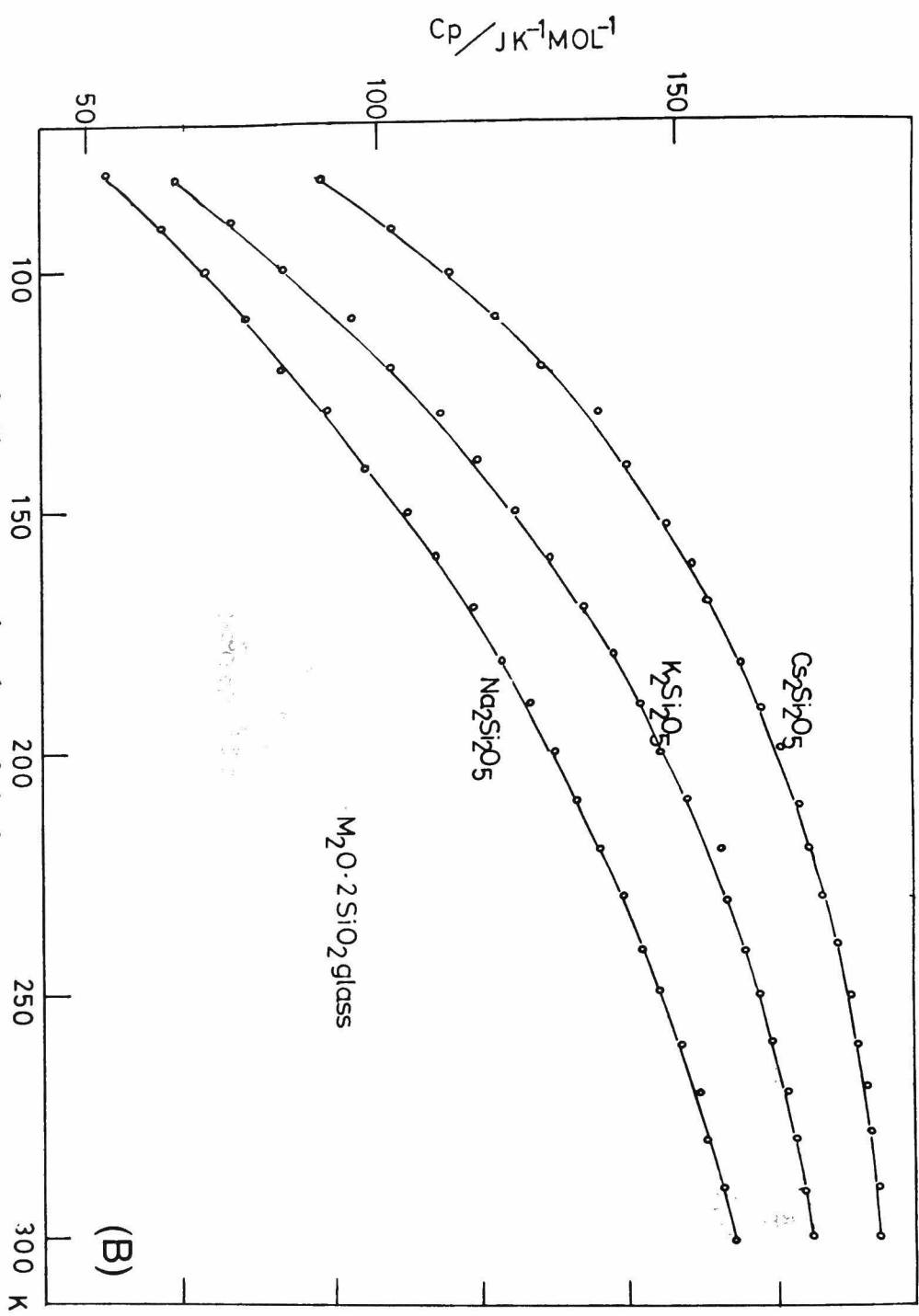
Fig. 2 The temperature dependence of the low temperature specific heat of $M_2O \cdot 2SiO_2$ glasses (M=Na, K, Cs)
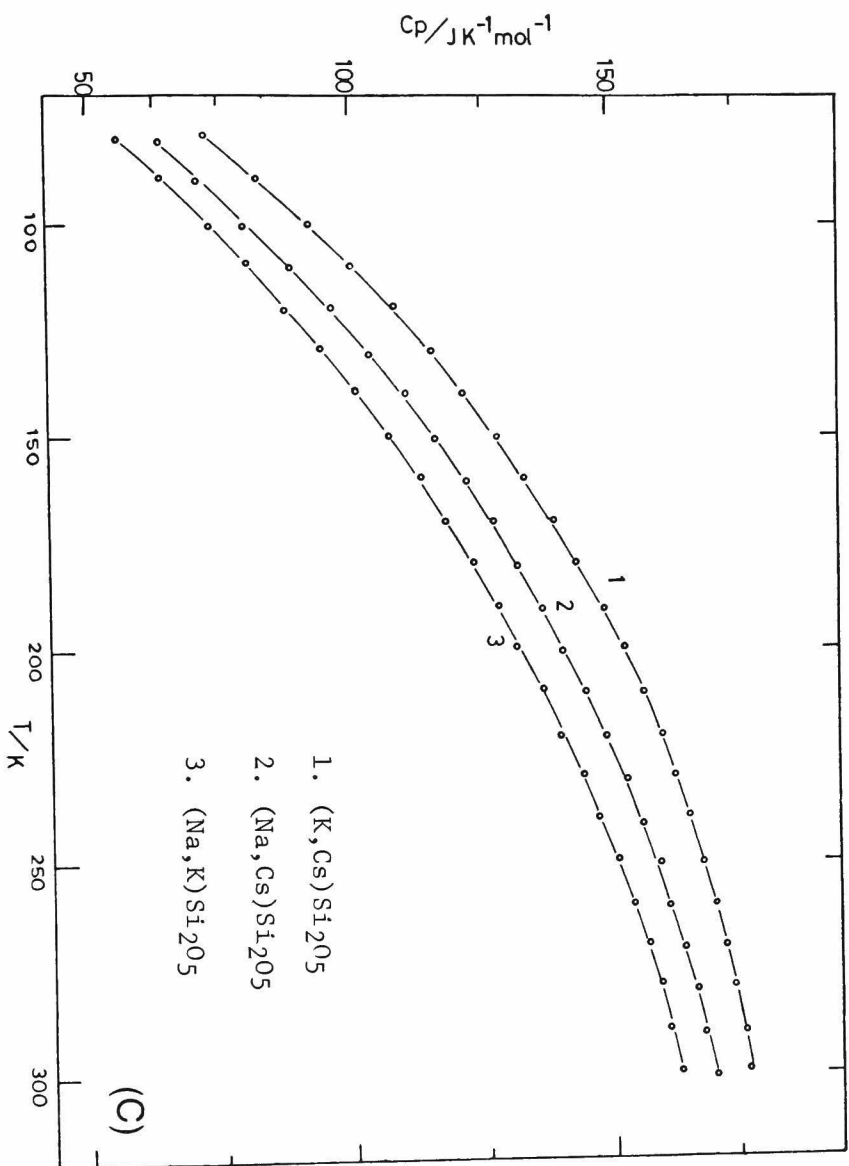
Fig.3 The temperature dependence of the low temperature
specific heat of mixed alkali silicate glasses
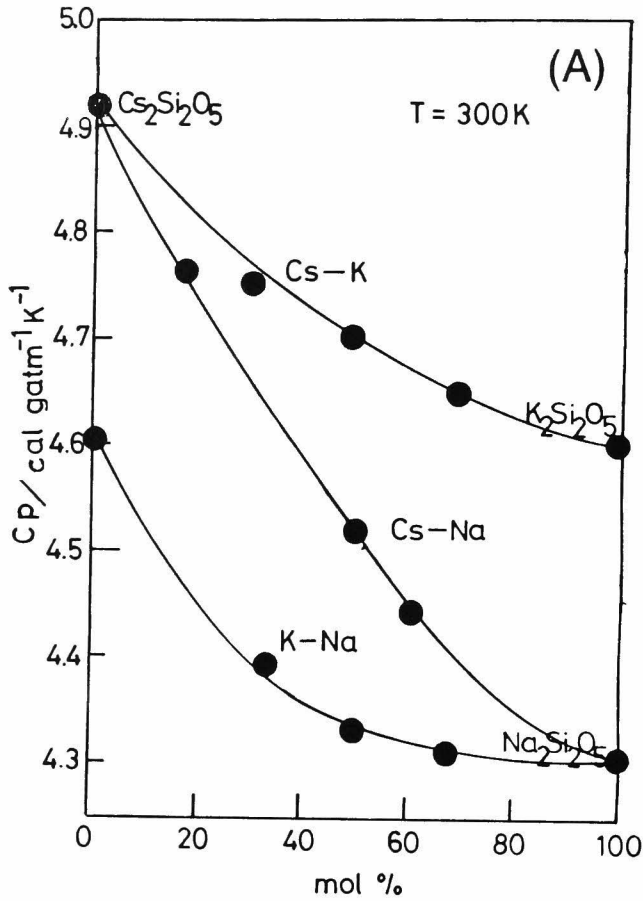
Fig.4 The specific heat capacity of mixed alkali silicate glasses at 300 K
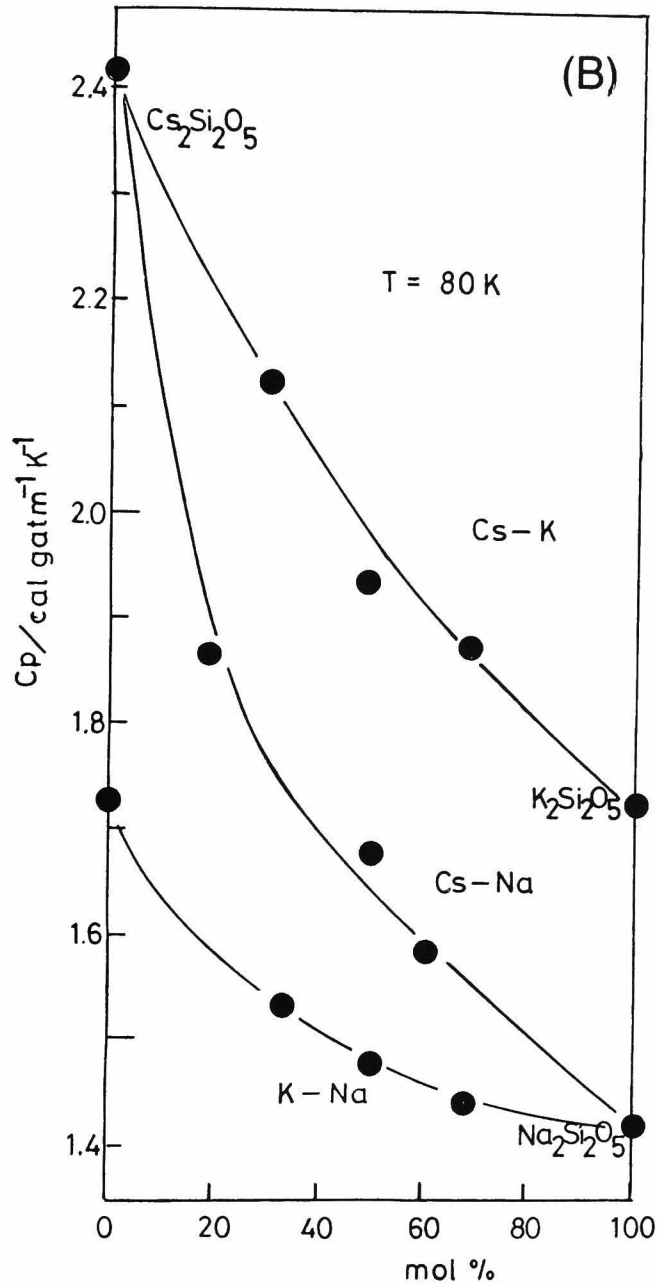
Fig.5 The specific heat capacity of mixed alkali silicate glasses at 80 K

If the Debye model were applicable, the corresponding Debye characteristic temperature calculated from the heat capacities at various temperatures should be constant over a wide temperature. The results of calculation for various alkali silicate glasses are shown in Fig. 6. Also included are the results for fused silica based on the heat capacity data by Westrum.[1] The values of Θ_D appear to vary with temperature. It is evident from this figure that the Debye theory is inadequate to represent the temperature dependence of heat capacity for alkali silicate glasses and other expression, such as the three band theory developed in Chapter 2, is required.
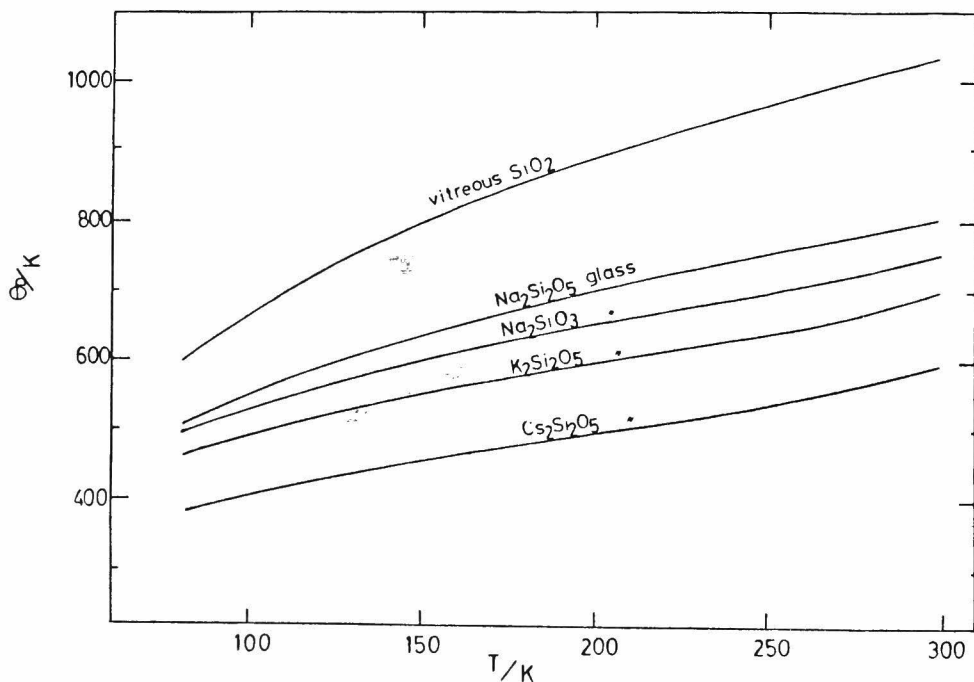
Fig.6 The corresponding Debye characteristic temperature by the application of Debye model
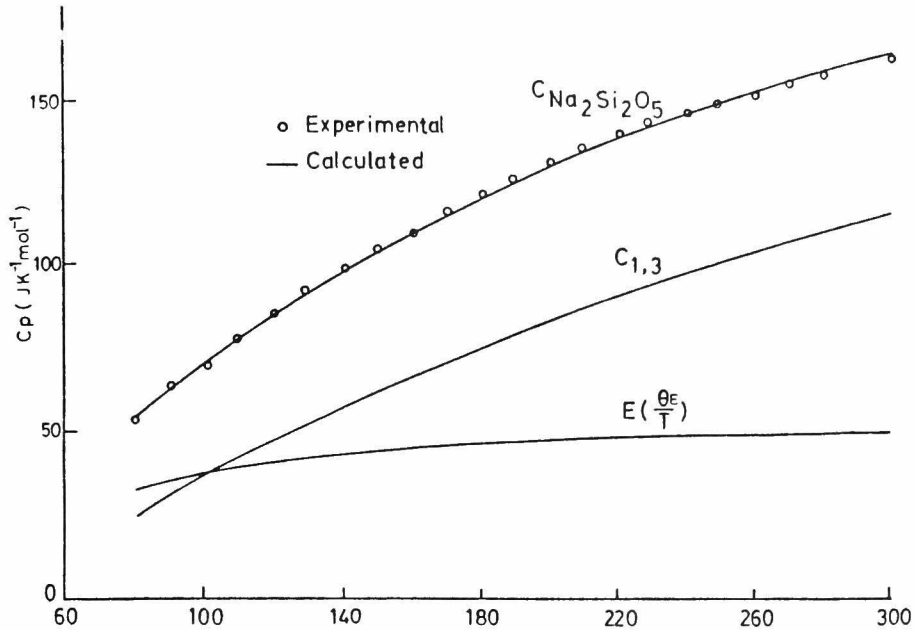
Fig.7 Temperature dependence of specific heat in sodium
disilicate glasses

The same data were analyzed on the basis of the three band

theory by fitting them to the equation (62) in Chapter 2 with an aid

of a computer at Kyoto University. An example for $Na_2Si_2O_5$ glass is

shown in Fig.7. The calculated curve represents the one for $\Theta_1=1300$

, $\Theta_3=400$ and $\Theta_E=230K$. A good agreement between the experimental and

calculated values is seen in this figure.

5.2   Comparison of characteristic temperatures Θ_1, Θ_3 and Θ_E

The independent analyses of the data shown in Table 1-4 based

on equation gave the value of $\Theta_E=220K$ for $Na_2O \cdot 2SiO_2$ glass and $260K$

for $Na_2O \cdot 6SiO_2$ glass. As can be seen in Eq.62 in Chapter 2, a small

variation in Θ_E for a glass containing low alkali content should not

cause any noticeable change in the best fit curve. Furthermore, the

above values of Θ_E are close each other.

When the three band theory was developed in Chapter 2, it was assumed that M-O bonds vibrate independently as the Einstein's model requires. Thus the value of 220K, which was obtained for the glass containing the highest amount of sodium oxide, was chosen as Θ_E for all the sodium silicate glasses, and the values of Θ_1 and Θ_3 were calculated. The results are shown in Fig.8 as a function of alkali mole ratio in glass composition. The standard deviation based on these three characteristic temperatures were about the same as the first try. This may be taken as a proof that the vibrations of alkali ions in silicate glasses are influenced little by the Si-O chains and they may be regarded as those of independent vibrators, as postulated by the Einstein function.

As described in Chapter 2, the first characteristic temperature Θ_1 is associated with the strength of elastic interchain Si-O bonds. The value of Θ_1=1550K for vitreous silica corresponds to the frequency of about 1080 cm^{-1}, and this is very close to the main peak of infrared absorption of vitreous silica.[2)-5)] The second characteristic temperature Θ_3, which represent the lateral interaction of the chains , is very low for vitreous silica in comparison with Θ_1 and thus the ratio Θ_3/Θ_1 is small (0.09). The introduction of alkali ions causes a decrease in Θ_1 and an increase in Θ_3, resulting in an increase in Θ_3/Θ_1 as shown in figure. As Na_2O is introduced into the SiO_2 network, the Si-O chain is broken and the directional bonding nature of Si-O bonds diminishes, resulting in weakening of the strength of
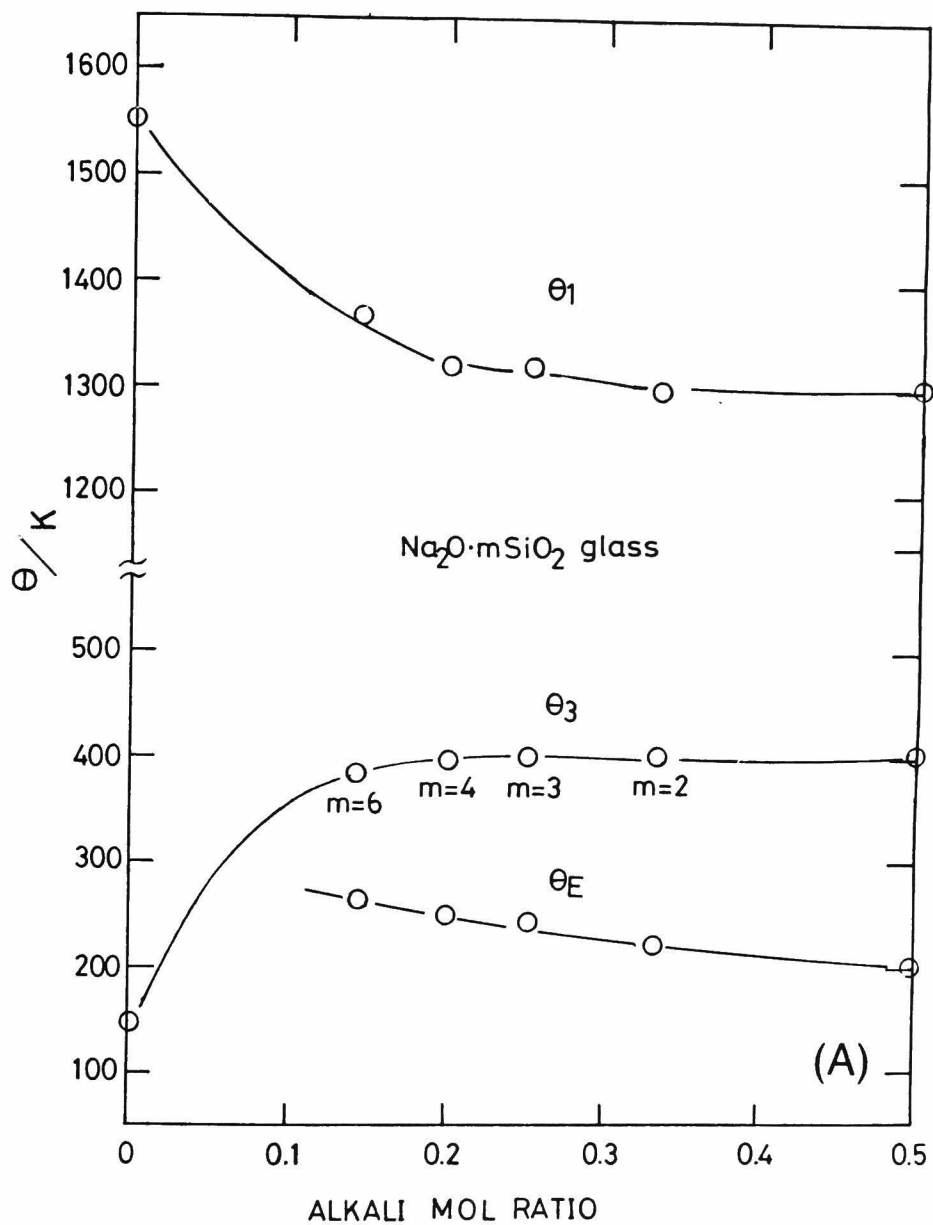
Fig.8 The three characteristic temperatures of sodium
silicate glasses

elastic interchain Si-O bonds and strengthening the lateral inter-
action of SiO_2 skeleton. Thus it may be considered that Θ_3/Θ_1 is
a kind of measure for non-directionality or ionic component of
bonding in silicates.

The effect of the kind of alkali ions in silicate glasses on
the characteristic temperatures is shown in Fig.9 for alkali disili-
cate glasses. It is clear that Θ_E increases in the order of Cs, K
and Na, which can be expected from the bond strength. Furthermore,
Θ_E for a mixed alkali silicate glass falls on a line drawn between
the values of two members. This additivity shows that there is no
mixed alkali effect on the vibrational modes of M-O bonds and these
bonds vibrate independently, satisfying the assumption of the present
three band theory.

Both Θ_1 and Θ_3 decreases as Na is substituted by K or Cs, in
the same manner as Θ_E. This result indicates that higher vibrational
frequencies are observable when SiO_4 tetrahedra are connected by
metal polyhedra of lighter atoms or the ones with strong interatomic
binding forces. This is consistent with the observations of infrared
spectra on alkali disilicate glasses that the stretching vibration
frequencies decrease in the order of Na, K and Cs.[6],[7]
The value of Θ_3/Θ_1 was found to vary little from 0.31 for $Na_2O \cdot 2SiO_2$
glass to 0.28 for $Cs_2O \cdot 2SiO_2$ glass in spite of a large variation
in Θ_1 and Θ_3. As discussed before, Θ_3/Θ_1 is considered as a measure
of ionic component of bonding in silicate glasses. Thus, this
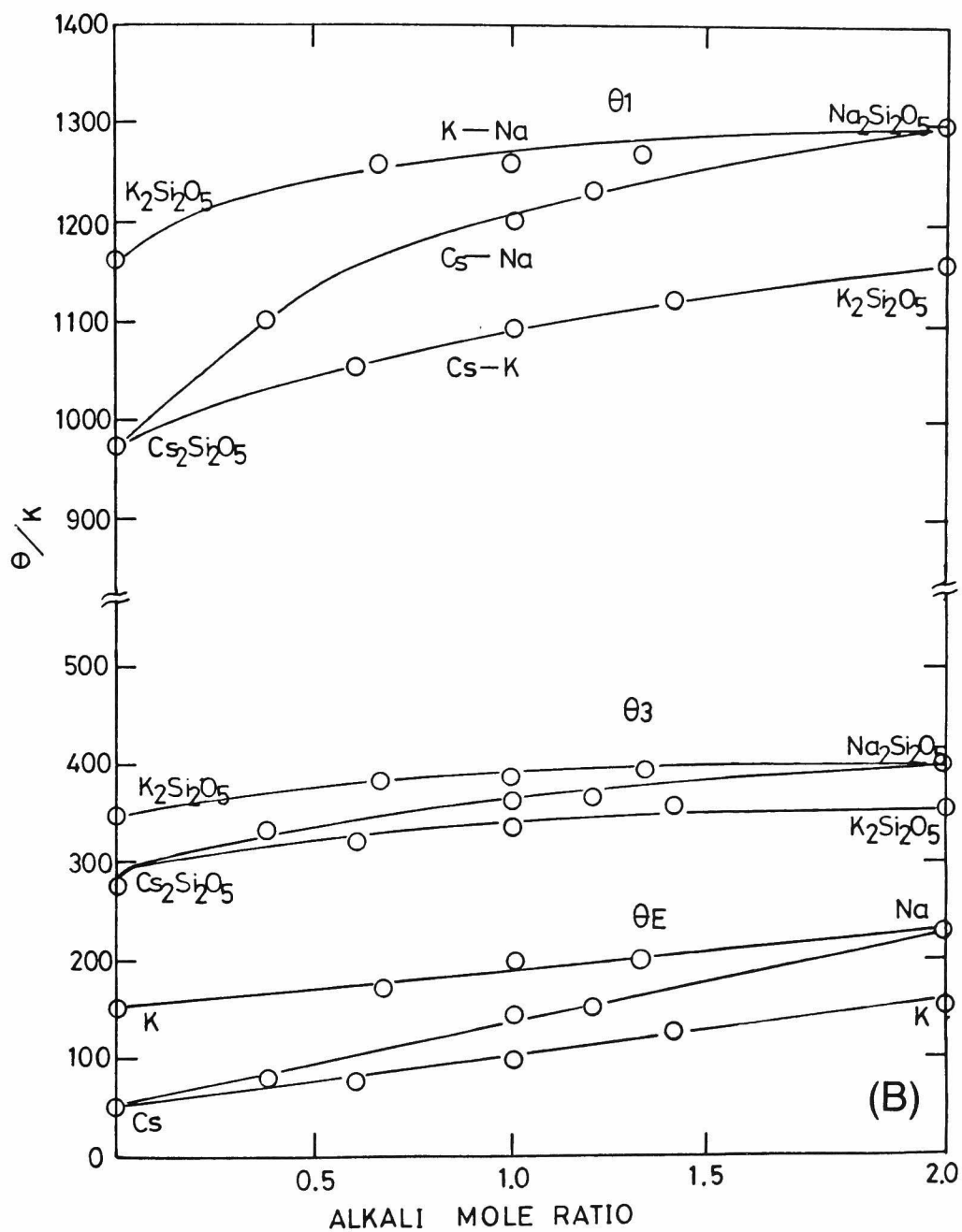
Fig.9   The three characteristic temperatures of mixed
        alkali silicate glasses

constancy in Θ_3/Θ_1 for alkali disilicate glasses indicates that the ionic components of bonding for these glasses are about the same. This result is consistent with the fact that the ionicity of M-O bond based on electronegativity is about the same for Na-O, K-O and Cs-O bonds. Thus, unless the ratio of M_2O/SiO_2 is changed, the ionic component of bonding in silicate glasses is expected to remain almost unchanged.

For mixed alkali disilicate glasses, both Θ_1 and Θ_3 show little positive deviations from the linear additivity, indicating that the Si-O chains are tightened slightly by mixing two kinds of alkali ions. This tightening effect might be related with the mixed alkali effect found on other physical properties.[8)-20)]

T	Cp	T	Cp
K	$JK^{-1}mol^{-1}$	K	$JK^{-1}mol^{-1}$
80.2	37.7	200.3	93.3
89.3	43.5	210.2	95.4
100.2	50.7	221.0	98.4
111.3	56.5	230.1	100.5
120.8	62.0	241.2	102.6
130.7	66.1	250.8	104.2
141.2	71.2	261.0	105.9
150.8	75.3	269.8	108.0
160.3	79.5	280.2	108.8
171.2	84.1	291.0	110.1
179.6	87.1	300.3	110.2
189.8	90.4		

Table 1.   Molar heat capacity of $Na_2O \cdot SiO_2$ glasses

T	Cp	T	Cp
K	$JK^{-1}mol^{-1}$	K	$JK^{-1}mol^{-1}$
80.3	53.6	200.1	130.6
91.8	64:0	210.5	134.4
100.5	70.7	220.3	138.1
110.3	77.9	230.2	141.5
121.2	85.8	241.0	145.3
129.8	91.3	250.2	147.8
141.0	98.4	260.9	151.1
150.9	104.7	270.2	154.0
159.7	110.5	279.5	156.1
170.9	116.4	290.2	158.2
181.2	121.4	300.5	160.3
190.3	126.0		

Table 2. Molar heat capacity of $Na_2O \cdot 2SiO_2$ ($Na_2Si_2O_5$) glasses

T	Cp	T	Cp
K	$JK^{-1}mol^{-1}$	K	$JK^{-1}mol^{-1}$
80.1	63.9	200.2	160.2
90.3	74.0	210.1	165.2
100.2	85.1	220.0	170.3
110.1	95.3	230.5	175.4
120.3	103.4	240.6	179.4
130.1	112.5	250.2	183.5
140.2	120.6	260.3	187.5
150.0	128.7	270.9	191.6
160.2	135.8	280.3	195.7
170.5	140.9	290.4	198.7
180.4	148.0	300.2	201.7
190.4	154.1		

Table 3. Molar heat capacity of $Na_2O \cdot 3SiO_2$ glasses

T.	Cp	T	Cp
K	$JK^{-1}mol^{-1}$	K	$JK^{-1}mol^{-1}$
80.1	73.4	200.2	191.0
90.4	87.3	210.5	196.1
100.5	101.2	220.3	202.4
111.3	111.3	230.1	208.8
120.6	122.7	241.3	213.8
130.7	132.8	250.2	218.8
141.2	143.0	260.9	222.7
150.9	153.1	269.8	229.0
159.7	160.7	280.2	232.8
170.2	168.3	291.0	237.8
181.2	175.9	300.3	241.6
190.1	183.4		

Table 4.   Molar heat capacity of $Na_2O \cdot 4SiO_2$ glasses

T	Cp	T	Cp
K	$JK^{-1}mol^{-1}$	K	$JK^{-1}mol^{-1}$
80.8	102.8	200.5	267.4
90.1	122.3	209.3	274.6
99.3	141.5	219.8	284.1
110.1	155.8	229.3	292.2
119.7	171.6	240.8	299.1
130.1	185.9	249.9	306.3
140.8	199.2	261.0	312.1
150.3	214.3	270.2	320.6
161.1	226.2	279.3	325.8
169.8	235.6	290.5	332.3
180.2	246.3	300.1	338.3
189.8	255.8		

Table 5. Molar heat capacity of $Na_2O \cdot 6SiO_2$ glasses

T	Cp	T	Cp
K	$JK^{-1}mol^{-1}$	K	$JK^{-1}mol^{-1}$
80.5	65.3	200.8	148.6
90.1	75.3	210.2	152.8
100.5	85.8	220.9	158.6
110.8	95.9	231.2	159.1
120.5	103.0	241.5	162.4
130.8	110.9	250.8	164.5
140.9	117.6	261.0	167.0
150.3	123.9	270.6	169.1
161.2	130.2	280.3	170.8
170.8	135.6	291.2	172.5
180.9	140.2	299.8	172.9
190.3	144.4		

Table 6. Molar heat capacity of $K_2O \cdot 2SiO_2$ ($K_2Si_2O_5$) glasses

T	Cp	T	Cp
K	$JK^{-1}mol^{-1}$	K	$JK^{-1}mol^{-1}$
80.2	91.3	200.3	168.7
92.0	103.0	211.3	171.6
101.8	112.6	220.8	173.7
110.6	120.6	230.6	175.8
120.3	128.9	241.3	177.9
130.6	136.0	250.9	181.3
142.0	142.7	261.3	182.1
153.5	150.0	270.8	183.3
162.2	154.0	279.8	184.2
169.6	157.0	291.2	185.0
182.3	162.4	300.8	185.4
191.8	165.3		

Table 7. Molar heat capacity of $Cs_2O \cdot 2SiO_2(Cs_2Si_2O_5)$ glasses

$\dfrac{T}{K}$	$\dfrac{Cp}{JK^{-1}mol^{-1}}$	$\dfrac{T}{K}$	$\dfrac{Cp}{Jk^{-1}mol^{-1}}$	$\dfrac{T}{K}$	$\dfrac{Cp}{JK^{-1}mol^{-1}}$
$(Na_{0.66}K_{1.34})Si_2O_5$		$(Na_{1.0}K_{1.0})Si_2O_5$		$(Na_{1.34}K_{0.66})Si_2O_5$	
80.1	57.8	80.6	55.7	80.1	54.4
90.3	65.7	89.8	63.6	90.3	62.8
100.5	74.5	100.4	72.0	100.5	71.6
110.3	82.9	111.2	80.8	110.4	80.0
120.8	90.0	120.4	87.9	120.6	86.7
131.0	97.1	130.6	95.0	130.3	93.8
139.9	103.0	140.0	101.3	140.9	100.0
150.0	109.7	151.8	107.6	151.3	106.3
161.1	115.1	160.5	113.9	160.3	113.4
170.3	121.0	170.4	118.9	170.2	118.0
180.2	126.4	180.4	124.3	180.1	123.1
191.0	131.0	190.2	128.5	190.1	128.1
200.5	134.8	200.5	133.1	200.9	131.9
210.2	137.7	211.4	136.0	210.9	135.2
221.3	143.2	221.0	140.6	220.3	139.4
230.1	146.9	230.4	144.8	231.0	143.2
240.8	150.7	240.8	148.2	240.5	147.8
251.3	154.0	250.6	151.5	250.3	150.7
260.9	156.6	260.2	154.5	260.8	153.6
270.1	159.1	270.6	157.0	270.2	155.3
280.1	161.6	280.9	159.5	280.7	158.2
291.2	164.1	291.5	161.6	291.0	156.1
300.5	165.3	300.4	163.3	300.4	162.0

Table 8. Molar heat capacity of $(Na_2O,K_2O)\cdot 2SiO_2$ glasses

T	Cp	T	Cp	T	Cp
$\overline{K}$	$\overline{JK^{-1}mol^{-1}}$	$\overline{K}$	$\overline{JK^{-1}mol^{-1}}$	$\overline{K}$	$\overline{JK^{-1}mol^{-1}}$
$(K_{0.6}Cs_{1.4})Si_2O_5$		$(K_{1.0}Cs_{1.0})Si_2O_5$		$(K_{1.4}Cs_{0.6})Si_2O_5$	
80.3	80.0	80.3	72.8	80.1	70.7
90.5	89.6	90.5	82.0	90.2	80.4
100.2	97.1	100.2	91.7	100.8	90.0
111.0	105.1	111.2	92.5	110.3	90.8
120.7	113.0	120.4	109.3	120.2	107.6
130.8	120.6	130.8	116.0	130.9	114.3
140.2	128.1	140.9	122.2	140.0	120.6
150.9	133.5	150.9	128.1	150.1	126.4
161.3	139.0	160.2	134.0	160.2	132.3
170.0	144.0	169.5	139.0	170.9	137.3
179.8	148.6	180.0	144.1	179.3	142.3
190.4	152.4	190.2	149.0	189.3	147.3
200.7	156.6	200.7	153.2	200.2	151.5
210.8	160.3	210.1	157.0	210.9	155.3
220.3	163.7	220.5	159.9	220.1	158.2
230.8	167.0	230.3	163.3	230.2	159.0
240.3	170.0	240.6	165.8	240.2	164.1
250.9	172.5	250.0	167.9	250.3	166.2
260.2	175.0	260.1	170.4	260.8	168.7
270.4	176.2	270.9	172.5	270.8	170.8
280.5	177.5	280.2	174.6	280.3	172.9
291.3	178.3	290.7	175.8	290.7	174.1
300.7	178.7	300.1	177.1	300.8	175.4

Table 9. Molar heat capacity of $(K_2O \cdot Cs_2O) \cdot 2SiO_2$ glasses

T	Cp	T	Cp	T	Cp
K	$JK^{-1}mol^{-1}$	K	$JK^{-1}mol^{-1}$	K	$JK^{-1}mol^{-1}$
$(Na_{0.38}Cs_{1.62})Si_2O_5$		$(Na_{1.0}Cs_{1.0})Si_2O_5$		$(Na_{1.2}Cs_{0.8})Si_2O_5$	
80.3	70.3	80.8	63.2	80.1	59.4
90.4	80.4	90.2	74.1	90.5	67.0
100.4	89.2	100.4	80.0	100.5	75.8
110.9	90.0	110.7	88.7	110.7	84.6
121.0	106.3	120.2	96.7	119.8	92.1
130.2	113.4	130.7	103.8	130.2	98.8
140.6	119.7	140.3	110.5	140.7	105.5
150.9	125.6	150.1	116.8	150.2	111.8
159.8	131.0	160.6	122.6	160.3	117.6
170.3	135.6	169.2	127.7	170.2	123.5
180.3	141.1	180.8	132.7	180.6	128.5
190.2	146.5	190.2	136.5	190.3	133.1
200.3	152.0	200.5	141.1	200.2	136.9
210.5	155.7	210.3	145.7	210.8	141.1
220.7	159.1	220.9	149.9	220.4	144.8
231.0	161.6	230.3	153.2	230.5	148.6
240.6	164.5	239.7	156.6	240.6	152.4
250.2	165.8	250.8	159.5	249.9	155.7
260.1	168.3	260.1	161.6	260.8	157.8
269.8	171.2	270.4	164.5	270.0	160.3
280.7	172.0	280.4	166.6	280.3	162.4
290.3	173.3	290.1	168.7	290.1	165.3
300.3	174.6	300.6	170.4	300.4	167.4

Table 10. Molar heat capacity of $(Na_2O, Cs_2O) \cdot 2SiO_2$ glasses

5.3   Thermal expansion

Although the thermal expansion coefficients for the binary lithium, sodium, potassium, rubidium and cesium silicate glasses[21],[22] have been reported by some authors between 25°C to 200°C, there exist no precise data on temperature dependence of thermal expansion coefficient. The thermal expansion coefficients were determined for alkali disilicate glasses between 77 to 350K by means of the precision dilatometer described in Chapter 3. All samples were prepared by grinding flats on opposite faces. The results of thermal expansion coefficients for alkali disilicate glasses are summarized in Fig.10. As shown in this figure, the thermal expansion coefficient increases with increasing a cation size in the order from Li to Cs. This observation is consistent with the tendency of bond stretching of Si-O with the addition of alkali ions in IR spectra.

It should be noted that at room temperature the thermal expansion coefficient varies with temperature for lithium and sodium silicate glasses but not so much for the potassium, rubidium and cesium silicate glasses. This behavior is similar to that of heat capacity.

The compositional dependence of thermal expansion coefficients for binary alkali silicate glasses are shown in Fig.11. In all cases, the thermal expansion coefficient increases with increasing alkali content.

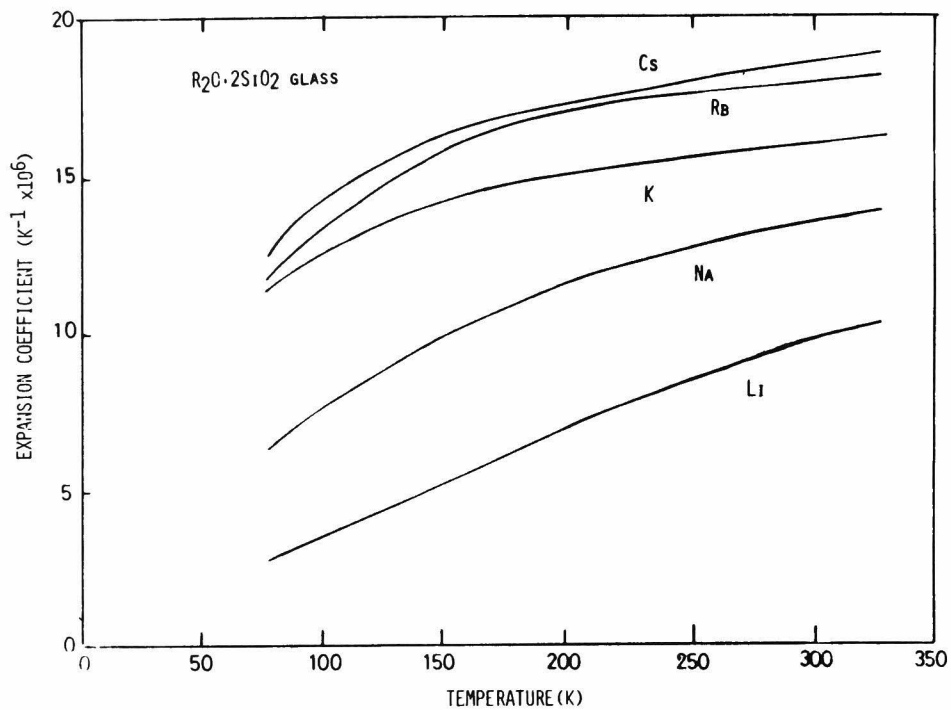The thermal expansion coefficients of mixed alkali silicate

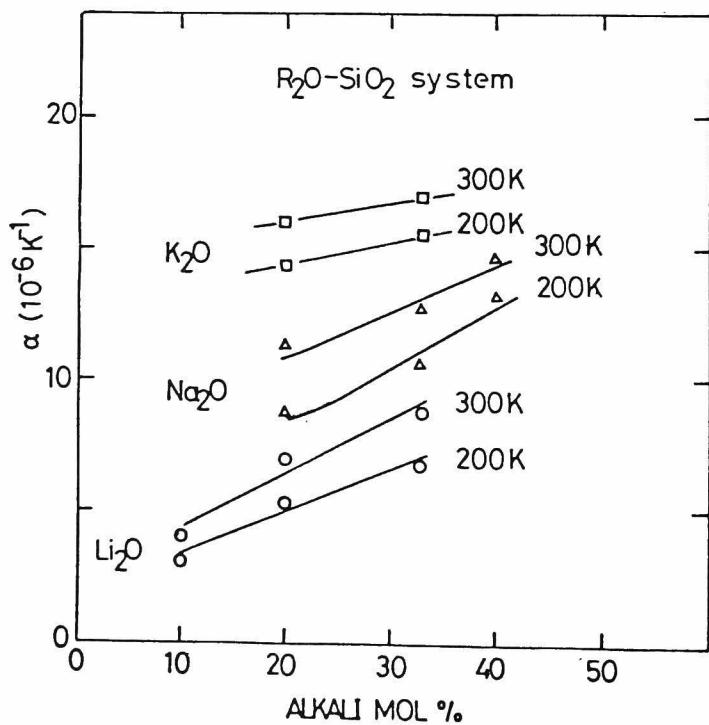Fig. 10 Thermal expansion coefficient for alkali
disilicate glasses

Fig.11

The compositional
dependence for
binary alkali
silicate glasses

glasses are shown in Fig.12-15 for the disilicate composition and Fig.16-19 for the pentasilicate composition. It is clear that the temperature dependence of thermal expansion coefficients for mixed alkali silicate glasses are different from that of the single alkali glasses. In order to observe these behaviors, thermal expansion coefficients are plotted against the composition at various temperatures in Fig.20 and 21. From these results, both series of sodium-cesium and lithium-cesium silicate glasses show a negative deviation from additivity, whereas both series of sodium-potassium and potassium-rubidium silicate glasses exhibit such a peculiar behavior that the deviation changes from negativity to positivity as the temperature increases. The data shown in Fig.20 and 21 can be used to determine the relative mixed alkali effect due to various pairs of alkali oxides. These figures indicate that the mixed alkali effect on thermal expansion coefficient is depending on the radius ratio of mixed alkali ions: the magnitude of the negative deviation from additivity at constant temperature decreased in the order of K-Rb, Na-K, Cs-Na and Li-Cs. This behavior is very similar to the results obtained from internal friction studies of identical glasses,[23],[24] which exhibit a large damping peak when two kinds of very different alkali oxides are present in the glass.

According to Shelby,[21] the mean expansion coefficients between 200-300°C for Na-K and Na-Rb glasses show a positive deviation from
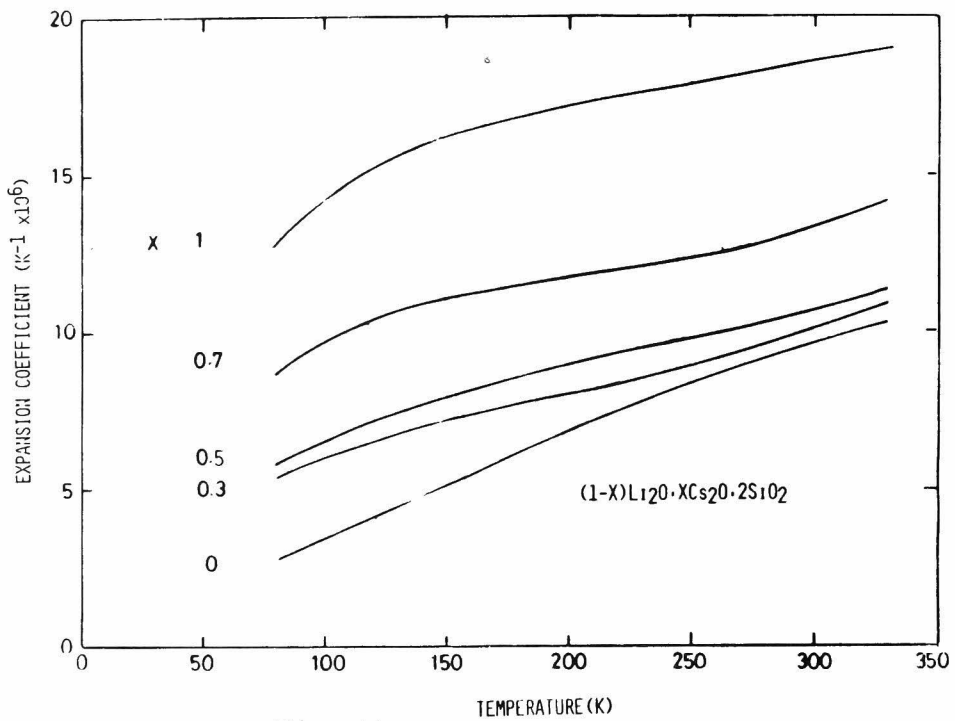
Fig. 12
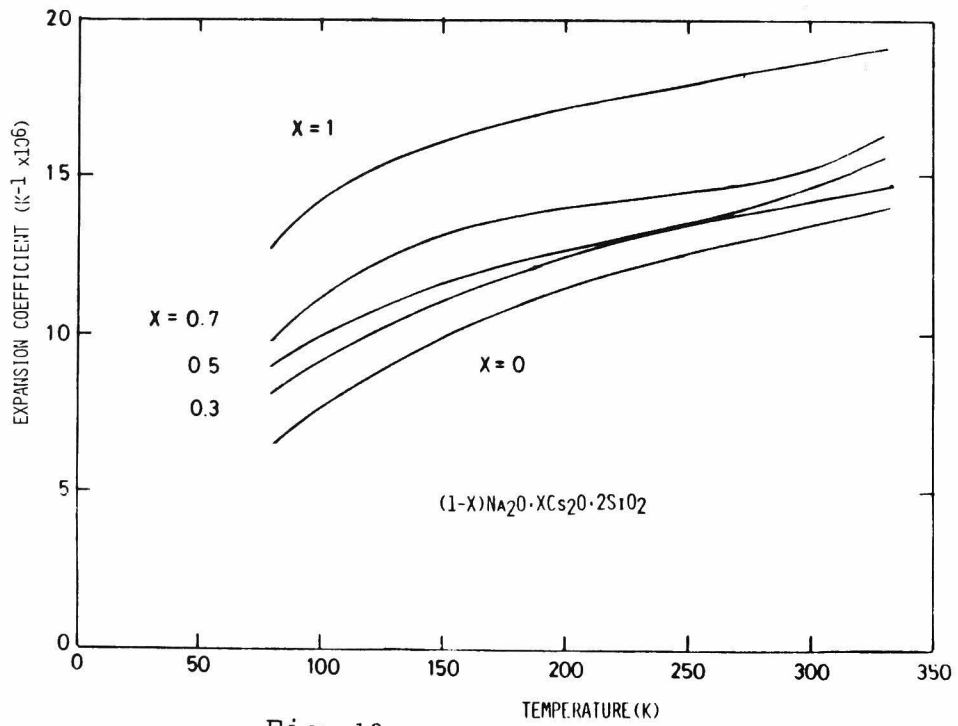
Fig. 13
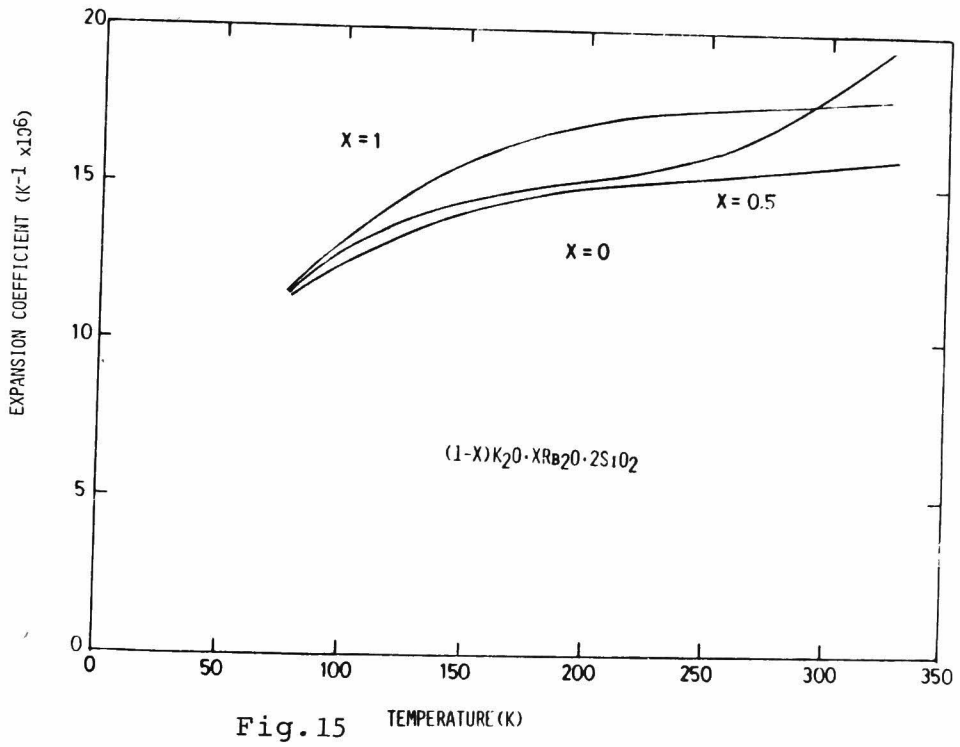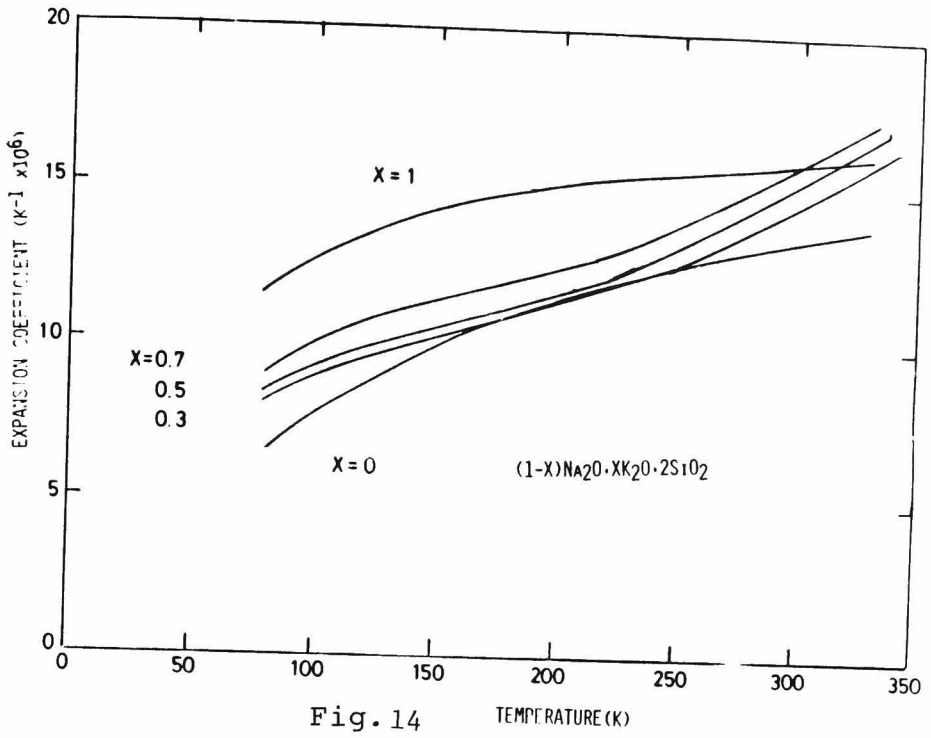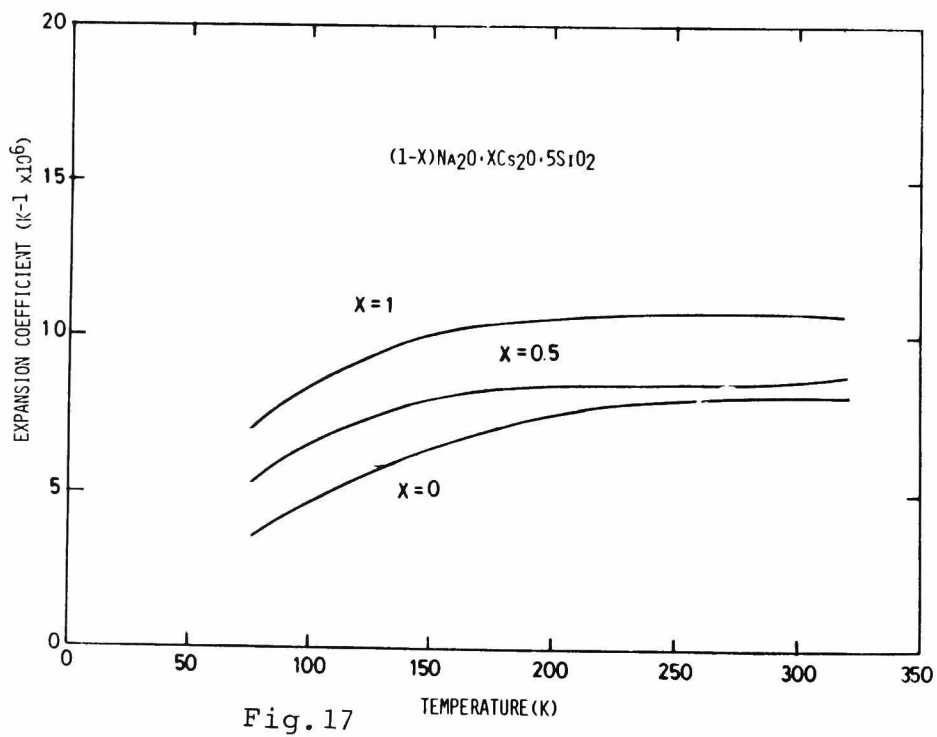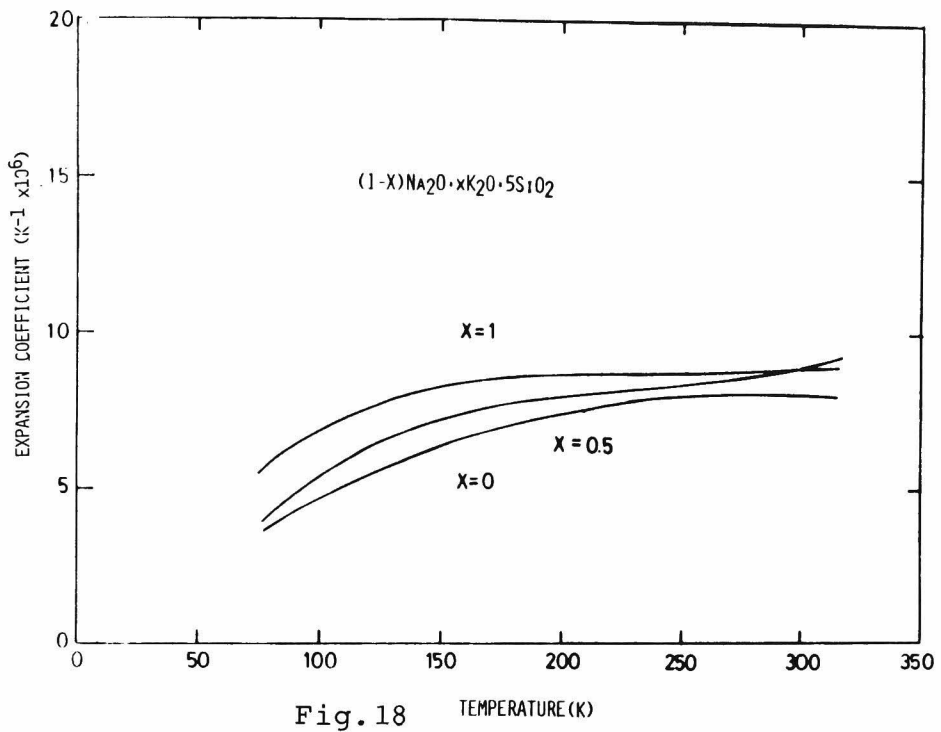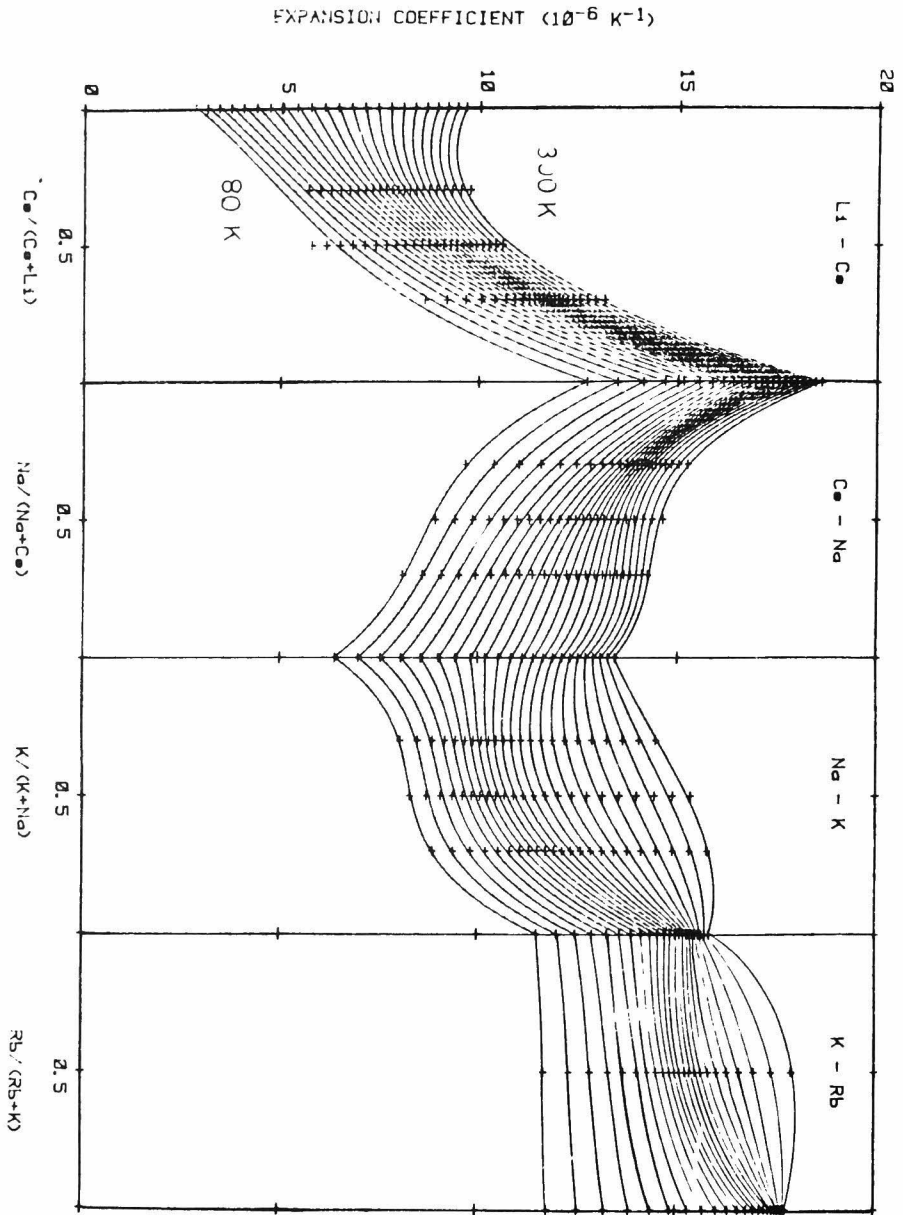
Fig. 14

Fig. 15

Fig. 16

$(1-X) Li_2O \cdot XCs_2O \cdot 5SiO_2$

X = 1

X = 0.5

X = 0

Fig. 17

$(1-X)Na_2O \cdot XCs_2O \cdot 5SiO_2$

X = 1

X = 0.5

X = 0

Fig.18   TEMPERATURE(K)

Fig.19   TEMPERATURE(K)

EXPANSION COEFFICIENT $(10^{-6} K^{-1})$

Fig. 20 Thermal expansion versus composition at various temperature for $R_2O \cdot 2SiO_2$ glasses

R_2O $2SiO_2$

EXPANSION COEFFICIENT (10^{-6} K^{-1})

$R_2O \cdot 5SiO_2$

Li – Cs

300 K

80 K

Cs'(Cs+Li)

2.5

Cs – Na

300 K

80 K

Na'(Na+Cs)

2.5

Na – K

300 K

80 K

K'(K+Na)

2.5

K – Rb

300 K

80 K

Rb'(Rb+K)

2.5
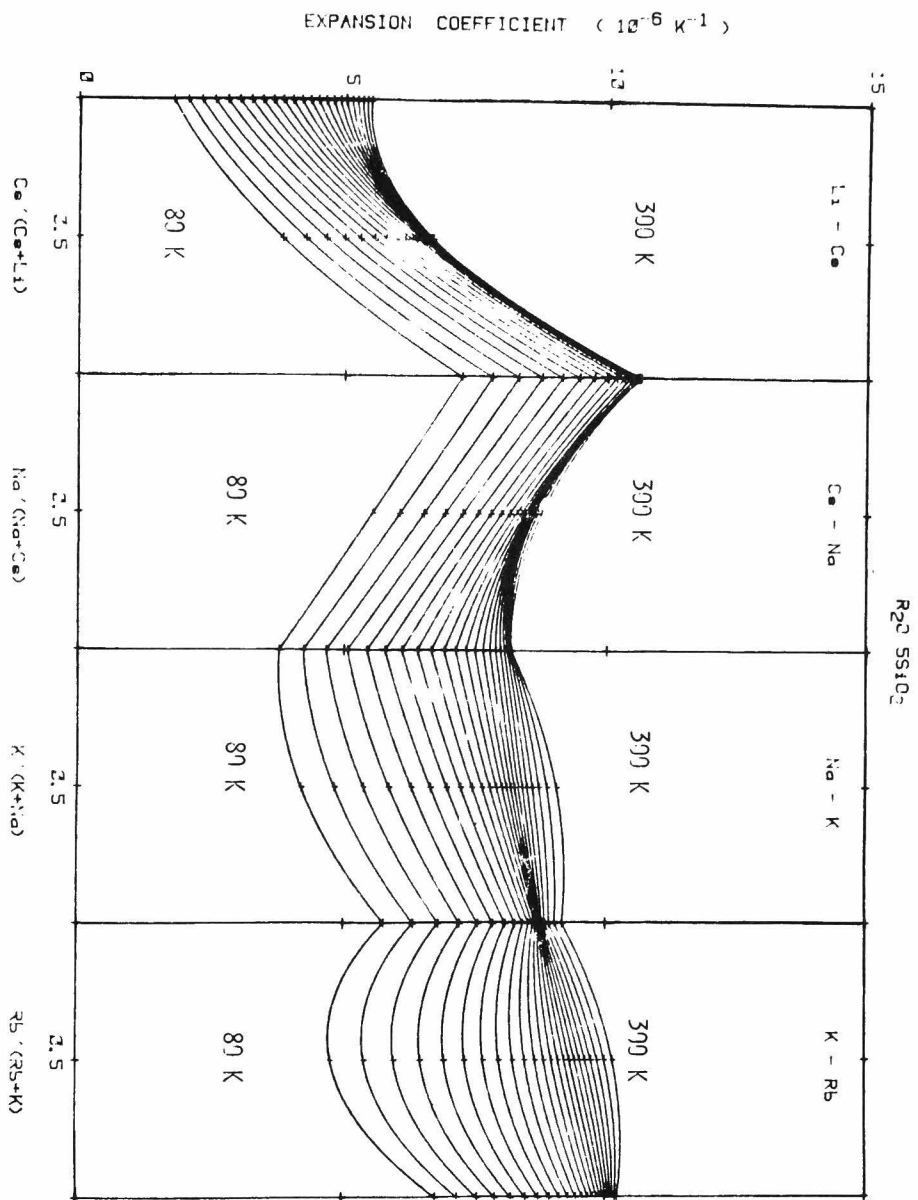
Fig. 21 Thermal expansion versus composition at
various temperature for R2O·5SiO2 glasses

additivity. However, the present results give that a negative deviation from the additivity exists for Na-K glasses at lower temperatures, even though a positive deviation is noticed at high temperatures. Since the thermal expansion coefficient generally decreases with increasing bond strength, a larger negative deviation means that the bond is tightened more in comparison with the case that the bonds of two end members are simply mixed.

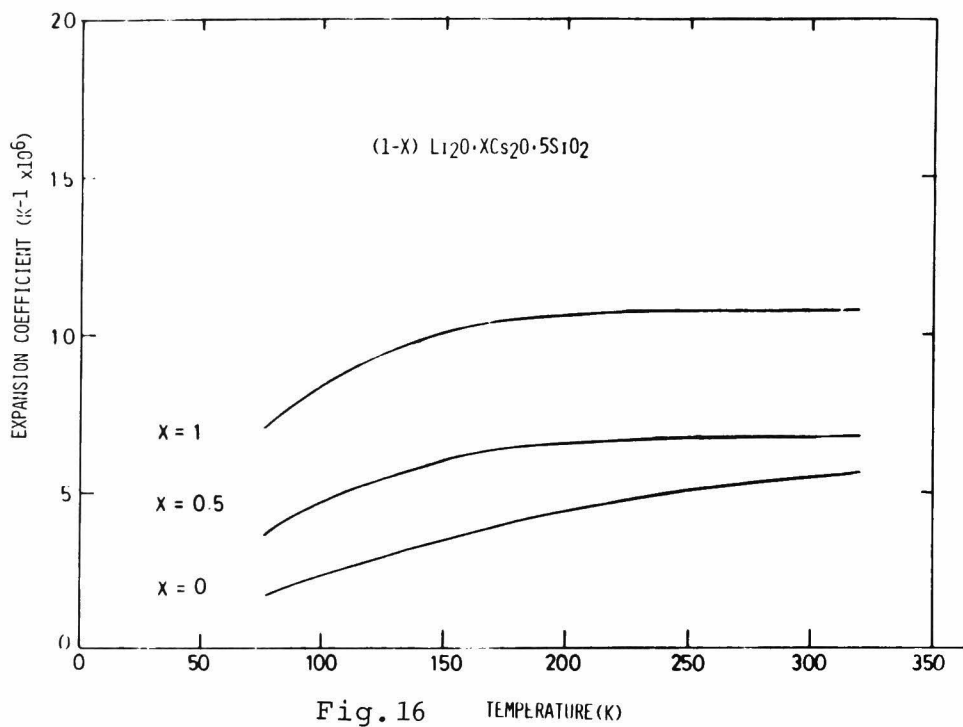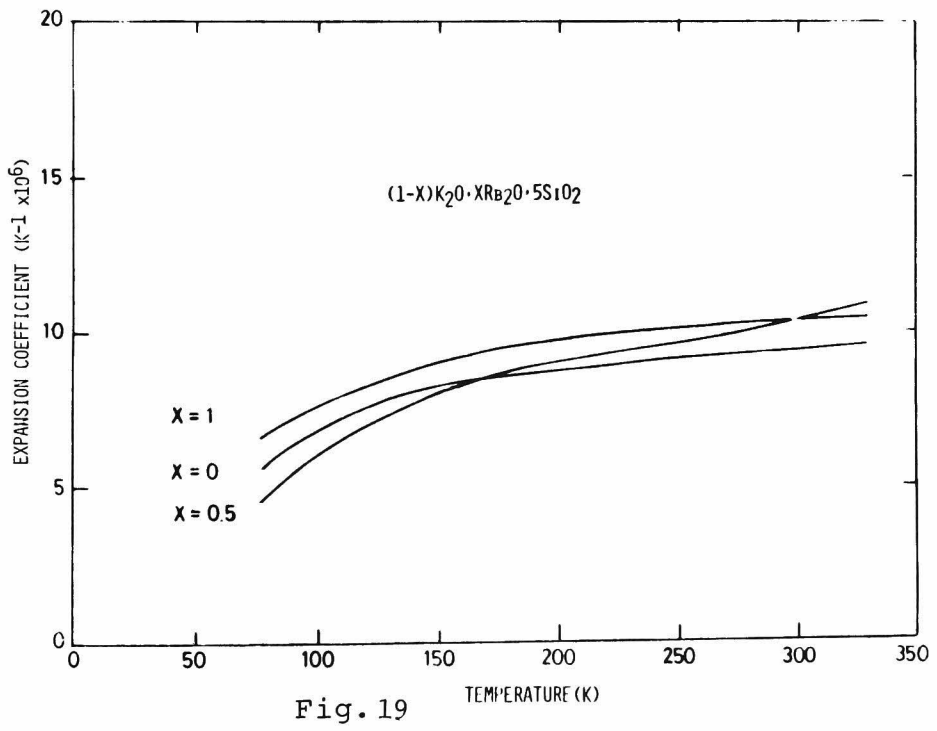It is interesting to compare these thermal expansion data with the heat capacity data in the previous section. From the analyses of the heat capacity data, it was found that both Θ_1 and Θ_3 showed a positive deviation from the linear additivity, indicating the strength of lattice modes for Si-O bond are increased by mixing two kinds of alkali ions. On the other hand, Θ_E approximately showed the linear additivity. The degree of the positive deviation for Θ_1 was larger for sodium-cesium silicate glasses than sodium-potassium or potassium-cesium glasses. Thus, the tightening of Si-O chains was stronger for the glasses having two kinds of alkali ions of dissimilar size than that for those having alkali ions of similar size. This is consistent with the above results of thermal expansion coefficient.

The cause of peculiar temperature dependence of thermal expansion coefficient for the glasses having alkali ions of similar size is not clear at this moment. A possible interpretation is the effect

of mixing two alkali ions which leads to produce the another volume dependent frequency, maybe the existence of R-O-R'.

This vibration may be very sensitive to the change of temperature and the strength of bond, as indicated by the study of dielectric relaxation and electrical conductivity.[25]-[34]

As for the effect of total alkali oxide content on the magnitude of the deviations from additivity, the degree of deviation for alkali pentasilicate glasses ($R_2O \cdot 5SiO_2$) was about the same for alkali disilicate glasses ($R_2O \cdot 2SiO_2$). This seems to indicate that the excess bonding, R-O-R', is independent of Si-O bonds.

SUMMARY TO CHAPTER 5

The heat capacity and thermal expansivity were determined on simple and mixed alkali silicate glasses in the low-to-moderate temperature range from 77 to 400K. The results were analyzed by the three band theory developed in this study, and the structural interpretation of thermal properties of alkali silicate glasses was made. The main results obtained are summarized as follows.

1. The temperature dependence of heat capacity in the low-to-moderate temperature range could not be expressed by a simple Debye temperature, but it was represented well by the three band theory developed in Chapter 2. The first characteristic temperature Θ_1, associated with the strength of elastic interchain Si-O bonds, was found to be 1550K for vitreous silica and decreased with increasing sodium content. The second characteristic temperature Θ_3, associated with the lateral interaction of the chains, was 150K for vitreous silica and increased with sodium content.
These behaviors of Θ_1 and Θ_3 were attributable to the breakage of Si-O bonds and the decrease in directional bonding nature of Si-O bonds caused by the introduction of sodium ions into glass network. The third characteristic temperature, Θ_E, was found to be almost constant satisfying the assumption of Einstein's independent vibrator concept in the present three band theory.

2. The substitution of sodium ions by larger alkali ions caused a decrease in all three characteristic temperatures. This is consistent with the theoretical consideration of lattice vibrations based on the bond strength of alkali metal-oxygen bonds. For mixed alkali silicate glasses, Θ_1 and Θ_3 showed a slightly positive deviation from the linear additivity, while Θ_E followed the linear additivity. This was attributed to the tightening of Si-O chains caused by mixing two kinds of alkali ions.

3. The thermal expansion coefficient increased with increasing cation size in the order from Li to Cs. The change in thermal expansion coefficient with temperature at near room temperature was large for lithium silicate glasses but became less with increasing cation size, as expected from the lattice dynamical theory as well as the above results of heat capacity. The behavior of thermal expansion coefficient for mixed alkali silicate glasses was different from that of single alkali silicate glasses and showed a different deviation from the linear additivity of two end members depending upon the temperature and glass composition. The deviation was found to be negative at low temperatures for most of the glasses but became positive for a few glasses at high temperatures. The magnitude of the negative deviation from the linear additivity decreased in the order of K-Rb, Na-K, Cs-Na and Li-Cs.

This order was consistent with the behavior of Θ_1 and Θ_3 of mixed alkali silicate glasses.

REFERENCES

1. E.F.Westrum,   IV Congres Inter. du Verre, Paris,
                     396 (1956)

2. J.Pirenne and P.Renson,
                     Physica, 28, 233 (1962)

3. J.Deltour and E.Kartheuser,
                     Physica, 31, 269 (1965)

4. B.Wunderlich,   J. Chem. Phys., 37, 1207 (1962)

5. V.V.Tarasov,   Phys. Stat. Sol., 20, 37 (1967)

6. H.Takashima and H.Saito,
                     J. Cer. Assoc. Japan, 85, 413 (1972)

7. A.N.Lazarev,   "Vibrational Spectra and the Structure
                     of Solids", Consultants Bureau, New York
                     (1972)

8. M.Born and K.Huang,
                     "Dynamical Theory of Crystal Lattice",
                     Oxford University Press (1954)

9. H.J.Mcskimin,   J. Appl. Phys., 24, 988 (1953)

10. M.E.Fine et al., J. Appl. Phys., 25, 402 (1954)

11. T.H.K.Barron and J.A.Morrison,
                     Canad. J. Phys., 35, 799 (1957)

12. O.L.Anderson,   J. Phys. Chem. Solids, 12, 41 (1959)

13. J.C.Lasjaunias and R.Maynard,

J. Non-Cryst. Solids, 6, 101 (1971)

14. G.K.White, S.B.Woods and M.T.Elford,

    Phys. Rev., 112, 111 (1958)

15. A.J.Leadbetter, Phys. Chem. Glasses, 9, 1 (1968)

16. R.Kaplow, T.A.Rowe and B.L.Averback,

    Phys. Rev., 168, 1068 (1968)

17. E.H.Henninger, R.C.Buschert and L.Heaton,

    J. Chem. Phys., 46, 586 (1967)

18. A.A.Antoniou and J.A.Morrison,

    J. Appl. Phys., 36, 1873 (1965)

19. P.Flubacher, A.J.Leadbetter, J.A.Morrison and B.P.Stoicheff,

    J. Phys. Chem. Solids, 12, 53 (1959)

20. E.F.Westrum, R.C.Lord and J.C.Morrow,

    J. Chem. Phys., 26, 230 (1957)

21. J.E.Shelby, J. Appl. Phys., 47, 4489 (1976)

22. J.E.Shelby, J. Appl. Phys., 46, 193 (1975)

23. Z.D.Alekseeva and N.V.Polozok,

    Izv. Akad. Nauk. SSSR. Neorg. Mater. 8,

    156 (1972)

24. J.E.Shelby and D.E.Day,

    J. Am. Ceram. Soc., 53, 182 (1970)

25. R.Terai, J. Non-Cryst. Solids, 6, 121 (1971)

26. R.M.Hakim and D.R.Uhlmann,

    Phys. Chem. Glasses, 8, 174 (1967)

27. J.O.Isard,   J. Non-Cryst. Solids, 1, 235 (1969)

28. J.E.Shelby,Jr., and D.E.Day,

         J. Am. Ceram. Soc., 4, 182 (1970)

29. G.L.Mcvay and D.E.Day,

         J. Am. Ceram. Soc., 53, 508 (1970)

30. J.W.Fleming,Jr., and D.E.Day,

         J. Am. Ceram. Soc., 55, 186 (1972)

31. R.J.Charles,   J. Appl. Phys., 32, 1115 (1961)

32. P.B.Macedo, C.T.Moynihan and R.Bose,

         Phys. Chem. Glasses, 13, 171 (1972)

33. J.E.Shelby,Jr. and D.E.Day,

         J. Am. Ceram. Soc., 52, 169 ,1969)

34. Y.Haven and B.Verkerk,

         Phys. Chem. Glasses, 6, 38 (1965)

35. G.J.Exarhos, P.J.Miller and W.M.Risen,Jr.,

         J. Chem. Phys., 60, 4145 (1974)

36. G.J.Exarhos, P.J.Miller and W.M.Risen,Jr.,

         Solid State Commun., 17, 29 (1975)

37. G.J.Exarhos and W.M.Risen,Jr.,

         Chem. Phys. Letters, 10, 484 (1971)

38. K.Matsusita, S.Sakka, A.Osaka, N.Soga and M.Kunugi,

         J. Non-Cryst. Solids, 16, 308 (1974)

39. K.Hirao, N.Soga and M.Kunugi,

J. Am. Ceram. Soc., 62, 570 (1979)

40.   K.Hirao, T.Kiyasu and N.Soga,

J. Appl. Phys., to be published.

CHAPTER 6

THERMAL PROPERTIES OF ALKALI ALUMINO SILICATE GLASSES

In the previous chapters, the applicability of the theoretical models developed in this study to analyze the heat capacity and thermal expansion data of glass systems was examined on alkali silicate glasses and the structural interpretation was made based on the results obtained. However, most commercial glasses are more complicated in their compositions. Thus, it is important to know that the similar treatment can be made for more complicated glass systems.

From the structural point of view, oxides are classified in three categories depending upon their glass forming tendency: the network former, intermediate and modifier. In this chapter, the effect of intermediate ions on the thermal properties of glasses is described. The glasses used were lithium alumino silicate and sodium alumino silicate glasses of $R_2O \cdot Al_2O_3 \cdot nSiO_2$ composition. In these alkali alumino silicate glasses, no breaking of network structure takes place in theory. In practice, however, it is likely that occasional terminations in the oxygen bridging may occur, and these may be compensated for by the formation of triclusters and, to a less extent, $(AlO_6)^{3-}$ octahedral groups. Nevertheless, the alkali ion will be predominantly associated with the margin of $(AlO_4)^-$ tetrahedra.

The study on these compositions presents, therefore, an opportunity to investigate the effects with introduction of alkali metal in the near absence of non-bridging oxygen and to compare with alkali silicate glasses which possess the non-bridging oxygen, as described in Chapter 5.[3)-5)]

6.1   Preparation of glass samples[1),2)]

Seven alkali alumino silicate glasses used in the present study were $Li_2O \cdot Al_2O_3 \cdot nSiO_2$ (n=2,4,6), $Na_2O \cdot Al_2O_3 \cdot nSiO_2$ (n=2,4,6) and $K_2O \cdot Al_2O_3 \cdot 6SiO_2$. The glass batches were prepared from reagent grade Li_2CO_3, Na_2CO_3, K_2CO_3, Al_2O_3 and SiO_2. The glasses were melted in platinum crucibles in a silicon carbide resistance furnace. After complete fusion, the melts were stirred several times with a Pt rod and poured onto a stainless steel plate. In order to obtain homogeneous glasses, the procedure of melting in an electric furnace for approximately 2 to 3 hours, cooling and crushing was repeated three times. The samples were lastly cooled through the glass transition region at a rate of about 20K/min. to give them a constant thermal history.

6.2   Heat capacity

The experimental molar heat capacities obtained for the glasses of the composition of $Li_2O \cdot Al_2O_3 \cdot nSiO_2$ (n=2,4,6) are shown in Table 1-3 and Fig.1. The molar heat capacity of glass was calculated by the formulae weight such as $LiAlSi_2O_6$. The temperature rise in
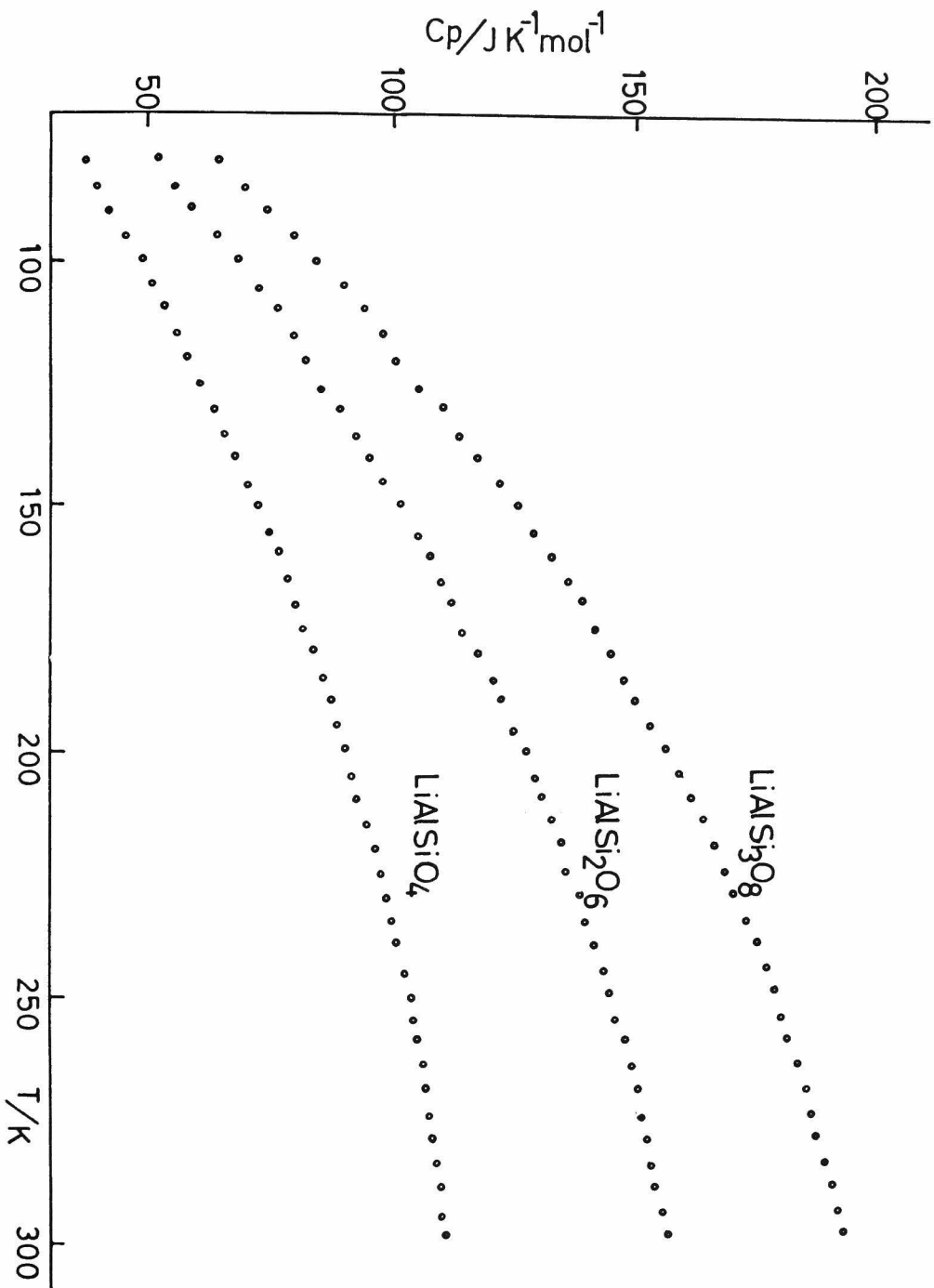
Fig.1 The temperature dependence of the low temperature specific heat of sodium alumino silicate glasses
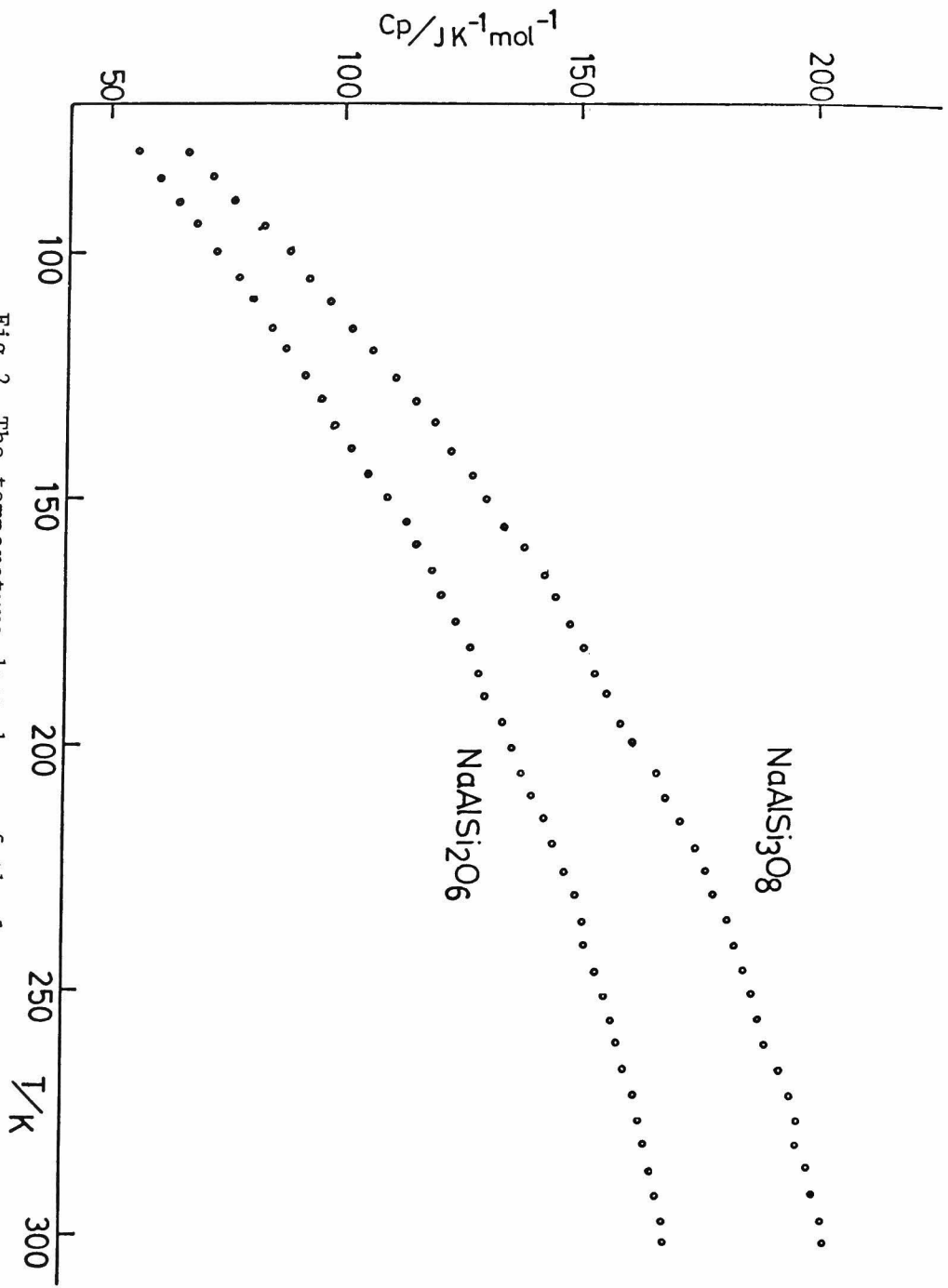
Fig.2 The temperature dependence of the low temperature specific heat of sodium alumino silicate glasses

$\dfrac{T}{K}$	$\dfrac{C_p}{JK^{-1}mol^{-1}}$	$\dfrac{T}{K}$	$\dfrac{C_p}{JK^{-1}mol^{-1}}$
80.1	37.2	194.3	88.5
84.8	39.8	199.2	90.0
90.1	42.2	205.1	91.4
95.2	46.0	210.0	92.6
99.9	49.3	214.8	94.6
104.8	51.0	220.0	96.2
109.6	53.5	224.9	97.5
114.8	56.0	230.1	98.5
119.6	58.3	235.0	99.6
125.0	60.2	239.8	100.3
130.2	63.2	245.3	102.5
135.1	65.1	250.1	103.6
139.8	67.5	255.0	104.2
145.7	70.0	259.1	105.1
149.8	72.1	264.2	106.2
155.8	74.2	269.1	106.5
159.0	76.5	274.8	107.3
164.6	78.3	279.9	108.7
170.6	80.0	285.1	109.0
175.2	81.5	289.1	110.1
179.1	83.4	295.3	110.0
185.2	85.3	299.2	111.1
189.4	87.1		

Table 1   Molar heat capacity of $LiAlSiO_4$ glass

T	Cp	T	Cp
K	$JK^{-1}mol^{-1}$	K	$JK^{-1}mol^{-1}$
79.1	52.5	196.1	124.5
85.2	55.6	200.1	127.2
89.2	59.0	205.7	129.0
94.9	64.0	209.3	130.3
99.8	68.1	214.1	132.3
105.6	72.5	218.2	134.5
109.8	76.5	225.0	135.0
115.8	79.8	229.8	138.0
120.1	82.0	235.6	139.1
126.0	85.2	240.2	140.9
130.1	89.1	245.8	142.8
135.8	92.0	249.9	144.0
140.1	95.3	255.1	145.7
145.6	97.5	259.2	147.3
149.2	101.4	265.1	148.5
155.8	105.0	269.2	150.0
159.7	107.3	275.6	150.5
165.8	109.9	281.1	151.6
169.5	112.0	286.0	152.5
176.0	114.1	289.9	153.0
180.1	117.3	295.2	155.1
185.8	120.7	299.3	156.0
189.1	122.0		

Table 2   Molar heat capacity of $LiAlSi_2O6$ glass

T	C_p	T	C_p
$\overline{K}$	$\overline{JK^{-1}mol^{-1}}$	$\overline{K}$	$\overline{JK^{-1}mol^{-1}}$
80.0	64.5	195.8	153.2
85.1	70.1	199.8	156.5
89.8	74.2	205.0	159.5
95.0	80.0	209.8	162.0
100.1	84.3	214.2	164.5
105.2	89.9	219.1	166.8
109.8	94.0	224.8	169.0
114.7	97.8	229.8	170.5
120.1	100.3	235.1	173.0
125.9	105.1	239.3	175.5
129.8	110.0	244.6	177.5
135.1	113.5	249.8	179.0
139.7	117.2	255.2	180.3
145.0	121.9	259.8	181.5
149.5	125.8	264.5	184.0
155.2	128.8	270.1	185.8
160.1	132.5	275.2	186.5
165.2	136.0	280.0	187.6
169.1	139.2	285.6	189.5
175.1	141.6	290.1	191.5
180.1	145.0	295.2	192.5
185.8	147.9	300.1	193.2
189.8	150.0		

Table 3   Molar heat capacity of $LiAlSi_3O_8$ glass

T	Cp	T	Cp
K	$JK^{-1}mol^{-1}$	K	$JK^{-1}mol^{-1}$
80.1	37.5	195.2	94.1
85.3	39.0	200.2	96.0
90.1	41.4	205.3	97.8
95.1	45.2	209.8	99.8
100.2	49.5	215.2	101.2
105.3	51.8	219.8	103.0
110.4	56.3	225.2	104.1
115.2	59.0	230.1	105.2
119.8	61.1	235.3	106.3
125.5	64.1	240.1	107.0
130.2	66.5	244.9	108.8
135.7	69.2	250.1	110.1
140.1	71.0	255.3	110.8
145.2	73.2	260.8	111.5
150.2	76.5	265.1	112.8
155.1	78.7	270.3	113.3
160.8	80.5	275.2	114.6
165.1	83.1	280.2	116.5
170.3	83.4	285.3	116.8
174.9	86.8	290.2	118.2
180.1	88.1	295.1	119.0
185.2	90.2	300.2	120.8
189.4	92.0		

Table 4   Molar heat capacity of $NaAlSiO_4$ glass

T	Cp	T	Cp
K	$JK^{-1}mol^{-1}$	K	$JK^{-1}mol^{-1}$
80.2	54.2	195.3	133.4
85.3	58.6	200.2	135.5
89.9	62.7	205.6	137.5
95.1	66.8	210.1	139.7
100.5	71.1	215.1	142.6
105.2	76.3	220.7	143.8
111.0	79.5	225.1	146.8
115.4	83.6	230.9	148.9
120.6	86.0	234.9	150.8
125.8	90.8	240.0	151.1
130.3	94.0	245.4	153.7
135.6	96.5	250.5	155.4
139.9	100.5	255.1	157.2
145.1	103.9	260.8	158.5
150.2	108.2	265.2	159.7
155.1	112.6	270.0	161.6
160.7	114.4	275.7	162.7
165.3	118.2	280.3	163.7
170.0	120.1	285.1	164.9
175.4	123.5	290.2	166.6
180.9	126.0	295.1	168.9
185.1	127.9	300.2	168.9
189.5	129.8		

Table 5   Molar heat capacity of $NaAlSi_2O_6$ glass

T	Cp	T	Cp
K	$JK^{-1}mol^{-1}$	K	$JK^{-1}mol^{-1}$
80.1	64.7	195.8	158.4
85.2	70.2	199.5	160.7
89.9	75.3	205.1	166.0
94.7	81.6	210.4	168.1
100.1	86.9	215.6	171.2
105.6	91.2	220.1	174.7
110.7	95.6	225.8	177.2
115.4	100.3	230.3	178.4
120.0	104.7	235.0	181.7
125.7	110.0	240.2	183.5
130.3	114.2	245.7	185.5
135.6	118.4	250.2	186.8
140.2	121.8	255.4	188.8
145.3	126.3	260.2	189.4
149.8	129.6	265.0	192.9
155.4	133.2	270.1	195.3
160.0	137.4	275.4	196.3
165.5	142.1	279.9	196.3
170.7	144.6	285.1	198.4
175.2	147.9	290.0	200.5
180.1	151.1	295.3	201.8
185.0	153.2	300.1	202.2
189.4	155.5		

Table 6   Molar heat capacity of $NaAlSi_3O_8$ glass

T	Cp	T	Cp
K	$JK^{-1}mol^{-1}$	K	$JK^{-1}mol^{-1}$
80.1	69.4	195.3	156.8
84.9	74.2	200.2	159.9
90.3	79.2	205.1	163.6
95.4	84.0	211.1	165.9
100.1	89.2	215.2	169.2
104.9	92.1	220.3	171.9
110.6	96.2	224.8	173.8
114.8	101.2	228.9	176.1
119.8	104.9	235.4	179.7
125.3	110.5	240.1	180.8
131.0	113.2	245.2	182.5
135.6	116.4	251.0	186.9
140.7	119.3	255.1	190.5
145.1	123.1	259.7	192.8
150.3	128.5	265.0	195.3
155.4	131.2	270.1	197.5
160.1	134.1	274.9	199.5
165.6	139.2	280.3	202.2
170.1	141.5	285.7	203.5
174.8	143.8	291.0	205.4
180.2	148.5	295.1	208.4
185.1	150.4	300.5	211.5
190.3	154.2		

Table 7   Molar heat capacity of $KAlSi_3O_8$ glass

each measurement was about 5K and raw data were plotted in Fig.1
without any correction.[6] The molar heat capacities for $Na_2O \cdot Al_2O_3 \cdot$
$nSiO_2$ glasses (n=2,4,6) are shown in Fig.2 and Table 4-6, and those
for $K_2O \cdot Al_2O_3 \cdot 6SiO_2$ glasses in Table 7.

The heat capacity data for alkali alumino silicate glasses
were interpreted in terms of the theory of the three band phonon
spectrum. The results of the calculations are given in Fig.3 and
listed in Table 8, together with the infrared spectra. Fig.3
indicates that the values of Θ_E for Na-O bond vibrations are almost
constant for all sodium alumino silicate glasses and furthermore
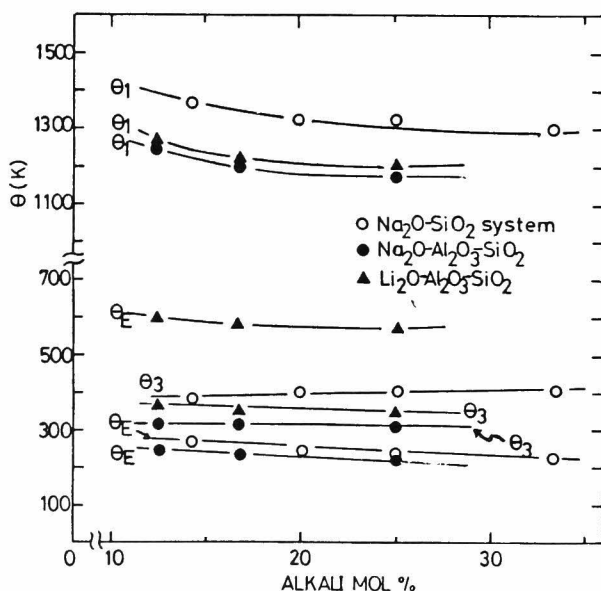close to those of alkali silicate glasses. As expected from the

Fig.3

The characteristic
parameters for alkali
alumino silicate glasses

Sample	Θ_1	Θ_3	Θ_E	Si-O bond (cm^{-1})
LiAlSiO$_4$	1209	360	571	1031
LiAlSi$_2$O$_6$	1220	349	580	1037
LiAlSi$_3$O$_8$	1258	344	593	1052
NaAlSiO$_4$	1195	314	223	1030
NaAlSi$_2$O$_6$	1201	312	232	1038
NaAlSi$_3$O$_8$	1250	310	239	1050

Table 8. The characteristic parameters for alkali alumino silicate glasses

strength of M-O bonds, Θ_E of lithium alumino silicate glasses is very much higher than that of sodium alumino silicate glasses,

The values of Θ_1 appear to be also close each other, although slightly lower than those for sodium silicate glasses with the same sodium contents. Thus, it is clear that the addition of aluminium oxide does not disturb the vibrations of network structures as well as of network modifiers. Thus, it may be said that Al-O bond behaves as the Debye chain continuum similar to Si-O bond rather than behaves as an independent vibrator. In other words, all the (AlSiO$_4$) or (AlSi$_2$O$_6$) are included in the continuum and vibrate in an unique monolithic system. As for the parameter (Θ_3/Θ_1), which represents the degree of non-directionality or

or ionicity, it almost remains constant irrespective of SiO_2 content in the both systems of lithium and sodium alumino silicate glasses, while it varies in Na_2O-SiO_2 glasses as shown in Fig.4. This result will be discussed later.
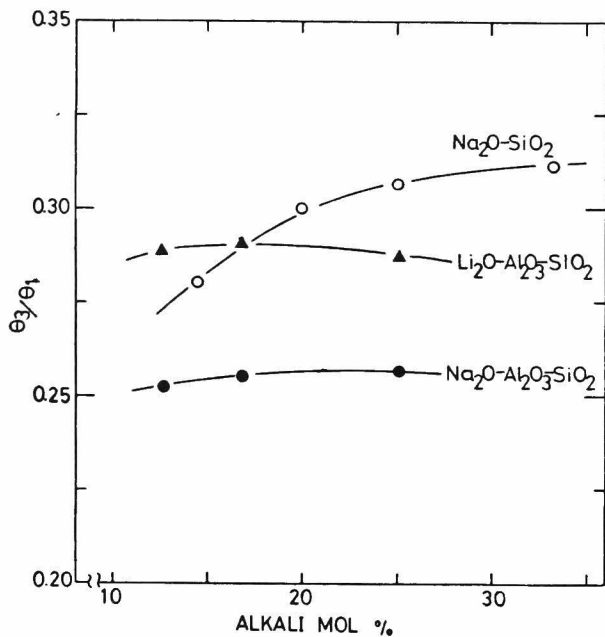

Fig. 4

The homodynamic coefficient of silicate glasses

6.3   Thermal expansion

The smoothed values of thermal expansion coefficient, α, were obtained at rounded temperatures as a function of temperature. The thermal expansion coefficient of lithium alumino silicate glasses of the composition $Li_2O \cdot Al_2O_3 \cdot nSiO_2$ (n=2,4,6) are shown in Fig.5, and those of sodium alumino silicate glasses of the composition

$Na_2O \cdot Al_2O_3 \cdot nSiO_2$ (n=4,6) in Fig.6. For $Na_2O \cdot Al_2O_3 \cdot 2SiO_2$ glass, it was not possible to obtain a bulk sample large enough to measure the thermal expansion and elastic constants. As expected, the effect of increasing silica content in both sodium and lithium system is to decrease the thermal expansion coefficient, which is similar to binary alkali silicate system. Furthermore, these figures also indicate α in lithium containing glasses is lower than that of sodium containing glasses when compared with the same molar content of SiO_2. The effect of the addition of Na_2O or Li_2O is shown in Fig.7, where α versus composition is plotted at different temperatures . This figure also indicates that α increases with increasing Li_2O and Na_2O content.
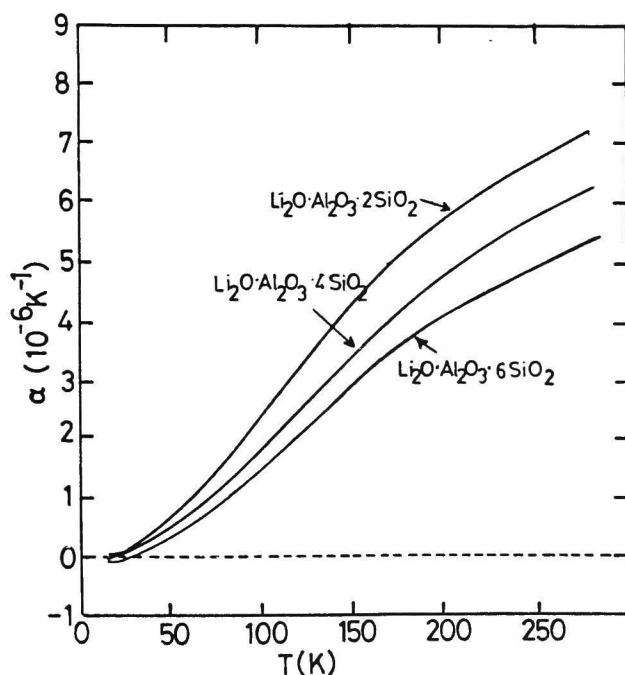

Fig.5

The temperature dependence of thermal expansion coefficient of lithium alumino silicate glasses
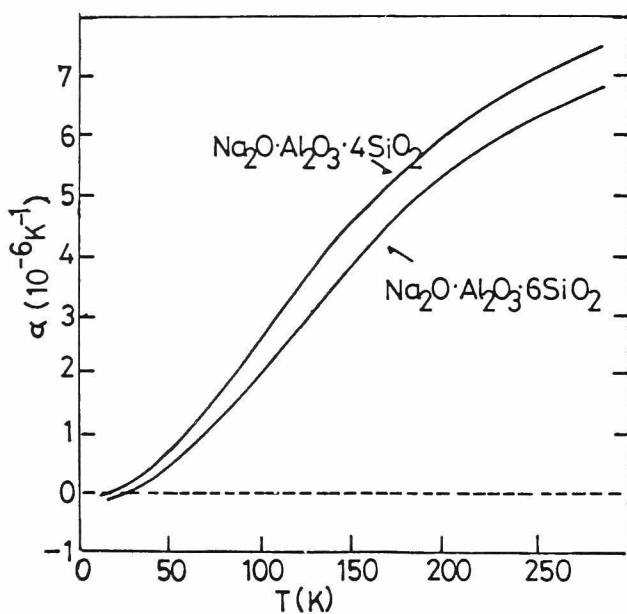
Fig.6
The temperature dependence of thermal expansion coefficient of sodium alumino silicate glasses
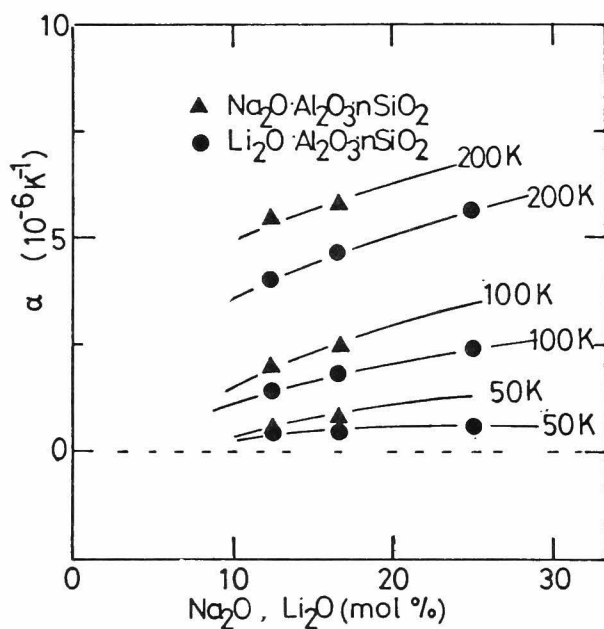

Fig.7
Thermal expansion coefficient versus alkali content

6.4   Grüneisen parameter

In order to examine the glassy state in the absence of non-bridging oxygens and also the influence of the substitution of [13] aluminium for silicon in the network, the anharmonic parameter such as Grüneisen parameter is useful. To obtain Grüneisen parameter for alkali alumino silicate glasses, the knowledge of bulk modulus and density is required in addition to heat capacity and thermal expansion coefficient.

The density of the glasses were determined by using Archimedes' method and are shown in Table 9. As the silica content in lithium alumino silicate glasses is varied from a molecular ratio of 1:1:2 to 1:1:6, the density varies from 2.447 to 2.386. The density of the glasses in the system of $Na_2O \cdot Al_2O_3 \cdot nSiO_2$ also decreases with increasing SiO_2 content.

The measurement of elastic constants[12] was made using the cube resonance method, which was reported previously.[9],[10] The results are given in Table 9. The bulk modulus decreases with increasing silica content, for both $Li_2O \cdot Al_2O_3 \cdot nSiO_2$ and $Na_2O \cdot Al_2O_3 \cdot nSiO_2$ glasses.

The Grüneisen parameter[14] of alkali alumino silicate glasses calculated from these data are illustrated in Fig. 8 as a function of temperature. In spite of a difference in the kind of alkali oxide and in the amount of alkali oxide content, the Grüneisen parameter behaves in a similar manner. In the case of alkali silicate

Composition	LiAlSiO$_4$	LiAlSi$_2$O$_6$	LiAlSi$_3$O$_8$	NaAlSi$_2$O$_6$	NaAlSi$_3$O$_8$
Density (g/cm^3)	2.447	2.426	2.386	2.458	2.444
Coeff. expansion (1/K·10^6)	7.60	6.66	5.25	7.80	7.21
Bulk modulus (kbar)	558.9	493.3	456.9	406.5	399.7
Heat capacity (J/mol·K)	110.8	155.8	192.7	169.1	202.9
Grüneisen parameter	0.59	0.49	0.38	0.46	0.45

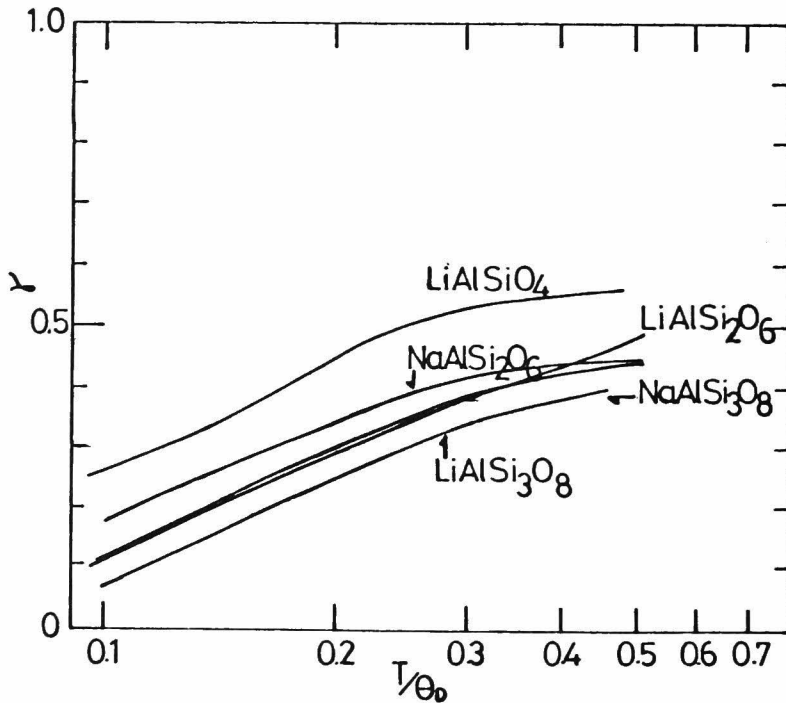Table 9. The density and bulk modulus of alkali alumino
silicate glasses

Fig.8 Grüneisen function of alkali alumino
silicate glasses

glass, the Grüneisen function of alkali silicate glasses varies largely depending upon the glass composition, because non-bridging oxygens are introduced with alkali ions. On the other hand, the introduction of aluminium ion with alkali ions into silica glass does not bring in non-bridging oxygens as described before. Consequently, the behavior of Grüneisen parameter is not so different, even if the alkali content varies from one glass to the other. This similarity in the behavior of Grüneisen parameter is reflecting in the constancy of (Θ_3/Θ_1) described in the previous section. In other words, the main difference in thermal behaviors between alkali silicate and alkali alumino silicate glasses results from the existence or lack of non-bridging oxygens, although the three band theory[11] is applicable to both glass systems.

SUMMARY TO CHAPTER 6

The heat capacity and thermal expansivity were determined on alkali alumino silicate glasses of $Li_2O \cdot Al_2O_3 \cdot nSiO_2$ (n=2,4,6), $Na_2O \cdot Al_2O_3 \cdot nSiO_2$ (n=2,4) and $K_2O \cdot Al_2O_3 \cdot 6SiO_2$ compositions in a wide temperature range. The results were analyzed by the three band theory and the effect of aluminium ions on thermal properties of glass was discussed. The main results obtained are summarized as follows.

1. The temperature dependence of heat capacity of alkali alumino silicate glasses was found to be expressed well by the present three band theory. The third characteristic temperature Θ_E was almost constant irrespective of alkali content, and was about the same value found for alkali silicate glasses. The first characteristic temperature Θ_1 was slightly lower than that for the alkali silicate glass of the same alkali content, and changed little with alkali content. The ratio of Θ_3/Θ_1, which represents the non-directionality or ionicity, remains almost constant for all glasses.
These results were explained by the intermediate nature of aluminium ions that aluminium ions are incorporated in glass network and thus behave as the Debye chain continuum similar to Si-O bonds.

2. The thermal expansion coefficients of alkali alumino silicate glasses increased with increasing alkali and aluminium oxides.

When compared at the same temperature and the same alkali content, a lithium containing glass has a lower thermal expansion coefficient than a sodium containing glass, as expected from the values of Θ_E or the bond strength of alkali ion-oxygen bonds.

3. The behavior of Grüneisen parameter was about the same for all alkali alumino silicate glasses in spite of the difference in alkali content or ionic size. This behavior was kind of alkali oxide or alkali content. This behavior was explained by the effect of the trivalent state of aluminium ions on network modifying alkali ions, or the disappearance of non-bridging oxygens by coexistence of aluminium and alkali ions. This effect also explains the constancy of Θ_3/Θ_1 for alkali alumino silicate glasses.

REFERENCES

1.   K.Hirao, N.Soga and M.Kunugi,

               J. Phys. Chem,, 80, 1612 (1976)

2.   R.G.Bohn,   J, Am. Chem., 45, 2133 (1974)

3.   M.B.Field and R,W.Tucker,

               J. Am. Ceram. Soc,, 54, 309 (1971)

4.   E.D.Lacy,   Phys. Chem. Glasses, 4, 234 (1963)

5.   P.J.Hayward,   Phys. Chem. Glasses, 17, 54 (1976)

6.   H.Suga and S.Seki,

               Bull. Chem. Soc. Japan, 38, 1000 (1965)

7.   D.C.Ginnings and G,T.Furukawa,

               J. Am. Chem. Soc., 75, 522 (1953)

8.   G.T.Furukawa, T.B.Douglas et al.,

               J. Res. Natl. Bur. Stand., 57, 67 (1956)

9.   H.H.Demarest,Jr.,

               J. Acoust. Soc. Am., 49, 768 (1971)

10.   I.Ohno,   J. Phys. Earth, 24, 355 (1976)

11.   K.Hirao, N.Soga and M.Kunugi,

               J. Am. Ceram. Soc., 62, 570 (1979)

12.   O.L.Anderson,   J. Phys. Acoustics, 3B, 43 (1965)

13.   D.E.Day and G.E.Rindone,

               J. Am. Ceram. Soc., 45, 489 (1962)

14.   G.K.White and J.G.Collins,

Proc. R. Soc., London, A333, 237 (1973)

15.   R.B.Stephens,   Phys. Rev., B8, 2896 (1973)

16.   P.Fulde and H.Wagner,

        Phys. Rev. Lett., 27, 1280 (1971)

17.   K.Hirao, N.Soga J. Ceram. Soc. Japan, (1981)

        to be published.

Summary

For the purpose of obtaining informations about the thermal behavior of glass and its relation to glass structure, a detailed experimental study was carried out on heat capacity and thermal expansivity of alkali silicate and alkali alumino silicate glasses from very low temperatures to moderately high temperatures, and the glass model systems were considered based on the lattice dynamic theory.

In Chapter 1, the general background and purpose of the present study was outlined. The difference in thermal behavior between the glassy and crystalline state was described, and the usefulness of the lattice dynamic theory for interpreting the thermodynamic data of glasses and obtaining information about glass structure was pointed out.

In Chapter 2, the application of the lattice dynamic theory to the thermal properties of glasses was described in detail. Two glass model systems were established in the present study to obtain the equations which are applicable to interpret the experimental data of thermodynamic properties of silicate glasses in a wide temperature range. The first model system, a homogeneous but structurally disordered simple system, was found to be useful to clarify the difference in vibrational properties between the glassy and crystalline states at very low temperatures. The effects of

compositional variation and temperature on the Grüneisen parameter were derived and a diagram showing these effects was made for vitreous silica and alkali silicate glasses. The second model, a more complicated system involving three different characteristic temperatures, was established to express the heat capacities of multicomponent glasses in the low-to-moderate temperature range. These three characteristic temperatures were taken to be associated with the interchain bonds of glass network, the lateral interaction of chains and the independent modifier-oxygen bonds. The way of structural interpretation of thermal properties of glasses was shown.

In Chapter 3, the experimental methods and the systems used in the present study were described in detail. The structure and performance of a newly constructed low temperature calorimeter system and a low temperature dilatometer system were presented. The test results of these systems for the standard samples were given and the deviation was found to be within 3% of the reported values in the entire temperature range from 1.6 to 400K.

In Chapter 4, the results of the measurements of heat capacity and thermal expansion coefficient for vitreous silica and sodium silicate glasses in the very low temperature range were presented. The specific heat of these silicate glasses did not obey the Debye continuum theory, but showed an excess heat capacity at about 10K. This excess heat capacity did not vary with composition, indicating

that this anomaly is related to the randomness of glass structure rather than the bending motions of glass network. A large anomaly in thermal expansion coefficient and its compositional dependence was found, which reflected to the variation in Grüneisen parameter with glass composition and temperature. The Grüneisen parameter for vitreous silica calculated from heat capacity, thermal expansion and elastic constants becomes negative below 150K and showed a large negative value at very low temperatures. When the network-filling sodium ions were added to silica glass, this negative value became less with increasing sodium content and disappeared with addition of 20% soda. This effect of alkali addition became more pronounced with increasing size of alkali ions from Na to K and to Cs. Such temperature and compositional effect on Grüneisen parameter were found to be in accordance with the diagram constructed theoretically in Chapter 2 based on the simple glass model system.

In Chapter 5, the thermal properties of simple and mixed alkali silicate glasses at low-to-moderate temperatures were described. The heat capacity was measured and analyzed by using the three band theory. For vitreous silica, the first characteristic temperature Θ_1 associated with the Si-O stretching modes was 1550K and the second characteristic temperature Θ_3 associated with the lateral interactions of networks was 140K and the ratio Θ_3/Θ_1 was small (0.09). Introduction of alkali ions to the vitreous silica network caused a small decrease in Θ_1 and a large in Θ_3, which was considered

due to the breakage of glass network by alkali ions. The third characteristic temperatures Θ_E associated with alkali metal-oxygen bonds independent of network vibrations were 220K for Na-O bonds, 150K for K-O bonds and 50K for Cs-O bonds. This order was in agreement with the bond strength of alkali metal-oxygen bonds. In the case of mixed alkali silicate glasses, both Θ_1 and Θ_3 showed a little positive deviation from the linear additivity, indicating that the Si-O chains are tightened by mixing two kinds of alkali ions.

The thermal expansion coefficient became larger with increasing alkali content as well as with increasing alkali ion size. However, the temperature dependences of thermal expansion coefficients of mixed alkali silicate glasses differed from those of simple alkali silicate glasses and could not be obtained from the linear additivity... This behavior became more pronounced for the glass containing two kinds of alkali ions of two very dissimilar ionic size. This was attributed to the interaction of two dissimilar ions.

In Chapter 6, the thermal properties of alkali alumino silicate glasses at low-to-moderate temperature were described and the applicability of the three band theory was examined. The heat capacity data were found to be represented well by the three band theory. The addition of intermediate cations such as aluminium to silica network showed only a slight decrease in Θ_1

and Θ_3 from those of a sodium silicate glass having the same sodium content and gave almost no change in Θ_E. This was interpreted on the basis that the Al-O bond in alkali alumino silicate glasses behave as the Debye chain continuum similar to Si-O bond rather than as an independent vibrator like network modifiers, because aluminium ions are incorporated into the glass network. The thermal expansion coefficient at any given temperature increased with increasing alkali content as observed in alkali silicate glasses. However, the behavior of Grüneisen parameter for alkali alumino silicate glasses was different from that for alkali silicate glasses in such a way that the dependence of Grüneisen parameter on alkali content was quite small. This independent nature was attributed to the lack of non-bridging oxygens in alkali alumino silicate glasses where no breaking of network structure takes place unlike in alkali silicate glasses.